TRANSCRIPTIONAL AND POST-TRANSCRIPTIONAL REGULATION OF MENKES COPPER ATPASE (ATP7A) GENE EXPRESSION DURING IRON DEFICIENCY

By

LIWEI XIE

A DISSERTATION PRESENTED TO THE GRADUATE SCHOOL
OF THE UNIVERSITY OF FLORIDA IN PARTIAL FULFILLMENT
OF THE REQUIREMENTS FOR THE DEGREE OF
DOCTOR OF PHILOSOPHY

UNIVERSITY OF FLORIDA

2013

© 2013 Liwei Xie

To my family who gave love and support over the past 6 years

ACKNOWLEDGMENTS

The past three years and half were the most exciting and memorable time in my life, which was filled with not only the effort and hard work, but also the most accomplishment and success I've ever made. Each of these points derives back to five and half years ago when I started my dream at SUNY at Buffalo.

First, I would like to give my deepest appreciation to my parents, my grandparents, and my wife. It was their support in most aspects of my life, which allowed me to utilize the available resources and limited time to study and conduct research work.

Secondly, I offer my acknowledgement to my academic advisor, Dr. James F. Collins. You offered me space and resource to participate in research where I learned basic biological techniques when I was still an undergraduate student with no background knowledge in biology. I learned the most basic things from where I started, and it turned out to be a precious experience when I moved forward to the advanced levels of my studies. During my Doctor of Philosophy work, you offered a comfortable working space and flexible working time, which allowed me to design and schedule my work based on my schedule. You also gave me a lot freedom to come up ideas, design the experiments, develop new techniques, and work independently, all of which led to my accomplishments and success, and will be helpful for future work in my life.

Thirdly, I want to thank my committee members, Drs. Cousins, Knutson and Lu for the significant and generous contribution toward my research work.

Fourthly, I would like to give appreciation to those people from other institutions for the useful research resources shared, the proofreading of a fellowship application,

and papers reviewed. I also want to acknowledge financial support from NIH, UF graduate school, and a generous donation from UF International Center.

Last, I would like to thank all the graduate students in the lab, Dr. Yan Lu, Ms. Lingli Jiang, Mr. Sukru Gulec, Ms. April Kim, and Dr. Genie, and other students and faculty in the department, as well for their support toward my work.

Without help from these people and organization mentioned above, I would not have been able to make these great achievements over the last three and half years. All of you are important components of my life, which have accelerated my success.

TABLE OF CONTENTS

page

LIST OF TABLES

LIST OF FIGURES

LIST OF ABBREVIATIONS

Atp7a	Menkes Copper ATPase
Ankrd37	Ankyrin Repeat Domain Protein 37
COX1	Cytochrome c Oxidase 1
Cp	Ceruloplasmin
Ctrl	Control
Ctr1	Copper Transport Protein 1
Cu	Copper
Cu^{1+}	Cuprous Copper
Cu^{2+}	Cupric Copper
Dcytb	Duodenal Cytochrome b
Dmt1	Divalent Metal Transporter 1
Fe	Iron
FOX	Ferroxidase
Fpn1	Ferroportin 1
FeD	Iron Deficiency
Heph	Hephaestin
HIF1α	Hypoxia-Inducible Factor 1α
HIF2α	Hypoxia-Inducible Factor 2α
HRE	Hypoxia Response Element
IEC-6	Rat Intestinal Epithelial Cells
IRE	Iron-Response Element
IRP	Iron-Response Protein
Mt	Metallothionein
SOD1	Cu/Zn Superoxide Dismutase 1

Sp1	Specificity Protein 1
Sp6	Specificity Protein 6
TfR1	Transferrin Factor Receptor 1
VEGF	Vascular Epithelial Growth Factor
UTR	Untranslated Region

Abstract of Dissertation Presented to the Graduate School
of the University of Florida in Partial Fulfillment of the
Requirements for the Degree of Doctor of Philosophy

TRANSCRIPTIONAL AND POST-TRANSCRIPTIONAL REGULATION OF MENKES COPPER ATPASE (ATP7A) GENE EXPRESSION DURING IRON DEFICIENCY

By

Liwei Xie

May 2013

Chair: James F. Collins
Major: Nutritional Sciences

Menkes copper ATPase (Atp7a) is a copper exporter in intestinal enterocytes of rodents. It is necessary to export copper from enterocytes and deliver Cu to blood circulation. In a well-characterized intestinal epithelial (IEC-6) cell model, Atp7a maintains intracellular copper homeostasis. In a previous study, Atp7a was shown to be strongly upregulated at the mRNA (~5-fold) and protein (~8-fold) levels in duodenal enterocytes, concomitant with copper loading and accumulation in intestine and liver. It was observed that *Atp7a* expression level also paralleled that of iron transport-related genes, such as divalent metal transporter 1 (*Dmt1*), and duodenal cytochrome B (*Dcytb*). Studies from different labs have proven that HIF2α robustly increases the expression of iron transported-related genes and iron absorption in small intestine during iron deficiency. A microarray study showed that *Atp7a* together with iron transport-related genes have GC-rich sequences (potential Sp1-like factor binding sites) on the promoters of these genes. The major gaps this study aims to fill are to elucidate the molecular mechanisms of Atp7a regulation during iron deficiency. These studies tested the hypothesis that *Atp7a* expression is regulated by HIF2α, Sp1, and copper at

transcriptional or post-transcriptional levels. *Atp7a* promoter was cloned into a luciferase reporter vector and characterized. Mutagenesis analysis showed that there are three evolutionarily conserved, functional Hypoxia Response Elements (HREs) and four functional Sp1-binding sites in the Atp7a promoter. Chromatin immunoprecipitation (ChIP) analysis proved that HIF2α and Sp1 directly bind to the Atp7a promoter. Further investigation looked into the copper-mediated stabilization of the Atp7a protein. The copper-Atp7a interaction increased Atp7a protein stability, which was investigated in the IEC-6 cells. These data indicated that Atp7a mRNA expression regulated by HIF2α and Sp1, in parallel with the iron transport-related genes, and that copper stabilized the Atp7a protein by a post-transcriptional mechanism. The major finding of this study is that Atp7a is coordinately regulated with iron transport-related gene by HIF2α, and that the Atp7a protein is stabilized by copper loading in the mammalian intestine during iron deprivation.

CHAPTER 1
INTRODUCTION

Iron

Chemistry and Biochemical Properties

Iron is essential for life, as it plays important roles in biological processes such as electron transport, enzyme activity, oxygen transport and gene regulation [1]. In nature, iron exists in various oxidation states. Ferrous (Fe^{2+}) and ferric (Fe^{3+}) iron are the most common states in biological systems [2].

Iron in the diet is found in two distinct forms: heme and non-heme (or inorganic) iron [3]. Heme iron, which is bound within the porphyrin ring structure of hemoglobin and myoglobin, is found predominantly in meat products [4]. Due to the protection of the ring structure, the absorption of heme iron is less influenced by dietary factors leading to higher bioavailability [4]. In contrast, non-heme iron that in nature exists mostly as ferric (Fe^{3+}) iron can be found in various dietary sources including meats and plants. Ferric iron is insoluble at physiological pH. However, in the small intestine, when ferric iron is released from digested food products, dietary and luminal factors, including ascorbic acid and gastric acid, help reduce the ferric iron to a soluble and more absorbable form, ferrous iron (Fe^{2+}) [5, 6]. Furthermore, some plant-derived dietary factors, such as phytate, fibers, polyphenol and tannic acid, tightly bind to ferric iron in the intestine, decreasing bioavailability and negatively affecting iron absorption [7].

Systemic Iron Homeostasis

Iron is abundant in the earth's crust. It is an essential nutrient, as organisms require adequate amounts of iron to maintain systemic homeostasis. However, organisms have to avoid absorbing too much iron as it will accumulate in organs and

cause toxic effects. Importantly, there is no known excretory pathway to eliminate excess iron.

Iron is absorbed from digested food into enterocytes, and is then exported into blood. Iron exported across the basolateral surface of enterocytes rapidly binds to transferrin (TF), which circulates iron to the major sites of utilization including the largest consumer of iron, the erythroid bone marrow [8, 9]. Absorbed iron goes first to the liver, where excess iron may be stored in ferritin inside the hepatocytes [10]. In tissues, no free iron exists as it is highly reactive and can produce oxygen free radicals [11]. Hepatocyte iron can be mobilized when needed. The rest of the absorbed iron is distributed to other tissues. When plasma iron is in excess, transferrin will be saturated, and massive amounts of iron accumulate in the liver [12]. As mentioned, the erythroid bone marrow is the largest iron consumer where iron is incorporated into hemoglobin in erythroid precursors. In muscle cells, the formation of myoglobin also requires a large amount of iron, however, the mechanism of iron acquisition by muscle cells is less clear [13].

Except for a small amount of absorbed iron in the small intestine (1-2 mg/d), the majority of body iron supply is derived from the recycling of iron already within the system (20-25 mg/d) [14]. The recovery and recycling of iron from senescent erythroid cells contributes most to this iron pool. Old or damaged erythrocytes are phagocytosed by tissue macrophages, particularly in spleen, and by Kupffer cells in the liver. Some iron remains in macrophages, and some is exported to plasma TF for use. TF-bound iron either circulates to hepatocytes for deposition or to the organ of iron utilization [14].

Massive iron overload and accumulation in liver results in hepatotoxicity, leading to liver fibrosis and cirrhosis, which eventually may cause liver cancer [15]. Iron accumulation is also a common feature of neurodegenerative diseases, including Parkinson's and Alzheimer's diseases and the much rarer disorders aceruloplasminemia, Hallervorden-Spatz disease, and neuroferritinopathy [16-18]. Iron has been implicated in pathogenic diseases for its capacity to produce free radicals and increase oxidative stress.

To avoid excessive iron absorption and accumulation leading to iron toxicity-related diseases, intestinal iron absorption, internal iron recycling from macrophages, and mobilization from hepatocytes have to be meticulously regulated. Thus, mammals have developed precise and sophisticated regulatory mechanisms that control intestinal iron absorption.

Molecular Mechanisms of Iron Absorption

Iron moves from dietary sources across the enterocyte to the portal circulation generally by three steps: 1) Iron flows from dietary sources across the apical surface of enterocytes; 2) Iron translocates from the apical to basolateral surfaces for delivery to portal blood circulation or it can be stored or utilized in enterocytes; 3) Iron is exported across the basolateral surface of enterocytes into the circulation, where it binds to *apo*-transferrin.

The majority of dietary non-heme iron is in the form of ferric iron (Fe^{3+}), which is insoluble at physiological pH. Ferric iron thus has to be reduced to a soluble form, ferrous iron, which is accomplished by an iron reductase on the brush-border surface of duodenal enterocytes [19, 20]. Duodenal cytochrome b (Dcytb), a multi-spanning membrane protein, was shown to have ferric iron reductase activity [21-23]. However,

mice with Dcytb deletion can still absorb iron, which suggests that Dcytb is not essential for iron absorption in mouse small intestine [22]. There may be some other iron reductase or iron reduction mechanism existing in mice, such as ascorbic acid. However, the relevance of this observation to iron homeostasis in humans is not clear.

Once reduced, ferrous iron is transported across the apical membrane by divalent metal transporter 1 (Dmt1) [24, 25]. In addition to the enterocyte of small intestine, Dmt1 expression is also detected in most body cells where it plays important roles in the uptake of TF-bound iron [26]. Studies indicated that either small intestine-specific deletion of Dmt1 or a mutated Dmt1 in small intestine will lead to a defect in iron absorption and severe anemia is observed [27, 28]. This suggests that Dmt1 is an essential pathway for iron absorption in the mammalian small intestine.

Once inside enterocytes, iron can be utilized by enterocytes, stored inside the iron storage protein ferritin, or transferred across the basolateral membrane to portal blood circulation [14]. First, the enterocyte may utilize newly absorbed iron for its metabolic purposes such as in mitochondria, where iron may be used for heme synthesis or iron-sulfur cluster protein synthesis, including cytochromes in the mitochondrial electron transport chain [29]. Newly absorbed iron may also participate in the regulation of genes encoding proteins involving in iron metabolism. Second, in addition to metabolic use and basolateral transport of excess iron in enterocytes, iron can be incorporated to ferritin. Last, if body has a high demand of iron, newly absorbed iron will be transferred across the basolateral membrane quickly for use by various tissues and organs.

Ferrous iron is pumped out of enterocytes into the portal blood circulation by a multi-spanning membrane protein, ferroportin 1 [30, 31]. On the basolateral membrane, before being bound to TF, effluxed ferrous iron needs to be oxidized to ferric iron. In small intestine, hephaestin (Heph) is strongly expressed in mature enterocytes and is known to be the major iron oxidase [32]. However, Heph is not essential as *sla* (Heph mutant) mice and Heph knockout mice do not strongly influence iron status [33]. There thus must be some other unidentified ferroxidases expressed in enterocytes that may work cooperatively with Fpn1 for iron export across the basolateral membrane of duodenal enterocytes [34, 35]. Ferrous iron in the basolateral iron-transport complex is oxidized to ferric iron, followed by picking up by *apo*-transferrin [36]. However, transferrin is not essential for iron transport, as mice lacking TF (called hypotransferrinemia mice) do not die [37]. These animals have massive iron overload in liver and nonhematopoietic tissues, and they develop severe iron-deficiency anemia, which suggests that TF is important for erythropoiesis to uptake sufficient iron for erythrocyte development to meet high levels of iron demand for hemoglobin synthesis [37]. Another plasma protein, ceruloplasmin (Cp) that has homology to Heph also has the ability to oxidize ferric iron to ferrous iron. Cp is synthesized in hepatocytes and secreted into blood [38]. It facilitates iron release from various tissues. However, Cp knockout in mice did not show a clear defect in iron absorption (unpublished observation). Since mice with double deletion of Heph and Cp are still viable, there must be some unidentified and uncharacterized ferroxidase that exists [35]. Recently, another ferroxidase has been identified with similar function to Heph and Cp [35]. Further studies are however necessary to understand the functional and physiological

importance of these novel ferroxidases. Both Heph and Cp are copper-dependent iron ferroxidases as copper is incorporated biosynthetically into both proteins. Thus, animals with copper deficiency will develop iron-deficiency anemia, as copper is required for Heph and Cp enzyme activity [39].

Regulation of Iron Absorption

Iron absorption in duodenal enterocytes is tightly regulated, as no active excretory pathway exists. Thus, the amount of body iron must be determined via regulation of intestinal iron absorption. Iron absorption increases at the times of high body demand, and decreases when iron stores are replete. Research has identified several regulatory mechanisms that regulate iron absorption.

The duodenum is the major site for intestinal iron absorption. Studies suggested a post-transcriptional regulatory mechanism is involved in expression of iron transport-related genes [40]. The iron response elements (IREs) are found in the untranslated region (UTR) of the mRNAs [41]. Iron regulatory proteins (IRPs) bind to IREs when intracellular iron is low. The binding of IRPs to IREs can either increase mRNA stability (e.g. Dmt1 [42] with IREs in the 3'-UTR) or block translation (e.g. Fpn1 [30] and ferritin [43] with IREs in the 5'-UTR). It was initially thought that IRPs sense the intracellular iron levels and regulate mRNA translation via direct interaction with mRNA. However, during iron deficiency, the system has a high iron demand. In this case, intestinal iron uptake and iron transport the across basolateral membrane are induced, while this conflicts with the IRPs-mediated mechanism of Fpn1 regulation. Furthermore, other iron transport-related genes such as Dcytb do not have IREs. It was thus hypothesized that other regulatory mechanisms must exist, especially during iron deprivation.

It was noted that during iron deficiency, iron is depleted in hepatocytes (the major iron deposition site) and in erythrocytes (the major iron utilization site) [44]. This causes a defect in hemoglobin synthesis in erythrocytes and eventually affects oxygen transport to different organs, leading to systemic hypoxia. Several studies have identified that iron deficiency-mediated hypoxia in small intestine stabilizes hypoxia inducible factor (HIF) in enterocytes [45]. HIF2α, but not HIF1α, robustly increases iron transport-related gene expression in enterocytes through direct binding to hypoxia response elements (HREs) on promoters of these genes [46]. At least two HREs were found on proximal region of the promoters, including Dmt1, Dcytb, and Fpn1 [45, 47]. During iron deficiency, HIF2α plays a major role in regulating iron transport-related gene expression in duodenal enterocytes to increase systemic iron level. Thus, another splice variant of the Fpn1 transcript without IREs in the mRNA is upregulated by HIF2α during iron deficiency [47]. Mice with intestine-specific deletion of HIF2α lose the induction on Dcytb and Fpn1 [45, 47] even during iron deficiency. Only a slight induction on Dmt1 is observed in mice with HIF2α deletion during iron deficiency, which suggests that intestinal iron absorption is mainly regulated by HIF2α when severe iron deficiency occurs [45].

Fpn1 is the only known iron transporter to carry iron across the basolateral membrane to the portal blood circulation, and this action is the rate-limiting step that is crucial for maintenance of systemic iron levels [30]. Hepcidin was originally identified in urine as a small antimicrobial peptide, and subsequently linked to iron homeostasis [48]. It is mainly produced by and secreted from hepatocytes [48]. Expression of hepcidin in liver is inversely related to intestinal iron uptake and this suggests that hepcidin is a suppressor of iron absorption [30, 31, 49]. Hepcidin exerts its function by interacting

with Fpn1, subsequently leading to the internalization and degradation of the whole complex to reduce iron export from enterocytes [30].

Copper

Chemistry and Biochemical Properties

Copper (Cu) is one of the essential trace minerals for most organisms, especially for rodents and humans. Cu ion exists in two oxidation states in biological systems, Cu^{1+} (cuprous) and Cu^{2+} (cupric). It plays important roles in biological systems and serves as a cofactor for enzymes and proteins involved in energy generation and release, iron oxidation (Cp and Heph), signal transduction (cytochrome c oxidase in mitochondria), formation and regulation of hormones, collagen formation (lysyl oxidase), red blood cell formation and cellular metabolism [50].

Systemic Copper Homeostasis

There is an average of ~1.3 mg/d of copper flowing from dietary sources into duodenal enterocytes [51]. The absorbed copper passes through enterocytes, and is exported into the portal blood circulation. The exported copper is picked up by albumin, which circulates and delivers copper to the liver for the cuproenzyme synthesis, such as Cp. Excessive copper is exported via hepatic Atp7b into bile and excreted through feces. Body copper homeostasis is coordinately regulated via intestinal copper absorption, copper storage in tissues (e.g. liver), and copper excretion by the liver [50].

Molecular Mechanisms of Copper Absorption

Copper absorption is regulated via coordinate interaction between membrane-bound transporters that pump copper in and out of cells and intracellular chaperones that deliver copper to their targets.

Copper uptake occurs from the lumen of small intestine via a copper transporter protein (Ctr1), which is structurally and functionally conserved from yeast to humans [52]. Accumulating evidence indicates that a metalloreductase is required to reduce Cu^{2+} to Cu^{1+}, which likely traverses the apical membrane of duodenal enterocytes via Ctr1. Recent studies suggested some possible candidates as the required metalloreductase. A Steap protein, which localizes to the plasma and intracellular membrane may work synergistically with Ctr1 to mediate Cu^{1+} uptake [53]. Alternatively, Dcytb located at the apical membrane of enterocytes, which mediates iron reduction, may also work with Ctr1 to mediate Cu^{1+} uptake [54].

Inside enterocytes, copper is delivered via specific copper chaperones to distinct target enzymes through direct protein-protein interactions. The copper chaperone, CCS is responsible to deliver copper to Cu/Zn superoxide dismutase (SOD1), while COX17 delivers copper to cytochrome c oxidase (COX1) in mitochondria [55, 56]. A third copper chaperone in enterocytes is the Atox1 protein, which delivers copper to a copper transporter (Atp7a), which is located inside the Golgi-complex and traffics between Golgi-complex and the basolateral membrane of enterocytes [57-59]. Following export across the basolateral membrane to the portal blood circulation by Atp7a, copper is bound to albumin, transcuprein, or low molecular weight ligands. Newly absorbed copper is taken up by hepatocytes, where copper is incorporated into newly synthesized ceruloplasmin, which is afterward released from hepatocytes into the blood and is

delivered to cells as a functional ferroxidase. In hepatocytes, excess copper is stored in metallothionein to avoid the generation of free radicals from the free Cu [60].

Regulation of Copper Absorption

Copper as a cofactor plays important roles in biological processes including growth and development. However, excessive copper, especially free copper, will be toxic in terms of the redox property of copper contributing to the generation of free radicals such as the hydroxyl radical [61]. Thus, excessive copper in duodenal enterocytes will be quickly exported across the basolateral surface into the portal blood circulation followed by binding to transport proteins such as albumin or transcuprein to circulate to hepatocytes for storage [50].

The concentration of copper in duodenal enterocytes is tightly regulated by the copper transporter located on the basolateral side of enterocytes, the Menkes Copper-Transporting ATPase (Atp7a). This protein is a unique copper-transporting P-type ATPase, which plays an essential role in maintaining copper homeostasis. Mutation on *Atp7a* gene may cause Menkes disease, which is an X-linked recessive disorder, identified and isolated in the 1960s by John Han Menkes and will lead to copper accumulation in enterocytes and systemic copper deficiency [62]. In 1993, Atp7a was isolated as a candidate gene for Menkes disease by positioning cloning and the supporting evidences indicated that this gene encodes a copper-transporting ATPase [63-65].

It was documented that genes involved in copper trafficking and transport are regulated at the transcriptional level in multiple systems [66-68]. However, in some organisms, copper does not affect the mRNA level and may be associated with protein degradation and maintenance of steady-state protein levels. Studies have demonstrated

that copper stimulates endocytosis of the membrane-bound copper transporter, Ctr1, followed by degradation via a post-translational mechanism in HEK293 cells [69]. Additionally, the copper chaperone for SOD1 (CCS) protein levels change inversely with copper concentration and CCS half-life via copper levels is regulated [70, 71]. This is achieved through the binding of copper to the cysteine residues (also known as CXC domain) at the N-terminus [72]. This domain is commonly found in several copper transporters and chaperones, including, Atp7a, Atp7b, CCS, and Atox1 [73, 74].

The Atp7a protein in duodenal enterocytes mainly was found in two subcellular locations, in the *trans*-Golgi network (TGN) and plasma membrane (PM) [75]. At normal copper concentrations, most Atp7a protein is localized to the TGN where it supplies copper to copper-dependent enzymes in the secretory pathway [59]. However, in the presence of increased copper concentration in duodenal enterocytes, the Atp7a protein trafficks to the PM to export excessive copper *in vitro [59]*. This phenomenon has been observed in both duodenal enterocytes and in intestinal epithelial cell models [76]. Studies investigated in various cell types showed that elevated intracellular copper concentration induces trafficking of Atp7a protein to PM and copper seems to maintain high level of Atp7a protein in the PM [77].

Iron-Copper Interactions

Copper is closely associated with iron absorption and transport. As ferrous iron traverses the basolateral membrane of enterocytes, it needs to be oxidized to ferric iron before being bound by *apo*-transferrin. This oxidation process is mediated via two known ferroxidases, hephaestin (Heph) that is synthesized by duodenal enterocytes [33] and ceruloplasmin (Cp) synthesized by hepatocytes [78]. These two ferroxidases (FOXs) are copper-dependent enzymes. When the copper level is low, copper-

dependent FOX activity and abundance are low, leading to a defect in intestinal iron absorption and the development of iron-deficiency anemia. In contrast, high copper uptake will be correspondingly associated with higher activity and abundance of FOXs. Increased copper levels in hepatocytes also robustly increase Cp activity and abundance in blood. Several *in vitro* studies have shown the link between copper and Cp levels and it was been demonstrated in HepG2 cells that induction of copper import into hepatocytes led to stabilization of HIF1α, which robustly increases Cp expression via direct binding to HREs on Cp promoter [79, 80]. Copper-mediated induction of Cp expression and activity has also been observed in rodent models [81]. However, the HIF1α-mediated regulatory mechanism of Cp expression could not be recapitulated in the *in vivo* animal models during iron deficiency. In humans and rodents, low copper level is associated with reduced ferroxidase activity, leading to iron-deficiency anemia. A similar phenomenon is also observed in mice with deletion of hephaestin or ceruloplasmin [35]. These observations demonstrated that copper is essential to maintain systemic iron homeostasis.

Dmt1 as an iron transporter on the apical membrane of duodenal enterocytes and it may also be involved in copper uptake [24]. Several studies have shown that Dmt1 can transport copper, although the physiological mechanism is not clear [82, 83]. Recent investigation in Belgrade rats (bearing a point mutation in Dmt1: b/b) have demonstrated that mutant Dmt1 abolishes the uptake of copper as a compensatory mechanism to increase iron absorption during iron deficiency [84]. This is supported by several key observations: 1) Dmt1 mutation abolishes the increase of liver and serum copper levels in Belgrade rats on low iron diets; 2) The documented induction of Cp

expression and activity was attenuated; 3) A decrease of copper levels in enterocytes was observed as exemplified by abolishing Mt expression and a lesser induction of Atp7a [84].

In duodenum of iron-deprived rats, a robust induction of iron-transport genes was observed, including Dmt1 and Dcytb [85]. The basolateral surface copper transporter, Atp7a is also strongly upregulated, perhaps responding to the influx of copper into enterocytes, eventually leading to increase on copper levels in liver and serum [85, 86]. The increased copper absorption is considered as a compensatory mechanism to activate the copper-mediated mechanism via increasing copper-based ferroxidase activity (Cp and Heph) to increase iron release from duodenal enterocytes. However, the regulatory mechanisms to mediate Atp7a induction during iron deficiency are still unknown. The major aim of this study was to delve into the mechanistic aspects of induction of Atp7a during iron deficiency.

First, preliminary studies demonstrated that endogenous Atp7a expression in rat intestinal epithelial (IEC-6) cells was induced by $CoCl_2$ treatment, a hypoxia mimetic and 1% oxygen exposure. A combination of Actinomycin D and $CoCl_2$ treatment suggested that the hypoxia-mediated induction is at the transcriptional level. We also identified three phylogenetically conserved hypoxia response elements (HREs; 5'-ACGTG- 3') across species in the Atp7a promoter. Thus, we hypothesized that Atp7a is transcriptionally regulated by hypoxia inducible factor (HIF2α) in IEC-6 cells.

Second, previous GeneChip studies found both iron transport-related genes and the Atp7a gene have GC-rich promoter sequences [87]. These GC-rich sequences are known to be bound by specificity protein (Sp-like factor) and furthermore, these GC-rich

sequences are located in the flanking region of HREs. Thus, we predicted that Atp7a is transcriptionally regulated by Sp1, which might be also involved in HIF2α-mediated transcriptional regulation.

Third, preliminary data demonstrated that Atp7a protein increases in IEC-6 cells with additional copper, however the mRNA level is unaffected. It was also noted that the induction of Atp7a protein level is stronger than that of mRNA [86]. Moreover, in duodenal enterocytes, studies have shown that copper is associated with Ctr1 and CCS protein stability and steady state protein levels [69, 71, 72]. Thus, we generated the hypothesis that copper stabilizes Atp7a protein in IEC-6 cells.

From these studies, three regulatory mechanisms are identified to be involved in regulation of Atp7a expression during iron deficiency: 1) HIF2α-mediated signaling pathway; 2) Sp1 involvement in HIF2α-mediated transcriptional regulation; 3) Copper-dependent stabilization of Atp7a protein. HIF2α and Sp1-mediated induction of Atp7a is at the level of transcription. Copper-dependent mechanism to increase Atp7a protein levels is at the level of post-transcriptional level, which is independent of HIF2α and Sp1-mediated induction of the Atp7a transcript. These investigations have thus identified novel regulatory mechanisms related to Atp7a expression in the mammalian intestine during iron deficiency.

CHAPTER 2
TRANSCRIPTIONAL REGULATION OF THE MENKES COPPER ATPASE (ATP7A) GENE BY HYPOXIA INDUCIBLE FACTOR (HIF2α) IN INTESTINAL EPITHELIAL CELLS

Summary

Iron homeostasis related genes (e.g. *Dmt1* and *Dcytb*) are upregulated by HIF2α during iron deficiency in the mammalian intestine. Menkes Copper ATPase (*Atp7a*) gene expression is also strongly induced in the duodenum of iron-deficient rats. The current study was thus designed to test the hypothesis that *Atp7a* is regulated by HIF2α. Rat intestinal epithelial (IEC-6) cells were utilized to model the intestinal epithelium, and $CoCl_2$ and 1% O_2 were applied to mimic hypoxia *in vitro*. Both treatments significantly increased endogenous *Atp7a* mRNA levels; mRNA induction with $CoCl_2$ treatment was blunted by a transcriptional inhibitor. The rat *Atp7a* promoter was thus cloned and studied. Various sized promoter constructs were inserted into a luciferase reporter vector and transfected into cells. A -224/+88 bp construct had full activity and was induced by $CoCl_2$; this promoter fragment was thus utilized for subsequent analyses. Interestingly, this region contains three phylogenetically conserved, putative hypoxia response elements (HRE; 5'-NCGTGN-3'). It was further noted that HIF2α over-expression caused a significant upregulation of promoter activity while HIF1α over-expression had little effect. To determine if *Atp7a* is a direct HIF target, three putative HREs were mutated individually or in combination; all were shown to be essential for transcriptional induction. Chromatin immunoprecipitation studies also demonstrated that

---

This work has been published: Am J Physiol Cell Physiol, 2011. June:**300**(6): C1298-305. Permission to reprint is not required.

HIF2α binds to the *Atp7a* promoter region. Lastly, Atp7a and HIF2α protein levels were shown to be increased by both treatments. In conclusion, the *Atp7a* gene is upregulated by direct interaction with HIF2α, demonstrating coordinate regulation with genes related to intestinal iron homeostasis.

Background

Intestinal iron absorption is the result of the coordinated action of iron import and export proteins, located on the brush-border and basolateral membranes of enterocytes, mediated by divalent metal transporter 1 (Dmt1) [24, 27] and ferroportin 1 (Fpn1) [30, 31, 49, 88], respectively. Also required are a coupled reduction of dietary ferric iron by duodenal cytochrome B (Dcytb; or other proteins) [21, 89] to the import process and an oxidation event mediated by hephaestin (Heph) [33] coupled to the export process. Absorption of iron is a regulated process, responding in the positive direction during states of iron deficiency. This enhancement of absorption is mediated partially via induction of genes related to enterocyte iron homeostasis; each of the genes mentioned above is modulated by physiological signals that increase expression during iron deprivation. Previous studies have also shown induction of copper transport related genes in the gut of iron deficient rats [85, 90], suggesting that alterations in copper homeostasis may be part of the compensatory mechanism to increase iron absorption. This is consistent with previous observations documenting increased copper in the intestinal epithelium , liver [91], and serum [92] of mammals during iron deficiency. The induction of iron and copper related genes in the intestine during iron deprivation suggests a possible common regulatory mechanism.

During iron deficiency, when levels of the liver derived, iron homeostasis regulating hormone hepcidin [93] drop precipitously, other regulatory mechanisms likely come into play. In some cases, genes are induced via interaction of intracellular iron sensing proteins (iron regulatory proteins) with stem loop structures (called iron response elements) in the 5' or 3' untranslated regions of mRNA transcripts encoding iron homeostasis related genes (*Dmt1*, *Fpn1*) [30, 42]. But interestingly, not all genes induced during iron deprivation have IREs and some genes respond in opposite directions than predicted by the location of the IRE, suggesting that other mechanisms are involved. Indeed, recent studies have shown that *Dmt1* and *Dcytb* (and possibly *Fpn1*) are upregulated during iron deficiency at the level of gene transcription via specific interaction with a hypoxia responsive *trans*-acting factor, HIF2α [45, 80]. These investigations and another recent study [94] suggested that during iron deficiency, when many tissues become hypoxic, the intestinal epithelium responds by preferential stabilization of HIF2α and that the hypoxic response drives fundamental changes in gene expression intended to overcome the iron deficient phenotype.

The current study was thus undertaken to test the hypothesis that the Menkes Copper ATPase (*Atp7a*) gene is regulated by HIF2α in the intestine of iron deficient rats. This supposition derives from the fact that *Atp7a* mRNA induction parallels that of *Dmt1* and *Dcytb*, as noted in previous publications [85]. *Atp7a* encodes an intestinal copper transporter, and its induction is particularly intriguing given the aforementioned potential link between iron and copper during conditions of low iron in the intestine. The induction of *Atp7a* was modeled in intestinal epithelial (IEC-6) cells in culture and hypoxia was applied (or mimicked). Data suggested transcriptional induction of *Atp7a* expression

during conditions that mimic hypoxia, so the promoter was cloned and studied. Extensive mechanistic studies identified specific HIF binding sites in the *Atp7a* promoter, which are shown to drive induction during hypoxia. Moreover, a critical role for Hif2α in this induction is revealed, strengthening the supposition that there is coordinate regulation of iron and copper homeostatic genes in enterocytes during iron deficiency.

Materials and Methods

Cell Culture. Rat intestinal epithelial (IEC-6) cells were obtained from American Type Culture Collection (ATCC, Manassas**,** VA) and cultured as previously described [76], essentially according to the distributor's recommendations. In some experiments, cells were grown in a hypoxia chamber (BioSpherix, Lacona, NY) with 5% CO_2 and 1% O_2 balanced with 94% N_2, according to the manufacturer's instructions, to set up low oxygen conditions.

Plasmid Construction. The rat *Atp7a* promoter was amplified by PCR with a proof reading polymerase (Invitrogen, Carlsbad, CA), utilizing a rat BAC genomic clone as a template (clone # CH230-423 C20; Children's Hospital of Oakland Research Institute, Oakland, CA). The forward primer was ~3000 bp upstream of the transcriptional start site (which was previously identified) [76] and the reverse primer was in the first exon of the gene (5' of the start codon). These primers were designed with overhanging *KpnI* (forward) and *EcoRV* (reverse) restriction enzyme cutting sites. Promoter fragments were cloned into pGL4.18 basic luciferase vector (Promega, Madison, WI). Further deletion constructs were created by PCR amplification using the 3 kb promoter fragment as a template, using the same reverse primer and different forward primers with overhanging *KpnI* restriction enzyme digestion sites. PCR products

and vector were double digested with restriction enzymes *KpnI* and *EcoRV* (Fermentas, Glen Burnie, MD) and ligations were performed with LigaFast Rapid DNA Ligation System® (Promega, Madison, WI). Deletion of putative hypoxia response elements (HRE; 5'-ACGTG-3') in the 224/+88 promoter construct was performed by amplifying the entire plasmid with AccuPrime™ Taq DNA Polymerase (Invitrogen, Carlsbad, CA) using primers flanking the putative HRE and going in opposite directions, thus deleting the HREs. For double and triple HRE deletions, plasmids having previously deleted HREs were used as templates in the same fashion. Linearized PCR products were subsequently circularized with the Quick Ligation™ Kit (New England BioLab, Ipswich, MA). All the promoter constructs were sequenced by the DNA Sequencing Core in ICBR® at the University of Florida. Sequences of each primer are shown in Table 2-1.

Transient Transfection and Luciferase Assay. IEC-6 cells were transfected in 24-well plates at ~80% confluence with 1 µg of *Atp7a* promoter construct and 150 ng pRL CMV vector (containing the Renilla luciferase reporter gene as internal control) using TurboFect® *in vitro* Transfection Reagent (Fermentas, Glen Burnie, MD) according to manufacturer's protocol. For HIF1α and HIF2α over-expression experiments, 1 µg *Atp7a* promoter construct, 1µg HIF1α or HIF2α expression vector and 150 ng pRL CMV vector were co-transfected into ~80% confluent IEC-6 cells in 24-well plates. Empty pcDNA3.1 vector was used as negative control (for the HIFs). Luciferase activity was measured using the Dual Luciferase Assay Kit® (Promega, Madison, WI) according to the manufacturer's instructions. Briefly, cells were lysed by incubating with 100 µL 1X Passive Cell Lysis Buffer for 20 minutes with gentle shaking. Cell lysates

were collected and 20 µL was used to measure Firefly and Renilla luciferase activity in a tube luminometer (CAN/CAS STD C22.2; Berthold Technologies, Oak Ridge, TN).

Total RNA Isolation and Real Time qRT-PCR. Total cellular RNA was isolated by Trizol® reagent (Invitrogen, Carlsbad, CA) according to the manufacturer's protocol. RNA concentration was measured by spectrophotometry and 1 µg RNA was reverse transcribed with iScript cDNA Synthesis kit® (BioRad, Hercules, CA) in a 20 µL reaction. After reverse transcription, the 20 µL reaction was diluted to 40 µL. 1µL was used for qRT-PCR reaction with SYBR® Green qRT-PCR master mix (BioRad), as previously described [76]. Sequences of each primer used for qRT-PCR are listed in Table 3-1.

Cytosol and Nuclear Protein Preparation and Immunoblotting. Cytosol and nuclear proteins were purified with the Nuclear Extract Kit® (Active Motif, CA) according to the manufacturer's protocol. Protein concentration was determined by BCA Protein Assay Kit® (Thermo Scientific, Rockford, IL). Cytosol or nuclear protein were resolved by 7% SDS-PAGE followed by electroblotting to a PVDF membrane which was then blocked in 5% non-fat milk. Membranes were reacted with a commercial available antibody against HIF2α (NB100-132H; Novus Biologicals, Littleton, CO) and one previously developed and characterized against Atp7a (called 54-10) [91]. The protein on the membrane was visualized by ECL and autoradiography film.

Chromatin Immunoprecipitation. Pre-confluent IEC-6 cells with or without $CoCl_2$ treatment in 10 cm cell culture dishes were crosslinked with 1X PBS containing 1% formaldehyde for 10 minutes and quenched with 2M glycine at a final concentration of 0.2M for 5 minutes at room temperature. Nuclei were isolated by using the Active Motif Kit® (Active Motif, Carlsbad, CA) and lysed with SDS lysis buffer (1% SDS, 10 mM

EDTA, 50 mM Tris-HCL pH 8.1 and protease inhibitor cocktail). Chromatin was sheered by a Bioruptor instrument (Diagenode, Sparta, NJ) following the manufacturer's instructions, using 45 cycles of one minute sonication followed by 30 seconds at 4^{o} C. The size of resulting fragments was determined by agarose gel electrophoresis. Nuclear samples were cleared by centrifugation at 16,000 x g for 30 minutes at 4^{o} C. The chromatin was subsequently immunoprecipitated with HIF2α antibody (NB100-122, Novus Biologicals, Littleton, CO) at 4° C. Protein and chromatin were reverse crosslinked with 1 M NaCl for 6 hours at 65° C following 1 hour incubation with RNase A (Fermentas) and overnight incubation with Proteinase K (Fermentas) at 37° C. Chromatin was extracted and purified with phenol/chloroform/isoamyl alcohol followed by precipitation with 100% isopropanol and glycogen. 1 µL sample was used for qRT-PCR as described above, with primers specific for *Atp7a* (covering a region containing the HREs and another upstream region with no HREs), *Dmt1* and ankyrin repeat domain protein 37 (*Ankrd37*). Phylogenetic footprinting and sequence alignments were utilized to identify regions in the rat *Dmt1* and *Ankrd37* genes that were homologous to the experimentally identified HRE containing regions in the mouse *Dmt1* [45] and human *Ankrd37* [95] genes. Amplification was also performed with the same primer sets using input DNA (i.e. before IP with the antibody). All primers are listed in Table 3-1.

Results

Regulation of Endogenous Atp7a Gene Expression by Hypoxia. In an attempt to recapitulate the induction of *Atp7a* seen in the intestinal epithelium of iron deficient rats, IEC-6 cells (which express *Atp7a*) [76] were treated with $CoCl_2$ (to mimic hypoxia) or subjected to hypoxia (1% O_2). qRT-PCR results demonstrated that endogenous *Atp7a* mRNA levels increased 1.8 and 1.6-fold following exposure to $CoCl_2$

or 1% O_2, respectively (Figure 2-1). The induction of *Atp7a* by $CoCl_2$ was abolished when cells were exposed to actinomycin D, a transcriptional inhibitor (ActD; 1µg/mg in H_2O), 1 hour prior to and during 16 hours $CoCl_2$ exposure (Figure 2-1).

Investigation of Atp7a Transcriptional Activity*.* The previously mentioned data suggested that the mechanism of *Atp7a* induction by hypoxia was transcriptional; regulation of the *Atp7a* promoter was thus investigated. The following promoter constructs were generated as described in the *Materials and Methods* section: bps -2995/ +88, -976/+88, -754/+88, -476/+88, -224/+88, -194/+88, -144/+88 and -15/+88 (all relative to the transcriptional start site). Forward primers utilized to amplify these fragments were designed from DNA regions that did not have predicted *cis*-elements. Reporter gene assays demonstrated that the activity of the longest construct (-2995/+88) had similar activity to the -224/+88 construct (Figure 2-2). The -976/+88 and -754/+88 constructs showed similar activity levels. Interestingly, the -476/+88 construct had significantly diminished activity suggesting that an inhibitory element exists in the region between bps -476 and -224; this element must be inactive or otherwise silenced by upstream elements as the -754/+88 construct retained full promoter activity. Promoter constructs with further 5' deletions had decreased activity, with the -15/+88 construct having the same background activity as the empty plasmid. As the -224/+88 construct had full activity, it was utilized for further studies.

Further data showed that the -2995/+88 (data not shown) and the -224/+88 constructs were significantly induced by $CoCl_2$ exposure (Figure 2-3; sequence indicating 5' ends of promoter constructs is shown in Figure 2-3, panel B). It was also noted that the -224/+88 construct contained 3 phylogenetically conserved, putative

hypoxia response elements (HREs; between bps -224 and -113). Additional 5' deletions were thus generated to assess the potential role of the HREs in this induction. Promoter constructs containing 5' ends from bp -224 to -160 all showed induction by $CoCl_2$ exposure while constructs ending from bp -113 to -57 were not responsive. These observations suggested that the HREs in the *Atp7a* gene may play a mechanistic role in induction by $CoCl_2$

HIFα Over-Expression and Atp7a Transcriptional Activity. Since $CoCl_2$ treatment and 1% oxygen exposure would presumably induce both HIFα isoforms, as has been described in many cell types [80, 96], and both isoforms bind to highly similar DNA sequences, it was important to determine experimentally which HIF was responsible for inducing the *Atp7a* gene. Additional experiments were thus performed in IEC-6 cells co-transfected with the -2995/+88 and -224/+88 *Atp7a* promoter/luciferase constructs and HIF1α or HIF2α expression plasmids. The Hif1α plasmid contained the human cDNA while the HIF2α plasmid contained the mouse cDNA [45]; cDNA expression was driven by the CMV promoter in the pcDNA3.1 plasmid (Invitrogen). Hif1α and Hif2α mRNA levels were significantly increased in co-transfected cells, as determined by qRT-PCR (data not shown). Results showed that HIF1α over-expression had only a minor effect on promoter activity of both constructs (Figure 2-4; 1.7- and 1.8-fold, respectively). HIF2α over-expression however resulted in a dramatic induction of promoter activity of both constructs, 5.2-fold for the -2995/+88 construct (Figure 2-4, panel A) and 4.7-fold for the -224/+88 construct (Figure 2-4, panel B; No Treatment). Further studies were performed to determine the effects of HIFα over-expression with $CoCl_2$ treatment or hypoxia (1% O_2) on *Atp7a* promoter activity. This was important as

even though there was a significant induction of *Hif1α* and *Hif2α* mRNA levels in transfected cells, it is likely that protein expression levels were not as significantly increased, as both HIFα subunits are unstable at normal oxygen tensions (21%). Studies described above were thus repeated using the -224/+88 promoter construct and $CoCl_2$ or 1% O_2. Basal promoter activity was increased 1.7 to 2.0-fold with these treatments (Figure 2-4, panel B; $CoCl_2$ pcDNA3.1 and Hypoxia pcDNA3.1). HIF1α over-expression had no additional effect on *Atp7a* promoter activity, while HIF2α over-expression resulted in a significant increase (although it was not greater than activity with HIF2α over-expression under normoxic conditions)

HIF2α Regulates Atp7a Expression by Direct Binding to cis-Elements in the Promoter. Since *Atp7a* promoter activity was induced by $CoCl_2$ treatment, hypoxia and Hif2α over-expression, the next logical step was to consider the role of the 3 putative HREs in the responsive promoter fragment. These sequences were thus deleted individually or in combination in the -224/+88 promoter construct and transfection experiments were done in IEC-6 cells. The wild type construct responded positively to HIF2α over-expression (~5-fold increase over empty vector transfected cells; Figure 2-5). Deletions of the HREs however resulted in a significant decrease in the level of induction (~2-fold), although there was no noticeable difference between individual deletions of an HRE, double deletions or deletions of all 3 HREs. Next, to prove HIF2α regulation of the *Atp7a* promoter, chromatin immunoprecipitation (ChIP) assays were performed with cross-linked, soluble chromatin isolated from $CoCl_2$ treated and non-treated IEC-6 cells. DNA fragments were found to be ~500 bp in length after the sonication protocol. qRT-PCR was subsequently performed on DNA samples pulled

down by a HIF2α specific antibody (Figure 2-6). As compared to input DNA (before pull down), there was a significant increase in the amount of DNA amplified from the $CoCl_2$ treated samples representing the region of the *Atp7a* promoter containing the HREs (Figure 2-6; Atp7a (+) HRE), while there was no amplification using primers targeting a region of the promoter upstream of the HRE region (Figure 2-6; Atp7a (-) HRE). Increased amplification was also noted from the $CoCl_2$ treated samples for two positive controls, *Dmt1* and *Ankrd37* (Figure 2-6). Previous studies demonstrated HIF2α regulation of *Dmt1* in the mammalian intestine [45, 46] and *Ankrd37* was also noted to be a HIF target (but regulated by HIF1α) [95].

Discussion

The hypothesis that common regulatory mechanisms are activated during iron deficiency stems from observations showing very similar patterns of gene expression in the intestine of iron deficient rats [85]. Several iron homeostasis related genes (e.g. *Dmt1*, *Dcytb*, *TfR1* etc.) were induced across several postnatal developmental stages, and in models of diet induced and genetic iron deficiency [97]. Genes related to copper homeostasis showed a parallel expression pattern. One particularly interesting gene, the Menkes Copper ATPase encoding an intestinal copper transporter, was induced in a strikingly similar pattern to the gene encoding the predominant iron transporter, *Dmt1* [85]. Furthermore, recent published works have demonstrated that *Dmt1* and other iron homeostasis related genes are regulated positively by HIF2α in the intestine during iron deficiency [45, 46]. This interesting observation leads to speculation that during iron deficiency, hepcidin-independent mechanisms are invoked to increase iron absorption, and that identifying additional genes regulated by this mechanism is likely to reveal novel participants in the compensatory response of the intestinal epithelium to iron

deprivation. Some of these participants may also play important, hitherto unrecognized roles in iron homeostasis as a part of normal physiology. The current study was thus undertaken to test the hypothesis that *Atp7a* is a novel HIF2α target in the intestine, which if true, would provide a mechanistic explanation for its strong induction during iron deficiency.

Atp7a is strongly expressed in IEC-6 cells [76], so this cell line was utilized as a model of the mammalian intestinal epithelium. Cells were exposed to 1% oxygen to recapitulate hypoxia which occurs in many tissues, including the intestine, during iron deficiency when hemoglobin levels are significantly reduced. Cells were also treated with $CoCl_2$, which mimics hypoxia by binding to the oxygen dependent degradation region of the Hifα subunits, which prevents oxygen from signaling their degradation [98]. Initial observations demonstrated that expression of the endogenous *Atp7a* gene was increased in response to both treatments; this induction was abrogated by a transcriptional blocker, indicating regulation at the level of transcription. The rat *Atp7a* gene promoter was thus cloned and characterized. The transcriptional start site (TSS) had been previously mapped by 5' RACE [76]; several 5' end most bases were identified suggesting alternative start sites, all within a ~30 bp region in exon 1 of the gene. Promoter constructs were generated representing almost 3000 bp 5' of the TSS, including 88 bp of the transcriptional unit covering all identified 5' end most bases (but not containing the putative start codon, which is in exon 2). Promoter constructs were transfected into IEC-6 cells, a well studied model of the intestinal epithelium.

The longest promoter construct (-2995/+88) and a shorter construct (-224/+88) both had similar reporter gene activity levels in transient transfection assays, so the

latter construct was selected for further analyses. This construct was significantly induced by $CoCl_2$ exposure; shorter deletion constructs containing 5' upstream sequence to bp -160 also responded but even shorter constructs were unresponsive. These data suggested the presence of the hypoxia responsive *cis*-elements (HREs) between bp -160 and -113. Interestingly, these putative HREs were conserved across three mammalian species (rat, mouse and human), when 1000 bp promoter sequences were used as input to run the FootPrinter web server (http://genome.cs.mcgill.ca/cgi-bin/FootPrinter3.0/FootPrinterInput2.pl). Further studies were designed to consider the role of these sequences in the induction of *Atp7a* gene expression by hypoxia.

Two HIFα subunits exist (HIF1α and HIF2α); either can heterodimerize with a binding partner (HIF1β) and transolcate to the nucleus to regulate gene transcription. This only occurs under conditions where the α subunit(s) are stabilized by hypoxia, or when cells are exposed to certain hypoxia mimics such as $CoCl_2$ or deferroxamine[46, 94]. In order to understand which HIFα subunit was important for the transcriptional induction of the *Atp7a* gene, experiments were performed to assess the effect of Hif1/2α over-expression on promoter activity. Data demonstrated that both the -2995/+88 and -224/+88 bp constructs were significantly induced by over-expression of HIF2α, while HIF1α over-expression only had a marginal effect on the activity of both constructs. Interestingly, identical studies carried out after cells were exposed to 1% oxygen or $CoCl_2$ demonstrated that there was no additional synergistic effect on promoter activity. This observation suggested that when HIF2α was over-expressed, even under conditions where it would normally be degraded (i.e. normoxia), protein levels must be sufficiently increased so as to overwhelm the degradative machinery. Both Hifα subunits

are degraded via interaction with an accessory protein, von Hippel-Lindau (VHL), that targets them for destruction in the lysosome [99, 100]. It is further speculated that hypoxia and $CoCl_2$ exposure had no additional influence on *Atp7a* promoter activity due to the fact that the HIF2α-mediated induction of *Atp7a* promoter activity was already at a predetermined maximum. It would seem logical that *Atp7a* induction would have an upper limit so as to avoid inducing copper deficiency in cells, as one important role of the *Atp7a* protein is in copper efflux.

Additional studies considered the function role of the HREs in the *Atp7a* promoter. The HIF2α over-expression system was thus utilized in co-transfection experiments using the wild type -224/+88 bp promoter construct and additional constructs with specific deletions of the putative HREs. Results showed that deletion of individual HREs or combinatorial deletions in two or three of the HREs all had the effect of minimizing the induction of promoter activity to around 2-fold (as compared to a >5-fold induction of the wild type construct). Surprisingly, none of the deletions, including deletions in all three sites in combination, resulted in complete loss of induction by HIF2α. This observation suggests that another *trans*-acting factor(s) is important in the response of the *Atp7a* gene to hypoxia. We previously speculated that Sp1 or a related G/C-rich binding *trans*-acting factor could play a role in the genetic response of the intestinal epithelium to iron deprivation [94, 101]. Interestingly, the *Atp7a* promoter contains a phylogenetically conserved Sp1 binding site and it was noted that mutation of this site in the -224/+88 bp promoter construct led to a >80% decrease in promoter activity (data not shown). The role of this *cis*-element in controlling *Atp7a* gene transcription will be the subject of further investigations.

Although the HRE deletion studies described above strongly suggested that the *Atp7a* gene was a direct HIF target, further studies were necessary to independently confirm this observation. ChIP assays were thus performed utilizing a well characterized HIF2α antibody and cross-linked DNA/protein isolated from control and $CoCl_2$ treated cells. Results showed a substantial increase in *Atp7a* promoter sequences containing the HREs with $CoCl_2$ exposure, while an upstream promoter region that did not contain the HREs was not detected in either condition. *Dmt1* and *Ankrd37*, two known hypoxia responsive genes, were utilized as positive controls. These data demonstrate that *Atp7a* is indeed a direct HIF2α target in the intestinal epithelium.

The last set of experiments was designed to address the issue of the potential physiological significance of the results reported in this manuscript. If the induction of *Atp7a* gene expression by HIF2α is of functional consequence, it would be predicted that 1) increased *Atp7a* mRNA expression would translate into increased protein levels, and 2) that the HIF2α protein would be stabilized in IEC-6 cells during hypoxia also resulting in increased protein levels. Well established Atp7a [76, 86] and HIF2α antibodies were thus utilized to perform immunoblots of proteins isolated from control, $CoCl_2$ treated and hypoxia exposed cells. In both cases (hypoxia and $CoCl_2$), Atp7a and HIF2α protein levels increased 4-6-fold as compared to untreated cells grown under normoxic conditions (Figure 3-7). These observations suggest that the induction of these genes during hypoxia is indeed of physiological relevance.

It is intriguing to note coordinate regulation of *Dmt1*, *Dcytb*, *Fpn1* and *Atp7a* gene transcription by HIF2α in intestinal epithelial cells, representing iron and copper homeostasis related genes. It has been previously suggested that alterations in copper

levels during iron deficiency may be part of the compensatory physiological response to iron deprivation [91]. Induction of *Atp7a* under these conditions, by a conserved regulatory mechanism of proven significance provides impetus for further consideration of this potential role for copper. As copper increases in the intestinal epithelium during iron deficiency and metallothionien is induced[68], it is tempting to speculate *Atp7a* induction could play a role in cellular physiology of enterocytes. There is a documented increase in the production of reactive oxygen species (ROS) in mitochondria with $CoCl_2$ exposure and hypoxia [102, 103], and copper may contribute to the production of ROS [104]. It is thus possible that Atp7a may play an essential role to protect cells from the enhancement in membrane lipid peroxidation, DNA damage and protein oxidation by ROS in the setting of iron deprivation when copper levels increase. This would be mediated by the copper efflux role for Atp7a in intestinal epithelial cells, which could partially mitigate ROS generation.

Table 2-1. Primer List

Construct	Primer Sequence
-2995/+88 Fwd	5' -AATAGGTACCCTGGCTGTCC TGAAACTC- 3'
-976/+88 Fwd	5' -AGCAGGTACCAGGGATGGAGTTCAGGTC- 3'
-754/+88 Fwd	5' -AGAGCGGTACCACGAGTAGGTAGTGCC TTG- 3'
-476/+88 Fwd	5' -ACCAGGTACCGCAACAAACCACGATGT- 3'
-224/+88 Fwd	5' -TATAGGTACCCACCTTGGCCGAGGATG C- 3'
-194/+88 Fwd	5' -AAAAGGTACCAGGGGGCGCACGGAG- 3'
-182/+88 Fwd	5' -AAAAGGTACCGGAGCTTTGGGCG- 3’
-160/+88 Fwd	5' -AACGGGTACCTTTCACGTGACGTGG- 3'
-144/+88 Fwd	5' -AAAGGTACCATTTCCCTAGTCGGCCCAG- 3'
-113/+88 Fwd	5' -AGTAGGTACCCTGGCATCACCCGGAG- 3'
-88/+88 Fwd	5' -ATTAGGTACCTCAGAGGCGGGCGGGGCGAA- 3'
-57/+88 Fwd	5' -ATTAGGTACCTGGGGAGGTTGGGGCT- 3'
-15/+88 Fwd	5' -AAAAGGTACCTCCGCCTGCGCCTAGACTC- 3'
Rev	5' -ATTAGATATCCAGGGCTGGGGTTCGAGC- 3'
ΔHRE 1 Fwd	5’-CACCAGGGGGCGCACG-3’
ΔHRE 1 Rev	5’-CATGCATCCTCGGCCAAGG-3’
ΔHRE 2 Fwd	5’-ACGTGGACCATTTCCCTAGTCGG-3’
ΔHRE 2 Rev	5’-TGAAAGGGAGCGCGCG-3’
ΔHRE 3 Fwd	5’-GACCATTTCCCTAGTCGGCCC-3’
ΔHRE 3 Rev	5’-TCACGTGAAAGGGAGCGCG-3’
Primer Name	qRT-PCR
18S Fwd	5’-TCCAAGGAAGGCAGCAGGC-3’
18S Rev	5’-TACCTGGTTGATCCTGCCA-3’
Atp7a Comm Fwd	5’-TGAACAGTCATCACCTTCATCGTC-3’
Atp7a Comm Rev	5’-TGCATCTTGTTGGACTCCTGAAAG-3’
Primer Name	ChIP Assay
Atp7a Fwd	5’-TGCTAGGGCCTAACCCACCTTG-3’
Atp7a Rev	5’-AAGCTGGGCCGACTAGGGAAAT-3’
Ankrd37 Fwd	5’- CTTGCAGACAGAAGCCCCAGTACA-3’
Ankrd37 Rev	5’-GGTTGATATCCTGGCCTTTGAGCT-3’
Dmt1 Fwd	5’-CTCTGCTTTGAAGTCTCCTAGTCC-3’
Dmt1 Rev	5’-TGAGATTTCATTTATGTGCCATTC-3’
Negative Control Fwd	5’-AGCCTGGCTTTGATGGATGATTTT-3’
Negative Control Rev	5’-TTTAGTCACCTCCCAACTCCAGGAAT-3’

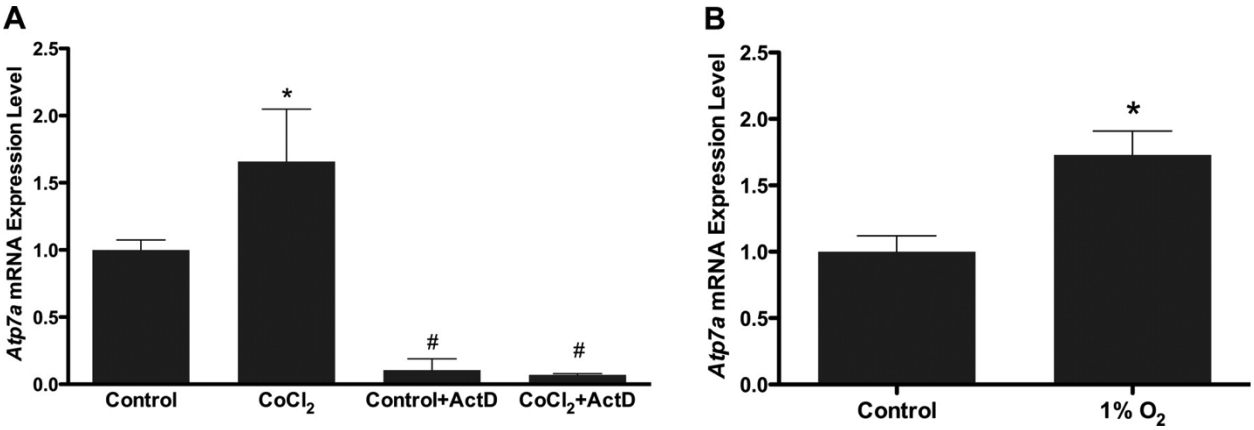

Figure 2-1. Real-time quantitative RT-PCR (qRT-PCR) analysis of Atp7a mRNA expression in rat intestinal epithelial (IEC-6) cells. Total RNA was extracted from IEC-6 cells that were treated with $CoCl_2$ (A) or cultured in 1% O_2 (B). Atp7aexpression was normalized to 18S. Similar experiments were performed with actinomycin D (ActD; 1 µg/mL) pretreatment 1 h before and during $CoCl_2$ treatment (A). Each bar represents the mean value ± SD. *P < 0.05, #P < 0.05, as compared with control, unpaired Student's t-test; n = 5.

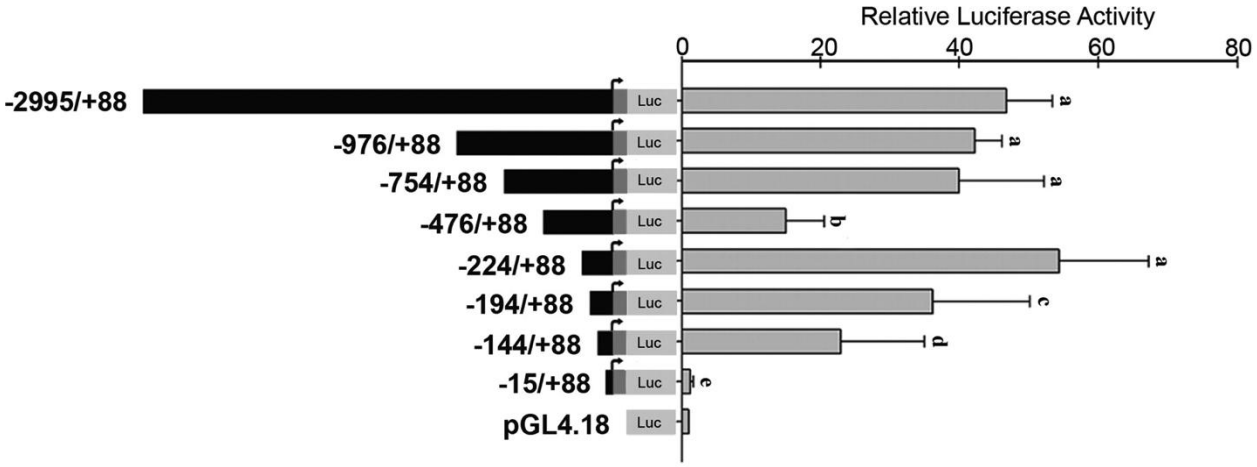

Figure 2-2. Analysis of rat Atp7a promoter transcriptional activity. Firefly luciferase (Luc) reporter vectors with various length Atp7a promoter fragments were constructed as described in MATERIALS AND METHODS. Each construct was transiently transfected into IEC-6 cells that were preseeded into 24-well plates at ~80% confluency. pGL4.18 empty vector (1 µg) was used as a control. Twenty-four hours after transfection, firefly and Renilla luciferase activity was measured by a Dual Luciferase Assay System; firefly luciferase activity was normalized by Renilla luciferase activity. Each bar represents the mean value ± SD. Different letters next to bars indicate statistical significance ($P < 0.05$), between constructs, unpaired Student's t-test; n = 3.

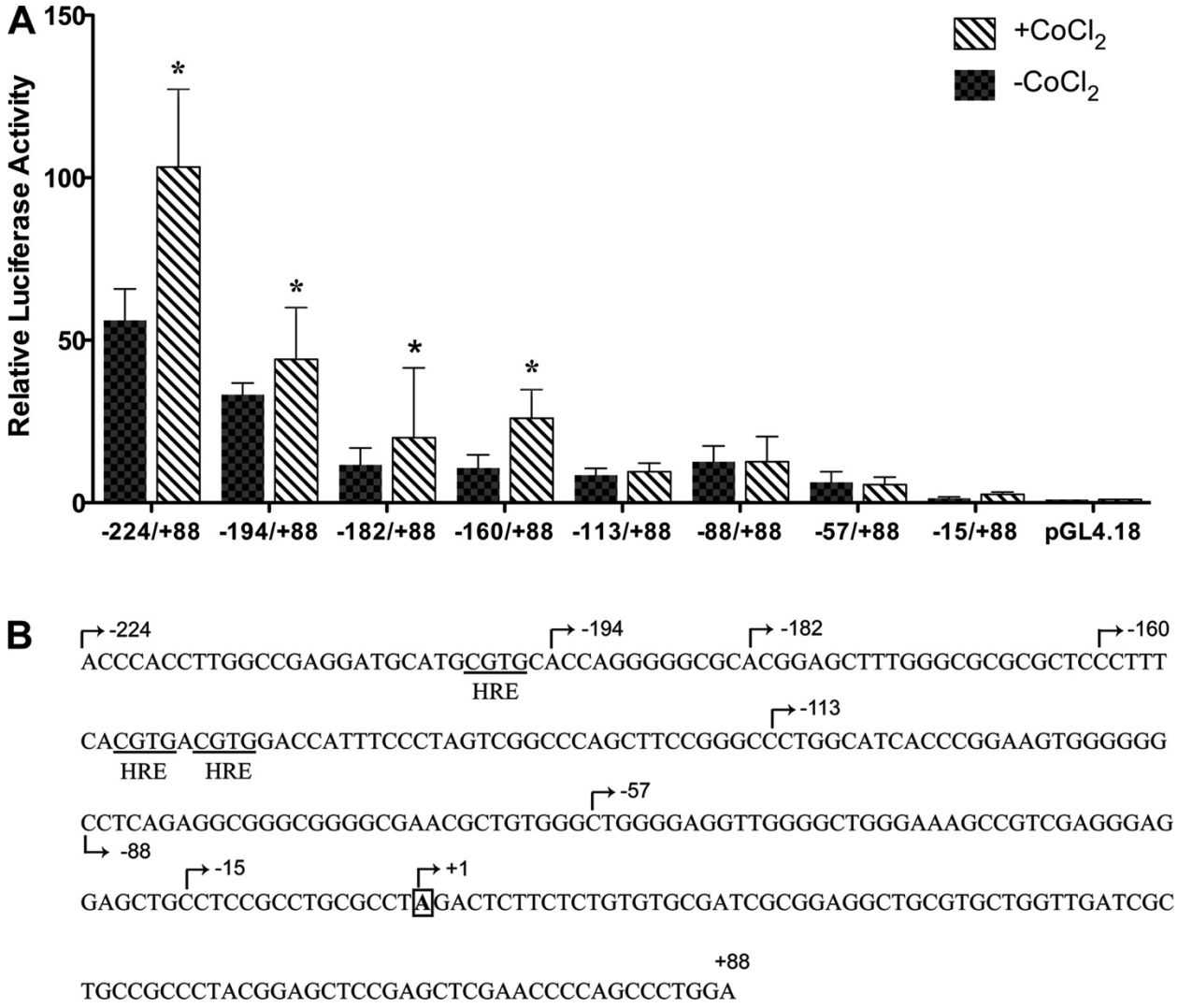

Figure 2-3. Deletion analysis of the −224/+88 bp construct containing putative hypoxia response elements (HREs). A: further deletions of −224/+88 promoter construct were made as described in MATERIALS AND METHODS. All of the constructs were transfected into preconfluent IEC-6 cells, followed by CoCl2 treatment for 16 h (200 μM). Each bar represents the mean value ± SD. *P < 0.05, +$CoCl_2$ vs. −$CoCl_2$ for each construct, unpaired Student's t-test; n = 3. B: sequence of the Atp7a promoter from −224 bp to +88 bp is shown. Putative HREs are indicated, and the 5′-endmost base of the different deletion constructs is shown.

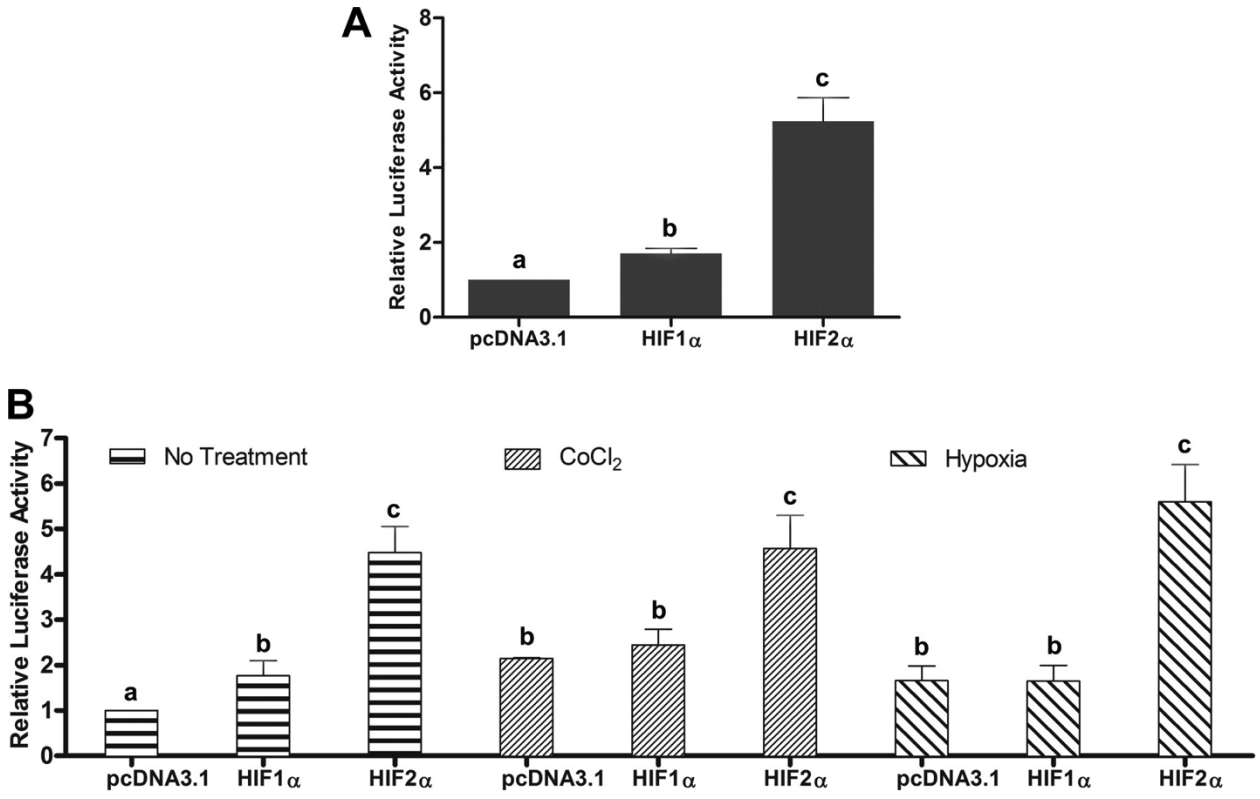

Figure 2-4. Cotransfection of −2,995/+88 and −224/+88 bp constructs with hypoxia-inducible factor (HIF) expression vectors. A: the −2,995/+88 promoter construct was cotransfected with HIF1α or HIF2α expression plasmid, and luciferase activity was determined. B: the −224/+88 promoter construct was cotransfected with HIF1α or HIF2α expression plasmids. Twenty-four hours after transfection, cells were treated with $CoCl_2$ (200 μM) or cultured in 1% O_2. Each bar represents the mean value ± SD. In A and B, different letters above bars indicate statistical significance ($P < 0.05$), between transfection or treatment conditions, unpaired Student's t-test; n = 3.

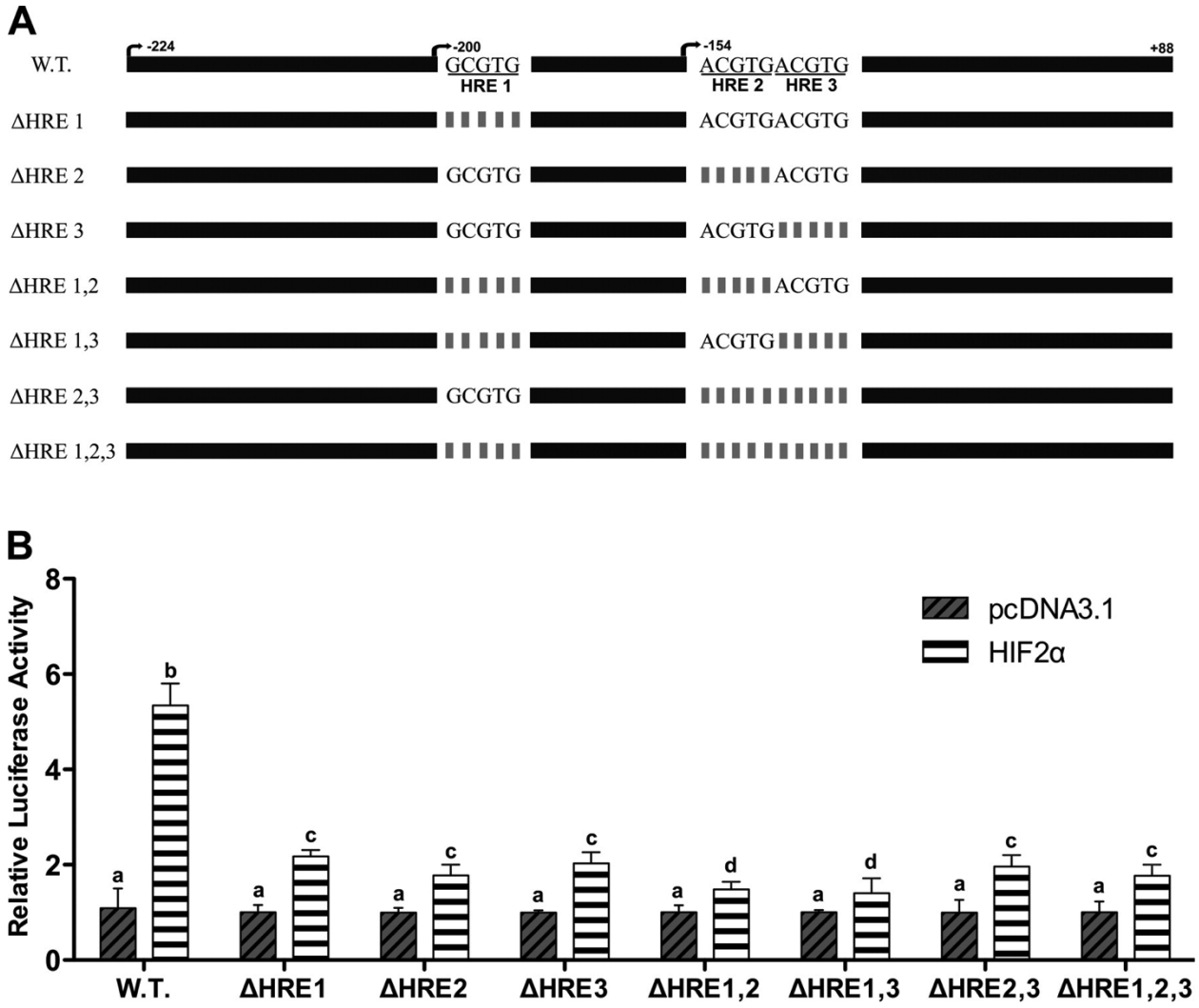

Figure 2-5. Deletion analysis of the putative HREs. HREs in the −224/+88 promoter construct were individually deleted or deleted in combination. Wild-type (WT) or deleted Atp7apromoter constructs were cotransfected with HIF2α expression plasmid (or empty vector) into IEC-6 cells. Constructs are shown schematically in A, while luciferase assay results are shown in B. Each bar represents the mean value ± SD. Different letters above bars indicate statistical significance ($P < 0.05$), unpaired Student's t-test; n = 3.

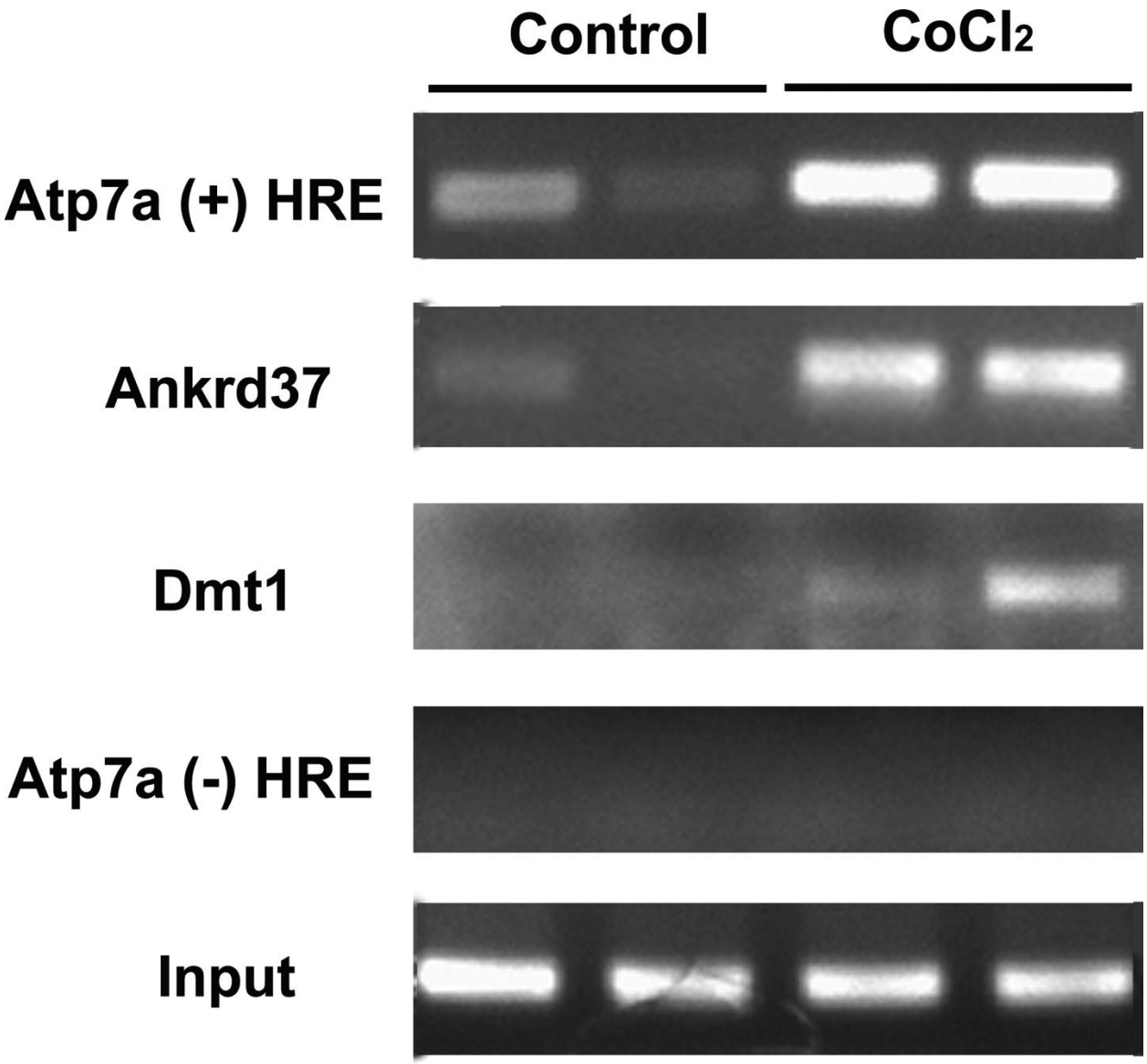

Figure 2-6. Chromatin immunoprecipitation (ChIP) analysis of HIF2α binding to putative HREs in the rat Atp7apromoter. DNA fragments containing cross-linked nuclear proteins were pulled down by HIF2α antibody from IEC-6 cell nuclear extracts prepared from control (untreated) or $CoCl_2$-treated cells. Primers were used to amplify the region of Atp7acontaining the HREs [Atp7a (+) HRE] or an upstream region not containing HREs [Atp7a (−) HRE]. Divalent metal transporter 1 (Dmt1) and ankyrin repeat domain protein 37 (Ankrd37) were utilized as positive controls. Input indicates amplification from DNA before pull down with the antibody using Atp7a primers covering the putative HREs. Input samples were also run for all other primer sets, and identical results were obtained (data not shown). Data from two independent experiments are shown.

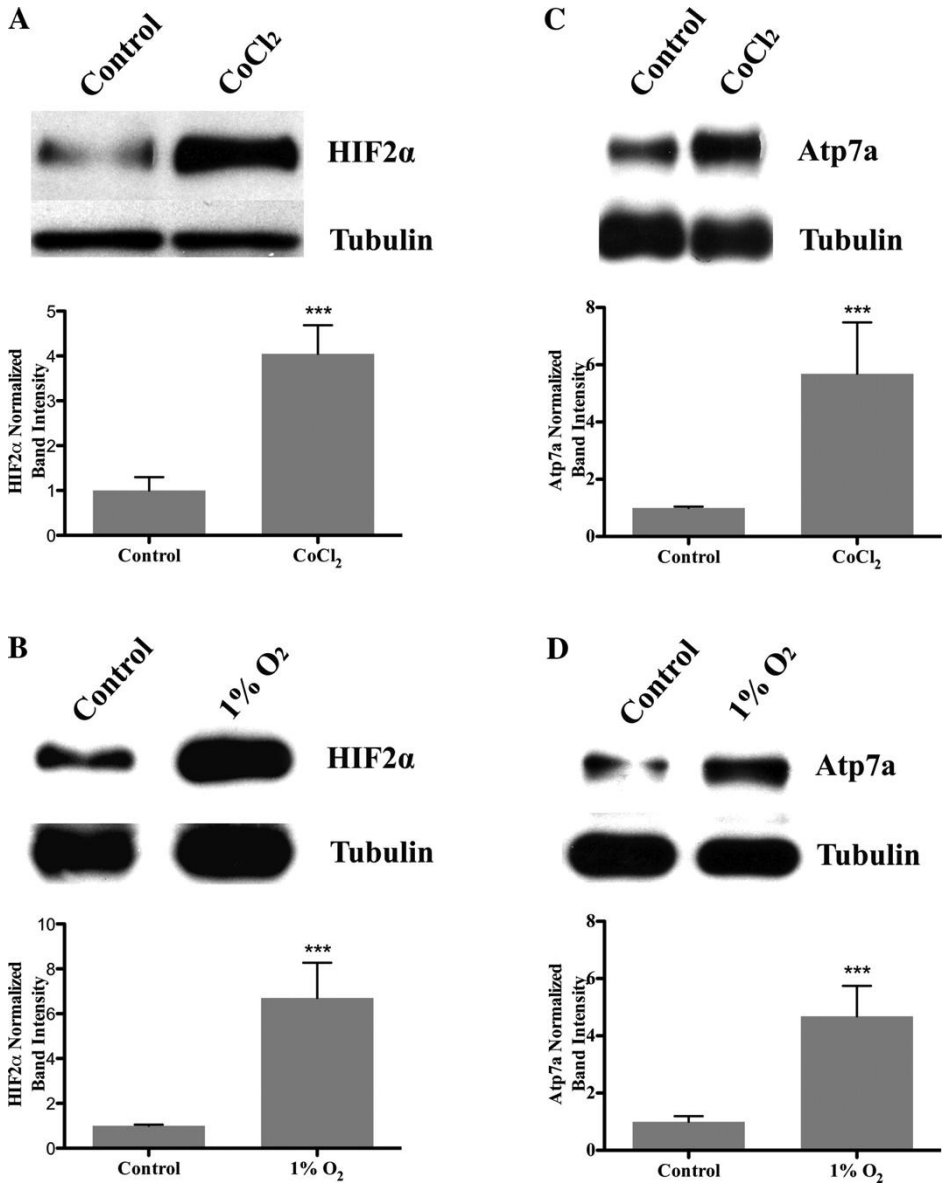

Figure 2-7. Immunoblot analysis of HIF2α (A and B) and Atp7a (C and D) protein expression in hypoxia and $CoCl_2$-treated IEC-6 cells**.** Eighty percent preconfluent IEC-6 cells were treated with $CoCl_2$ (200 μM), cultured in 1% O_2, or cultured in normoxia (21% O_2; control). Nuclear (for HIF2α) and cytosolic (including membrane for Atp7a) proteins were extracted and resolved by 7% SDS-PAGE, and blots were reacted with specific antibodies against these proteins. Images shown are from one representative experiment. Quantitative data from three independent experiments are shown below each representative blot. ***$P < 0.05$.

CHAPTER 3
SP1 AND HIF2A MEDIATE TRANSCRIPTIONAL INDUCTION OF *ATP7A* DURING HYPOXIA

Summary

Genes with GC-rich promoters were preferentially induced in the rat duodenal epithelium during iron deficiency, including those encoding iron (e.g. *Dmt1*, and *Dcytb*) and copper (e.g. *Atp7a*, and *Mt1*) homeostasis-related genes. We previously demonstrated that *Atp7a* was co-regulated with iron transport-related genes by HIF2α. In this study, we sought to test the role of Sp1 in transcriptional regulation of *Atp7a*, as phylogenetic footprinting revealed conserved GC-rich sequences 5' of the transcriptional start site. Initial studies in IEC-6 cells showed that an Sp1 inhibitor (mithramycin) reduced expression of endogenous Atp7a and iron transport-related genes, and also blocked their induction by the $CoCl_2$ mimetic hypoxia. Moreover, overexpression of Sp1 increased endogenous Atp7a mRNA and protein expression, and also *Atp7a, Dmt1,* and *Dcytb* promoter activity. Site-directed mutagenesis of a basal *Atp7a* promoter construct revealed several functional Sp1 binding sites, which were necessary for HIF2α-mediated induction of promoter activity. Furthermore, chromatin immunoprecipitation (ChIP) assays confirmed that Sp1 specifically interacts with the *Atp7a* promoter and this interaction was blocked by mithramycin treatment. Furthermore, to determine the physiologic relevance of these observations, studies were performed in a rat model of iron deficiency. ChIP experiments confirmed that the *Atp7a* gene in duodenal enterocytes is indeed a direct Sp1 and HIF2α target. This investigation has thus revealed a novel aspect of hypoxia-related gene expression in the mammalian intestine in which Sp1 is necessary for the HIF-mediated induction of

gene expression during iron deficiency. This regulatory mechanism may have broader implications for understanding the genetic response to intestinal hypoxia.

Background

Iron is essential for life, as it plays important roles in biological systems; it is involved in such processes as electron transport, enzyme activity, oxygen transport, and gene regulation [1]. Systemic iron levels are maintained by intestinal absorption, which is precisely controlled, as there is no regulated excretory mechanism in mammals. Thus, precise and sophisticated regulatory mechanisms have evolved to control iron absorption in duodenal enterocytes to maintain appropriate cellular iron levels and to avoid iron overload [14]. The absorption process is regulated coordinately via signals derived from different organs involved in iron transport, utilization, and storage. Intestinal iron absorption is mediated first via reduction of dietary ferric iron by duodenal cytochrome c reductase (Dcytb) [21, 23, 105] and transport of ferrous iron by divalent metal transporter (Dmt1) [24, 27, 42], located on the apical surface of enterocytes. Newly absorbed iron is exported by ferroportin 1 (Fpn1) [30, 31, 49] on the basolateral side of enterocytes, followed by oxidization by hephaestin (Heph) [33] expressed in enterocytes and/or ceruloplasmin (Cp) [106, 107] synthesized and released from hepatocytes into blood.

Iron absorption is induced during iron deprivation reflected by the increased expression of iron transport-related genes including Dmt1, Dcytb, and Fpn1 in duodenal enterocytes [85]. Studies found that the copper transporter (Menkes copper ATPase; Atp7a) located on the basolateral surface of enterocytes was also upregulated during iron deficiency, and increased copper concentrations were noted in enterocytes, liver, and serum of iron-deficient rats [85, 86]. In enterocytes, Atp7a expression paralleled

that of iron transport-related genes, suggesting that a copper-dependent mechanism was activated in response to low iron levels to increase iron absorption via increased activity of copper-dependent enzymes (Heph and Cp) [81].

Low body iron stores activate intestinal iron absorption via physiological signals to increase iron uptake from dietary sources. In response to low tissue iron levels, some iron transport-related genes are regulated via a post-transcriptional mechanism. Iron response elements (IREs), which are short, conserved stem-loops, are found in either 5'- (TfR1 [108], Fpn1 [31]) or 3'- (Dmt1 [42], ferritin [109]) of untranslated regions (UTRs) of these mRNA molecules. IREs are bound by the iron regulatory proteins (IRPs) in the cytosol of cells. IRP binding to IREs increases mRNA stability (3' end binding) or blocks translation (5' end binding) of target genes [41, 43]. In the Dmt1 mRNA with IREs in 3'-UTR, IRP binding increases transcript stability, leading to accumulation of Dmt1 protein on the apical side of enterocytes to increase iron uptake during iron deficiency. Other genes, including Fpn1 and TfR1, have IREs in the 5'-UTR where IRP binding blocks translation. Although some key iron-related genes are regulated by the IRP/IRE-mediated regulatory mechanism, other genes related to iron homeostasis do not have IREs (e.g. Dcytb, hephaestin). Moreover, the downregulation of Fpn1 via the IRP/IRE-mediated post-transcriptional mechanism conflicts with the overall concept to increase systemic iron levels through duodenal enterocytes during iron deficiency. Thus, there must be some additional regulatory mechanisms involved in maintaining systemic iron homeostasis.

Resent studies have demonstrated that low body iron stores (and hemoglobin in red blood cells) result in systemic hypoxia, leading to stabilization of hypoxia-inducible

trans-acting factors (the HIFα-subunits: either HIF1α or HIF2α). HIFα-subunits translocate to the nucleus and dimerize with a β-subunit to form the functional HIF-complex, which binds to HREs on gene promoters with additional recruitment of co-activators (such as p300 and C/EBPα) to regulate gene expression [110-112]. Intestinal hypoxia stabilizes HIF2α in duodenal enterocytes, where iron transport-related genes are upregulated by HIF2α via direct binding to HREs on promoters to increase systemic iron levels [45-47]. In previous work, we reported that Atp7a is also upregulated by HIF2α in IEC-6 cells via $CoCl_2$ mimetic hypoxia [113]. It was speculated that the HIF2α-mediated upregulation of Atp7a in enterocytes during iron deficiency to increase body copper concentration to induce the copper-dependent ferroxidase activity as a secondary mechanism to increase iron absorption during low body iron storage.

In addition to HREs found on the promoter of iron transport genes (e.g. *Dmt1*, *Dcyt B* and *Fpn1*) for a HIF2α-mediated regulatory mechanism, it was noted that these genes that were highly induced in rat intestinal epithelium during iron deficiency also contain evolutionary conserved GC-rich sequences [87]. The *Atp7a* gene was strongly induced during iron deficiency and also co-regulated with iron transport-related genes by HIF2α. GeneChip analysis identified that *Atp7a* gene has GC-rich sequences promoter, especially in the proximal region to the transcriptional initiation sites, where HREs were found. Thus, in the current study, we sought to test the role of Sp1 involved in transcriptional regulation of Atp7a, especially its involvement in HIF2α-mediated induction of Atp7a. This hypothesis is derived from the observation that gene promoters enrich of GC-rich sequences. Atp7a encodes a copper transporter protein, which is located on basolateral surface of enterocytes. Its induction during iron deficiency

provides a potential interface between iron and copper. An initial observation made in IEC-6 cells showed that an Sp1 inhibitor (mithramycin) reduced expression of endogenous Atp7a and iron transport-related genes, and also blocked their induction by the $CoCl_2$ mimetic hypoxia. Moreover, Sp1 overexpression robustly increased Atp7a mRNA and protein expression, and also Atp7a, Dmt1, and Dcytb promoter activity in IEC-6 cells. Phylogenetic foodprinting indicated that several evolutionally conserved putative Sp1-binding sites were found on Atp7a promoter in rats and mice, and Chromosome Immunoprecipitation (ChIP) assay suggested that the induction of Atp7a was mediated via a direct binding of Sp1 on the promoter and mithramycin decreased the Sp1 binding to promoter. Furthermore, to determine the physiological relevance of these observations, the in vivo rat model on iron-deficient diet was used. ChIP experiment confirmed both HIF2α and Sp1 to promoter. This study suggested a coordinate interaction between Sp1 and HIFα exits and Sp1 is required for HIF2α-mediated induction of gene expression to increase iron absorption during iron deficiency.

Methods

Cell Culture: Rat intestinal epithelial (IEC-6) cells were obtained from the American Type Culture Collection (ATCC; Manassas, VA) and cultured according to the manufacturer's instructions and as described previously [113, 114]. For hypoxia experiments, 85% pre-confluent IEC-6 cells were cultured in a hypoxia chamber with 1% O_2 and 5% CO_2 (with the balance being nitrogen). To mimic hypoxia, 200 μM $CoCl_2$ was used to treat IEC-6 cells at 85% confluence for 60 hours. To interrupt Sp1 binding, IEC-6 cells were treated with mithramycin (a specific Sp1 inhibitor) at various concentrations at 7 days post-confluence for 24 hours.

Animals and Diets: Weanling Sprague-Dawley rats (male) were purchased from Harlan, raised in overhanging, wire mesh-bottomed cages under 12-hour light/dark cycle and sacrificed at 10 am. A total of 12 rats were used for this study. Rats were split into two diets group and fed AIN-93G based diets (Dyets, Bethlehem, PA), including a control diet (Ctrl) containing 198 ppm iron and an iron-deficient diet (FeD) containing 3 ppm iron for five weeks. The diets were otherwise identical. Animal body weights was measured weekly. At the end of the feeding regime, each rat was anesthetized by CO_2 exposure and killed by cervical dislocation. Blood was collected by cardiac puncture and transferred to a 1 mL tube. Hemoglobin and hematocrit were measured by routine methods. The duodenum was excised and inverted on a wooden stick, followed with isolating enterocytes using well-established, previously published methods [81, 84]. Duodenal enterocytes were used for mRNA isolation, western blot analysis, and chromatin immunoprecipitation experiments, as described in *Methods*. All animal studies were approved by Institutional Animal Care and Use Committee (IACUC) at the University of Florida.

RNA Isolation and Real-Time Quantitative RT-PCR: Total RNA was isolated from IEC-6 cells or duodenal enterocytes by TRIzol® (Life Technologies, Grand Island, NY), according to the manufacturer's instructions and as described before [113]. RNA concentration was measured by spectrophotometery, and 1 µg total RNA was reverse transcribed using the iScript™ cDNA Synthesis Kit (Bio-Rad, Hercules, CA) in a 20 µL reaction. After reverse transcription, the 20 µL reaction was diluted to 120 µL with nuclease-free water, and 3 µL was utilized for qRT-PCR reactions with SYBR® Green PCR Master Mix (Bio-Rad). Primers were designed to span large introns to avoid

amplification from genomic DNA. Furthermore, standard curve reactions were run in pilot experiments to validate each primer pair; linear amplification was documented over a range of template concentrations for each primer set prior to experiments being performed. Expression of experimental genes was normalized to the expression of 18S rRNA. Primer sequences are listed in the Supplementary Table.

Plasmid Construction: The rat Sp1 open reading frame (ORF) was cloned by PCR from cDNA derived from IEC-6 cells using Phusion High Fidelity DNA Polymerase® (Fermentas, Waltham, MA). The forward primer contained the translational start codon and the reverse primer ended just at 5' of the translation stop codon. Primers were designed with overhanging Kpn I (Forward) and EcoR V (Reverse) restriction enzyme cutting sites. PCR-amplified Sp1 ORF and pcDNA 3.1 vector were double digested with Kpn I and EcoR V, followed by column purification. Sp1 ORF was sub-cloned into double digested pcDNA 3.1 with LigaFast® Rapid DNA Ligation System (Promega). An HA-tag was inserted onto the 3' end of Sp1 ORF by PCR amplifying the entire pcDNA-Sp1 plasmid with primers containing the HA sequence. Primers were designed with the forward primer at the end of Sp1 ORF without a stop codon, and reverse primer at the EcoR V site on the pcDNA 3.1 vector. Each primer contained half of the HA-tag sequence and the 5'-end of each primer was phosphorylated.

Atp7a promoter constructs with mutations in putative Sp1-binding sites were prepared by PCR-amplifying the entire wild type (WT) -224/+88 bp promoter construct with QuickChange® Lightning Site-Directed Mutagenesis Kit (Agilent Technologies, Santa Clara, CA) using primers with mutations in putative Sp1-binding sites, going in opposite directions. PCR products were digested with Dpn I restriction enzyme (Agilent

Technologies) to remove the template DNA. All DNa constructs were sequenced by the DNA Sequencing Core in ICBR® at the University of Florida to confirm that amplicons did not contain mutations. Primer sequences are listed in Supplementary Table 3-1.

Transfection and Luciferase Assay: Atp7a WT or mutated promoter constructs (1 μg) were transiently transfected to IEC-6 cells at ~60% confluence and cultured in 24-well plates. For Sp1 and HIF2α overexpression experiments, 1 μg of Atp7a promoter construct (WT or mutated) was co-transfected with 1 μg of either Sp1 or HIF2α overexpression vector. pRL CMV plasmid expressing Renilla luciferase was used to normalize expression of firefly luciferase driven by experimental promoters. 36 hours after transfection, luciferase activity was measured with the Dual-Luciferase® Reporter Assay System (Promega, Madison, WI) according to the manufacturer's instructions.

Stable Sp1 Overexpression: IEC-6 cells in 6-well plates were transfected with pcDNA 3.1 (empty vector) or pcDNA-Sp1-HA vector with TurboFect® *in vitro* Transfection Kit (Fermentas). 60 hours after transfection, IEC-6 cells were treated with G418 (at a predetermined concentration) to kill non-transfected cells, allowing transfected cells expressing the Neomycin gene in pcDNA 3.1 or pcDNA-Sp1-HA vectors to survive. The selected IEC-6 cells with stable expression of Sp1 were used to analyze Atp7a and Sp1 mRNA expression using qRT-PCR and protein expression by western blotting.

Protein Isolation and Western Blot Analysis: Total cytosolic and nuclear protein was isolated from IEC-6 cells cultured in 10 cm cell culture dishes as described previously [114]. Briefly, cells were washed 3 times with ice-cold PBS (pH 7.4) and harvested with a cell scraper. Cells were lysed using a hypotonic buffer (Active Motif;

Carlsbad, CA) and a tissue homogenizer and membrane-bound proteins were solubilized with NP-50 (0.05%), followed by centrifuging at 16000 rpm for 1 minute. The nuclear pellet was resuspended with nuclear lysis buffer (Piercenet, Rockland, IL), and incubated on ice for 30 minutes, followed by 30 seconds of vortexing every ten minutes. Nuclear lysate was collected by centrifugation at 16000 rpm in a microcentrifuge for 15 minutes, and the supernatant was collected. Cytosolic and nuclear protein concentrations were determined with BCA Protein Assay (Piercenet, Rockford, IL). 30 µg cytosolic and 50 µg nuclear proteins were resolved on 7.5% SDS-PAGE gels, followed with transfer to PVDF membranes. The membrane was blocked with 5% non-fat milk and then incubated with anti-Atp7a (54-10 as characterized before), anti-Sp1 (Millipore, Temecula, CA) or and anti-phophorylated-Sp1 (Abcam, Cambridge, MA) primary antibodies followed by an anti-rabbit secondary antibody. Antibody binding was visualized using home-made ECL reagent as described before [81] followed by exposure to X-ray film. For some experiments, protein expression was normalized to the total proteins on stained blots. Protein expression was normalized to total Sp1 for the phosphorylation of Sp1.

Chromatin Immunoprecipitation (ChIP) Assay: Chromatin Immunoprecipitation (ChIP) assay was performed as described and published before [113]. Briefly, IEC-6 cells or rat duodenal enterocytes were cross-linked with 1.1% chloroform for 10 minutes, followed with quenching with 0.3 M glycine. IEC-6 cells or enterocytes were lysed with hypotonic buffer (Active Motif) and homogenized. Nuclei were collected and resuspended in nuclear lysis buffer, followed by sonication with a BioRuptor for 30 cycles with 30 seconds on and 30 seconds off. The target DNA with

bound protein was pulled down with Sp1 or HIF2α antibody. DNA samples were analyzed by PCR with primer sets listed in Supplementary Table.

Statistical Analysis: ANOVA (Tukey: compared all pairs of columns) and paired student t-test (Graphpad, La Jolla, CA) were used to statistically compare data across groups. $p<0.05$ was considered statistically significant.

Results

Mithramycin Selectively Inhibits Sp1-Mediated Transcriptional Regulation: Endogenous Atp7a expression in 7 days post-confluent IEC-6 cells was analyzed by qRT-PCR with mithramycin for 24 hours treatment at various concentrations. Concentrations of mithramycin from 100-1000 nM did not cause significant cellular stress, as determined by microscopic observation. Mithramycin at 100 nM started to reduce Atp7a mRNA expression ~50% in IEC-6 cells. Higher concentrations led to further reduction of Atp7a expression (e.g. 500 nM caused >70% reduction). Concentrations between 700 and 1000 nM did not cause further reductions in Atp7a mRNA level (Figure 3-1A). The iron transport-related genes including Dmt1, Dcytb, and Fpn1 also have GC-rich promoter sequences, as shown by previous microarray studies [87]. The mRNA levels of these genes also decreased as mithramycin concentration increased (Figure 3-1B, C and D). Ankyrin repeat domain 37 (Ankrd37), which also has a GC-rich promoter expression and is a known HIF target [95], also showed a decreasing expression pattern with mithramycin treatment (Figure 3-1E). HIF2α and Sp1 were selected as positive control genes, as it was reported that Sp1 regulates both at the mRNA level via direct DNA binding (Figure 3-1F and G). Sp6 and TfR were selected as negative control (Figure 3-1H and I).

Selective Inhibition of Sp1 Blocked Hypoxia-Mediated Induction: Iron transport-related genes including *Dmt1*, *Dcytb* and *Fpn1* are upregulated by HIF2α in duodenal enterocytes during iron deficiency. In a previous study, we proved that Atp7a was upregulated by the hypoxia mimic $CoCl_2$ via HIF2α binding to HREs on the promoter [113]. In IEC-6 cells, the combination of $CoCl_2$ and mithramycin was utilized to access the role of Sp1 in HIF2α-mediated induction of endogenous Atp7a expression. 7 days post-confluent IEC-6 cells were treated with $CoCl_2$ for 60 hours, as described in a previous study [113]. 36 hours after $CoCl_2$ treatment, 500 nM mithramycin was added to cells with and without $CoCl_2$ treatment. 24 hours later, mRNA expression levels were analyzed by qRT-PCR. $CoCl_2$ robustly increased Atp7a, Dmt1, Dcytb, and Fpn1 mRNA expression levels, and mithramycin treatment led to a reduction in transcript levels, consistent with observations shown in Figure 3-1. For the combination of $CoCl_2$ and mithramycin treatment, HIF2α-mediated induction of Atp7a and iron transport genes was blocked by mithramycin treatment, possibly via the interruption of Sp1 binding to the promoter. Additional experiments were performed in the expression of Ankrd37, and VEGF for combined of $CoCl_2$ and mithramycin treatment. Several previous studies indicated that Ankrd37 and VEGF are regulated by HIF1α and HIF2α [47, 95, 115, 116]. Here, we shown that even though mithramycin treatment inhibited Sp1-binding, blocking HIF2α-mediated effect, the expression was still induced with the hypoxia mimic $CoCl_2$ (Figure 3-2). This induction may thus be exerted by a HIF1α-mediated mechanism.

Regulation of Atp7a Expression by Sp1: We have shown that inhibition of Sp1 DNA binding blocks target gene expression. Sp1-binding was necessary and required for HIF2α-mediated induction of Atp7a expression. To recapitulate the Sp1-mediated

regulatory mechanism on induction of Atp7a in response to iron deficiency, IEC-6 cells were transfected with HA-tagged Sp1 expression vector. qRT-PCR and western blot confirmed the overexpression of Sp1 in IEC-6 cells (Figure 3-3A and C) and also demonstrated that both Atp7a mRNA and protein were induced in IEC-6 cells by Sp1 overexpression (Figure 3-3B, D, and E).

Since endogenous Atp7a expression was induced in IEC-6 cells by Sp1 overexpression, the effect of Sp1 overexpression on promoter activity was tested. Sp1 overexpression resulted in an induction of Atp7a promoter activity (~2.5 fold; Figure 3-3F). Previous microarray analysis showed that iron transport-related genes contained GC-rich sequences on the promoter and that sequences were highly conserved between mouse and rat [113]. Therefore, mouse Dmt1 and Dcytb promoter constructs (shared by Dr. Shah's lab at the University of Michigan, Ann Arbor, MI) were co-transfected with Sp1 expression vector. Dmt1 (~5-fold; Figure 3-3G) and Dcytb (~4-fold; Figure 3-3H) promoter activity was induced in IEC-6 cells with Sp1 overexpression

Sp1 Regulated Atp7a Expression Via Direct Binding to the Promoter: It has been shown that in IEC-6 cells, Sp1 robustly increased endogenous Atp7a expression and promoter activity, and that of iron transport-related genes. Therefore, to delve into mechanistic aspects of Sp1-mediated induction, the -224/+88 bp *Atp7a* promoter bearing basal transcriptional activity, as described before [113], was analyzed. Phylogenetic footprinting analysis across species (human, rat, mouse) has shown multiple GC-rich sequences in this promoter region (data not shown). TFSEARCH (http://www.cbrc.jp/research/db/TFSEARCH.html) was thus utilized to predict putative Sp1-binding sites. Four evolutionarily conserved, putative Sp1-binding sites across species

were identified in the region of -224/+88 bp (Figure 3-4A). Promoter constructs with mutation of the putative Sp1-binding sites were generated. Constructs with multiple mutations were generated by introducing subsequent mutations. Either WT or mutated promoter constructs were transiently transfected into IEC-6 cells, and promoter activity was analyzed. Single site mutations of sites 2 and 3 led to ~50% reduction of promoter activity. Mutations of sites 1 or 4 led to ~60% and ~75% decreases in promoter activity, respectively (Figure 3-4B). Double mutations of sites 2 and 3 reduced promoter activity to 70% of WT. It is surprising to note that mutations of both site 1 and 4 brought promoter activity down to the background level (Figure 3-4C). However, triple mutation (sites 1 & 2 & 3 and sites 2 & 3 & 4) and quadruple mutations on all four putative Sp1-binding sites led to only 70% reduction of Atp7a promoter activity.

Sp1 Regulated Atp7a Expression ByDirect Binding to Promoter Cis-Elements: Four evolutionarily conserved, putative Sp1-binding sites across species were identified on the Atp7a promoter, and the site-specific mutations affected Atp7a basal promoter activity. Thus, to prove Sp1-mediated regulation via direct binding to the promoter, the chromatin immunoprecipitation (ChIP) assays were performed with cross-linked, soluble chromatin isolated from IEC-6 cells. With an established sonication protocol, ~200 bp DNA fragments were generated (Figure 3-5C) Target fragments were pulled down by ChIP-grade, Sp1-specific antibody. PCR was subsequently performed on DNA samples with three separate primer sets, targeting the putative Sp1 binding sites, with 100 bp flanking regions between forward and reverse primer (Figure3-5A). The predicted putative Sp1-binding sites were all successfully PCR-amplified (Figure 3-5D), while there was no noticeable amplification using primers targeting upstream or

downstream regions with no predicted Sp1-binding sites (Figure 3-5B and D). To confirm the effect of mithramycin treatment to inhibit Sp1 binding, WT *Atp7a* promoter-transfected IEC-6 cells were treated with increasing concentrations of mithramycin. As the concentration of mithramycin increased, promoter activity decreased progressively (Figure 3-5E). Additional ChIP assay experiments were performed with samples from mithramycin-treated IEC-6 cells. Primers targeting the region containing four Sp1 binding sites were used. PCR-amplification suggested that mithramycin treatment of IEC-6 cells resulted in a significant reduction in DNA amplification from the mithramycin-treated samples as compared to input DNA (Figure 3-5F). This demonstrated the effect of mithramycin to be able to inhibit Sp1 binding to the *Atp7a* promoter.

Involvement of Sp1 in the HIF2α-Mediated Upregulation of Atp7a Expression: Previously, we reported that the *Atp7a* gene is upregulated by HIF2α in IEC-6 cells with $CoCl_2$ treatment, which recapitulates the iron deficiency-induced hypoxia seen in rat small intestine. Thus, we used this cell line to further elucidate the synergistic relationship between Sp1 and HIF2α to determine whether these *cis*-elements on the Atp7a promoter were necessary for HIF2α-mediated upregulation of Atp7a expression. The co-transfection experiment with Atp7a promoter (with or without mutation of the Sp1-binding site) and Sp1 or HIF2α expression vector was performed. Co-transfection resulted in an induction of WT Atp7a promoter activity with overexpression of HIF2α (~5-fold induction; Figure 3-6A) or Sp1 (~3-fold induction; Figure 3-6A). Next, the promoter bearing individual, or combinations of two, three or four mutations was co-transfected with HIF2α or Sp1 expression vector. Mutation of Sp1-binding sites resulted in decreased promoter activity induced by HIF2α or Sp1.

Compared to WT promoter activity, single mutation only led to a slight decrease of promoter activity with Sp1 overexpression (~25% reduction). ~50% reduction of Atp7a promoter activity induced by HIF2α was observed (Figure3- 6B, C, D, and E). Double mutations either of sites 1 & 4 or 2 & 3 blocked the HIF2α-mediated induction of Atp7a promoter activity completely, while only mutation of sites 2 & 3 blocked Sp1-mediated induction (Figure 6F & G). Triple mutations of the *Atp7a* promoter caused further decreases of HIF2α (~70%) and Sp1 (~50%)-mediated induction (Figure 6H & I). Mutation on all four Sp1-binding sites blocked the induction of promoter activity mediated by both HIF2α and Sp1 (Figure 3-6J).

HIFα and Sp1-Regulated Gene Expression Via Direct Binding to the Promoter In Vivo: To recapitulate the *in vitro* observations in an *in vivo* setting, SD rats were placed on specialized diets (Control: Ctrl or Iron deficient: FeD) for 5 weeks. Body weight was measured each week for each of the five weeks when they consumed the special diets. The growth rate of iron-deficient rats started to decrease at the third week (Figure 3-7A). At the end of the fifth week, all rats were sacrificed, and hemoglobin and hematocrit levels were measured. Hemoglobin and hematocrit levels decreased ~75% for FeD diet fed rats (Figure 3-7B & C). In response to iron deficiency, Dmt1, Dcytb, and Atp7a expression was induced in duodenal enterocytes (Figure 3-7D, E, F, & H). Ceruloplasmin (Cp) is a ferroxidase protein synthesized and released from liver to blood to oxidize ferrous iron for release from various organs. Cp protein level in blood increased ~1.5-fold in iron deficient rats (Figure 3-7G), consistent with our previous study [81]. In duodenal enterocytes of iron-deficient rats, HIF2α protein accumulated (Figure 3-7I). Stabilization of HIF2α in enterocytes led to induction of Atp7a expression

via direct binding to the Atp7a promoter, as shown in ChIP results (Figure 3-7J). ChIP assays also confirmed the direct binding of Sp1 to the Atp7a promoter *in vivo* Figure 3-7K).

Discussion

The perturbation of iron and copper levels in the intestinal epithelium was associated with the upregulation of the *Atp7a* gene [85, 86]. Atp7a expression in enterocytes parallels that of iron transport-related genes. However, the regulatory mechanism of *Atp7a* gene regulation was unclear. To determine the molecular mechanisms of this induction, an established cell culture model of mammalian intestinal epithelium was utilized. A recent investigation noted that *Atp7a* is co-regulated with iron transport-related genes by HIF2α during iron deficiency [113]. Furthermore, we found that genes with GC-rich sequences promoter were strongly induced in rat duodenal enterocytes during iron deficiency [87]. This included a copper transporter (*Atp7a*) and iron transport-related genes (e.g. *Dmt1*, and *Dcytb*) [87]. This seemed more plausible, given that the GC-rich sequence binding proteins (e.g. Sp1-like factors) may be involved in regulation of gene expression in duodenal enterocytes. In the current study, we sought to test the role of Sp1 in transcriptional regulation of Atp7a in the intestinal epithelium during hypoxia.

Accordingly, we used a well-characterized anti-tumor drug (mithramycin), which selectively inhibits Sp1-binding to DNA to block Sp1-mediated transcriptional regulation [117-119]. Concentrations of mithramycin ranging from 100 to 1000 nM progressively decreased Atp7a, Dmt1, Dcytb, Fpn1, Ankrd37, Sp1 and HIF2α mRNA expression. Concentrations of mithramycin >500 nM had no additional effect on mRNA expression.

This may be due to cellular tolerance or some protective mechanisms activated at higher concentrations for non-tumor cells. Studies have demonstrated that in various tissues both the *Sp1* and *HIF2α* genes have functional Sp1-binding sites, and that mutation of putative Sp1-binding sites blocked mRNA expression [120, 121].

Furthermore, we sought to understand whether Sp1-binding was necessary for HIF2 α -mediated induction, as phylogenetic footprinting showed that conserved HREs and GC-rich sequences were located in the proximal region of 224 bp upstream of the transcriptional initiation site. IEC-6 cells were treated with $CoCl_2$ and/or mithramycin. $CoCl_2$ mimics hypoxia and can thus stabilize the HIF1 α and HIF2 α proteins; however, in the intestinal epithelium, it was demonstrated that HIF2 α (not HIF1 α) upregulates gene expression (e.g. *Atp7a*, *Dmt1*, *Dcytb*, and *Fpn1*) during iron deficiency [45-47, 113]. Here, our results suggested that inhibition of Sp1-binding by 500 nM mithramycin blocked the induction by HIF2α. However, disruption of Sp1-binding did not affect VEGF and Ankrd37 induction by $CoCl_2$, because HIF1α and HIF2α can upregulate their expression [47, 95, 115, 116]. These observations suggested that Sp1 may be involved in the regulation of expression of HIF2α target genes with GC-rich sequences promoter induced during iron deficiency/hypoxia, and Sp1 involvement may be necessary for HIF2α-mediated induction. Additional experiments were thus designed to delve into the mechanistic aspects of Sp1-mediated induction.

To recapitulate Sp1-mediated upregulation, an Sp1 overexpression system was established to access the role of Sp1 in endogenous Atp7a expression and promoter activity. Stable expression of Sp1 in IEC-6 cells induced both Atp7a mRNA and protein expression. Sp1 overexpression also induced the promoter activity of Atp7a, Dmt1, and

Dcytb. Further investigation looking into the putative binding sites was performed by introducing mutations into the predicted Sp1-binding sites. To understand whether the predicted binding sites were essential for Atp7a basal promoter activity and Sp1-mediated induction, mutated promoter constructs were generated. Mutation analysis experiments suggested that these sites were essential for basal promoter activity. However, why double mutation of site 1 & 4 brought expression down to background levels, while mutations of all four sites only led to ~60% reduction of promoter activity is unclear.

To prove that Sp1 regulates Atp7a expression through a direct interaction with predicted GC-rich sequences on the promoter, ChIP assays were performed, utilizing a ChIP-grade Sp1-specific antibody to pull down the DNA/Sp1-complex isolated from non-treated IEC-6 cells. To do this, three sets of primers were designed to amplify the DNA sequence from pull-down samples with 100 bp flanking regions between forward and reverse primers. A well-established sonication protocol from previous studies generated ~200 bp DNA fragments [113]. Results proved that all of these sites were important for Sp1 binding to upregulate Atp7a expression. Further experiments to explore the effect of mithramycin interruption of Sp1 binding to the GC-rich sequences were performed. *Atp7a* promoter activity and Sp1 binding to the promoter in IEC-6 cells with mithramycin treatment were assessed. *Atp7a* promoter activity decreased progressively with increasing concentrations of mithramycin, and ChIP results showed that mithramycin treatment in IEC-6 cells decreased Sp1-binding to the *Atp7a* promoter. These data demonstrated that *Atp7a* is a direct target of Sp1 in the intestinal epithelium.

In a previous study, deletion of all HREs did not result in complete loss of induction by HIF2 α , which led to the speculation that other *trans*-acting factors may be important for the *Atp7a* genomic response to hypoxia [113]. In the current study, we noted multiple GC-rich sequences on the *Atp7a* promoter and demonstrated these Sp1-binding sites were functionally important for Sp1 and HIF2α-mediated induction in response to iron deficiency/hypoxia. Additional experiments considered the functional roles of GC-rich sequences in the *Atp7a* promoter in terms of Sp1-mediated transcriptional regulation and the involvement of Sp1 in HIF2α-mediated induction. A HIF2α and Sp1 overexpression system was utilized to assess the role of Sp1-binding sites by using the WT and mutated -224/+88 bp *Atp7a* promoter constructs. HIF2α and Sp1 overexpression led to ~5- and ~2.5-fold induction of Atp7a promoter activity, respectively. Mutation of individual Sp1-binding sites led to only a slight reduction of promoter activity. However, double mutation of site 2 & 3 blocked Sp1-mediated induction completely. This was reasonable because *Atp7a* has a TATA-box less promoter; we thus predicted that Sp1 has function in a similar role as TATA-box binding protein to recruit the transcriptional initiation complex[122, 123].

The triple mutation progressively decreased the induction of promoter activity by Sp1 and mutation on all four Sp1-binding sites blocked the induction. These data suggested that all sites were functional Sp1-binding sites. In terms of the effect of mutation on HIF2α-mediated induction, single mutation, or combinations of two, three or four mutations on Sp1-binding sites effectively attenuated HIF2α-mediated induction (as compared to the induction of the WT promoter construct by HIF2α), especially double mutations of sites 1 & 4 or 2 & 3, which completely blocked HIF2α-mediated induction.

However, there was still a 1.5-fold induction by HIF2α observed in promoter constructs bearing triple mutations (either sites 1 & 2 & 3 or 2 & 3 &4). Mutation of four Sp1-binding sites also blocked the HIF2α-mediated induction. This suggested some synergistic relationship between each Sp1 binding site in HIF2α-mediated induction.

To determine the physiologic relevance of these observations, ChIP experiments were performed in duodenal enterocytes isolated from rats fed Ctrl or FeD diets for 5 weeks after weaning. At the end of fifth week, animals were sacrificed for enterocyte isolation. The iron-deficient rats showed a similar phenotype as observed in previous studies, such as slow growth rate, lower hemoglobin and hematocrit levels (about 25% of rats on Ctrl diet), induction of iron transport protein-encoding genes (*e.g. Dmt1*, *Dcytb*, *Fpn*) and copper homeostasis protein-encoding genes (*e.g. Atp7a*: both mRNA and protein) [85], and induction of serum ferroxidase activity (*e.g*. Cp) [81]. In duodenal enterocytes, HIF2α but not HIF1α protein accumulated in response to iron deficiency/hypoxia. Importantly, ChIP experiments showed that *Atp7a* is indeed a direct target of Sp1 and HIF2α in duodenal enterocytes of iron-deficient rats.

Sp1-binding to promoters may be enhanced by post-translational modifications such as phosphorylation or acetylation. Studies indicated that phosphorylation of Sp1 could increase protein/DNA binding affinity [124]. Here we report that hypoxia (1% O_2 or $CoCl_2$) increased phosphorylation of the Sp1 protein in relation to total Sp1 protein levels (Figure 3-8). Additional investigations also suggested Sp1 may interact with HIF2α directly in some cancer cells, for example in in ovarian clear cell carcinoma [125], and this interaction between Sp1 and HIF1α may also exist in some tumor cells involved in tumor progression [126].

This investigation has successfully identified the *trans*-acting factor involved in induction of Atp7a by HIF2α in an *in vitro* model. This is what may occur to upregulate *Atp7a* and iron transport-related genes in the rat intestinal epithelium during iron deficiency, when enterocytes iron levels are low and hypoxia occurs. It is intriguing that iron perturbation affected both iron homeostasis-related gene expression (e.g. Dmt1, Dcytb, and Fpn1) and copper transport-related gene expression (Atp7a) during iron deficiency. As GC-rich promoters were preferentially induced in the intestinal epithelium during iron deficiency, it was notable that genes with such promoter sequences included these same iron and copper homeostasis protein-encoding genes. The Sp1-mediated regulatory mechanism was integral to HIF2α-mediated induction, most likely functioning to increase iron homeostasis-related gene expression during iron deficiency and copper transport-related genes as a compensatory mechanism to increase iron absorption. Therefore, this study provides novel insight into iron deficiency/hypoxia-responsive genes in the mammalian small intestine, where Sp1 is necessary and required for the hypoxic response. This regulatory mechanism may have broader implications for the understanding of the intestinal iron and copper homeostasis.

Table 3-1. Primer List

Primer Name	qRT-PCR
18s Forward	5'-TCCAAGGAAGGCAGCAGGC-3'
18s Reverse	5'-TACCTGGTTGATCCTGCCA-3'
Atp7a Forward	5'-TGAACAGTCATCACCTTCATCGTC-3'
Atp7a Reverse	5'-TGCATCTTGTTGGACTCCTGAAAG-3'
Dmt1 Forward	5'-GTGTTGGATCCTGAAGAAAAGATTCC-3'
Dmt1 Reverse	5'-GGGATTTTCTCATCAAAGTAGGTGGT-3'
Dcytb Forward	5'-AGTGCAGCAAGTTCTTGATGAAAT-3'
Dcytb Reverse	5'-CGTGGCAATCACTGTTCCAA-3'
Fpn1 Forward	5'-TCGTAGCAGGAGAAAACAGGAGC-3'
Fpn1 Reverse	5'-GGAACCGAATGTCATAATCTGGC-3'
Ankrd37 Forward	5'-TGCTGGAGACAGGAGCATCAGT-3'
Ankrd37 Reverse	5'-CCACCAGGAGGCTAAGGCAC-'
HIF2α Forward	5'-GCGACAATGACAGCTGACAAGG-3'
HIF2α Reverse	5'-CCTCCAAGGCTTTCAGGTACAAGT-3'
Sp1 Forward	5'-CCAGACCATTAACCTCAGTGCATTG-3'
Sp1 Reverse	5'-CCCTCACTGTCTTTACAATAGGGGC-3'
Sp6 Forward	5'-TGTGCTACCAAGACAACCTT-3'
Sp6 Reverse	5'-AAGTGGGTTCACAGCAGTT-3'
TfR Forward	5'-ATTGCGGACTGAGGAGGTGC-3'
TfR Reverse	5'-CCATCATTCTCAGTTGTACAAGGGAG-3'
VEGF Forward	5'-ACTGCTGTACCTCCACCATGCC-3'
VEGF Reverse	5'-CTTTCTGCTCCCCTTCTGTCGT-3'
Primer Name	Promoter construct with mutation on Sp1-binding site
Site 1 Forward	5‘-TGCGTGCACCAGGGGAAAACACGGAGCTTTGGGC-3'
Site 1 Reverse	5'-GCCCAAAGCTCCGTGTTTTCCCCTGGTGCACGCA-3'
Site 2 Forward	5'-GGGGGGCCTCAGAGATAGGCGGGGCGAACGC-3'
Site 2 Reverse	5'-GCGTTCGCCCCGCCTATCTCTGAGGCCCCCC-3'
Site 3 Forward	5'-GGGCCTCAGAGGCGGATAGGGCGAACGCTGTGG-3'
Site 3 Reverse	5‘-CCACAGCGTTCGCCCTATCCGCCTCTGAGGCCC-3’
Site 4 Forward	5'-GCTGGTTGATCGCTGCTATCCTACGGAGCTCCGAG-3'
Site 4 Reverse	5‘-CTCGGAGCTCCGTAGGATAGCAGCGATCAACCAGC-3’
Site 2 & 3 Forawrd	5'-GTGGGGGGCCTCAGAGTACGTACGGGCGAACGCTGTGGGC-3'
Site 2 & 3 Reverse	5'-GCCCACAGCGTTCGCCCGTACGTACTCTGAGGCCCCCCAC-3'

Table 3-1. Continued

Primer Name	ChIP Assay
HRE Forward	5'-TGCTAGGGCCTAACCCACCTTG-3'
HRE Reverse	5'-AAGCTGGGCCGACTAGGGAAAT-3'
Negative Control Forward	5'-AGCCTGGCTTTGATGGATGATTTT-3'
Negative Control Reverse	5'-TTTAGTCACCTCCCAACTCCAGGAAT-3'
Sp1 Forward 1	5‘-CCCACCTTGGCCGAGGA-3'
Sp1 Reverse 1	5‘-GGGCCGACTAGGGAAATGGT-3'
Sp1 Forward 2	5'-GGGCCCTGGCATCACCC-3'
Sp1 Reverse 2	5'-GCTCCTCCCTCGACGGCTT-3'
Sp1 Forward 3	5'-GAGCTGCCTCCGCCTGC-3'
Sp1 Reverse 3	5'-GGTTCGAGCTCGGAGCTCC-3'
Negative Control Forward 1	5’-GCCAGGGTAGAGAAACCCTGTCT-3‘
Negative Control Reverse 1	5'-GCCCTGGCAGTAAATGCCC-3'
Negative Control Forward 2	5'-TGAAACGGGTGGGAGGAGG-3'
Negative Control Reverse 2	5'-CCCAAGTTCAGTTCCCAGTGATAA-3'
Negative Control Forward 3	5'-ATGGGGTGATGTCAAATTAAGACAG-3'
Negative Control Reverse 3	5'-AGTTAGTGAGGTTGGCAGAACCAC-3'

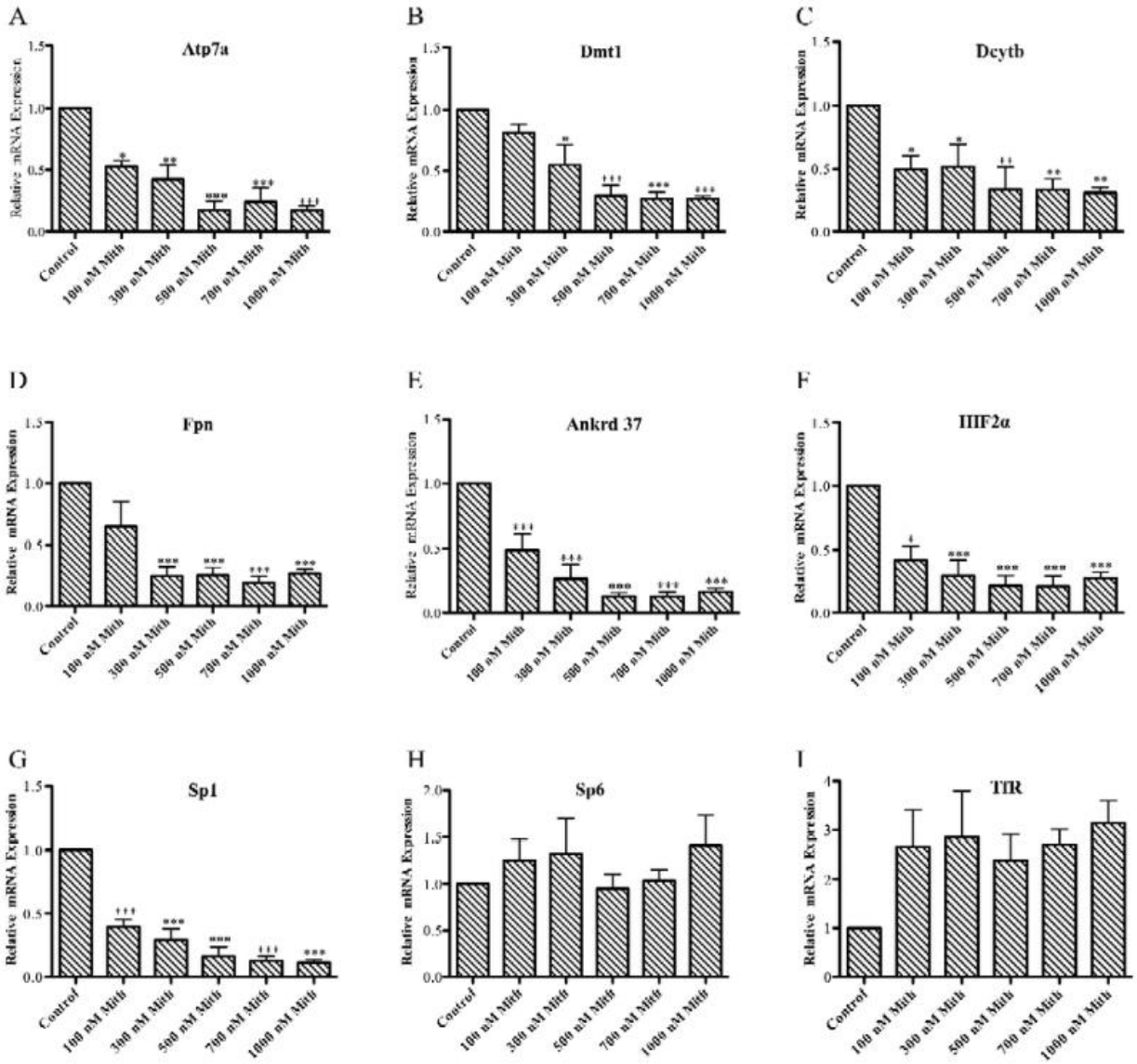

Figure 3-1. Effect of mithramycin on mRNA expression in rat intestinal epithelial (IEC-6) cells. IEC-6 cells at 7 days post-confluence were treated with mithramycin at different concentrations ranging from 100 nM to 1000 nM for 24 hours. Relative mRNA expression levels were determined. A: Atp7a. B: Dmt1. C: Dcytb. D: Fpn1. E: Ankrd37. F: HIF2α. G: Sp1. H: Sp6. I: TfR. Values are mean ± SD. *P<0.05, **P<0.01, ***P<0.005; unpaired Student's t-test, n=3.

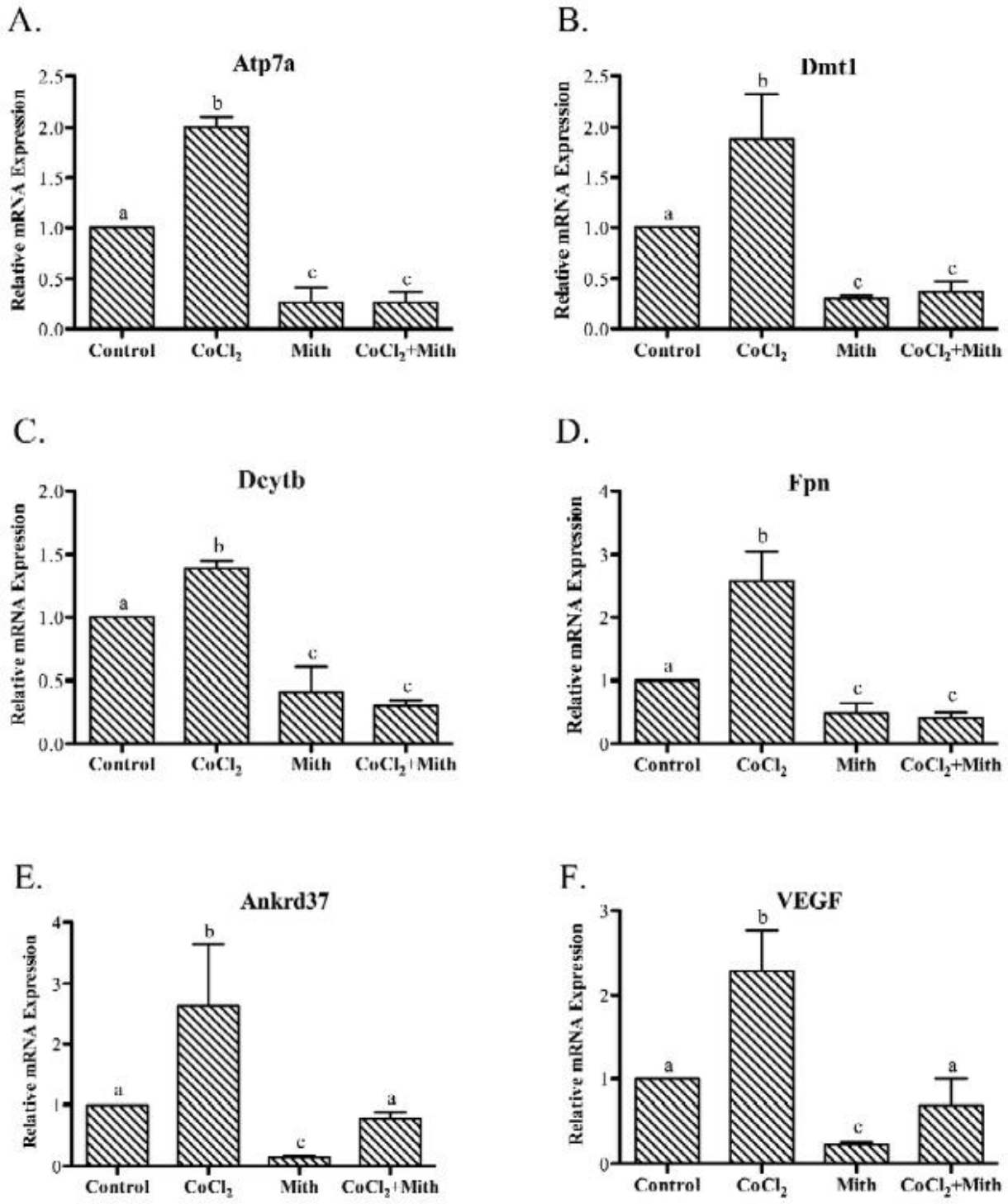

Figure 3-2. Effect of mithramycin on $CoCl_2$-mediated transcriptional induction in IEC-6 cells. IEC-6 cells at 7 days post-confluence were treated with $CoCl_2$ (200 μM) for 36 hours, followed by adding mithramycin (500 nM) with/without $CoCl_2$ to cell cultures for another 24 hours. Gene expression levels were determined by qRT-PCR. A: Atp7a. B: Dmt1. C: Fpn1. D: Ankrd37. E: VEGF. Each bar represents mean ± SD. Different letters above each bar (a, b, c) indicate significant differences ($P<0.05$, ANOVA).

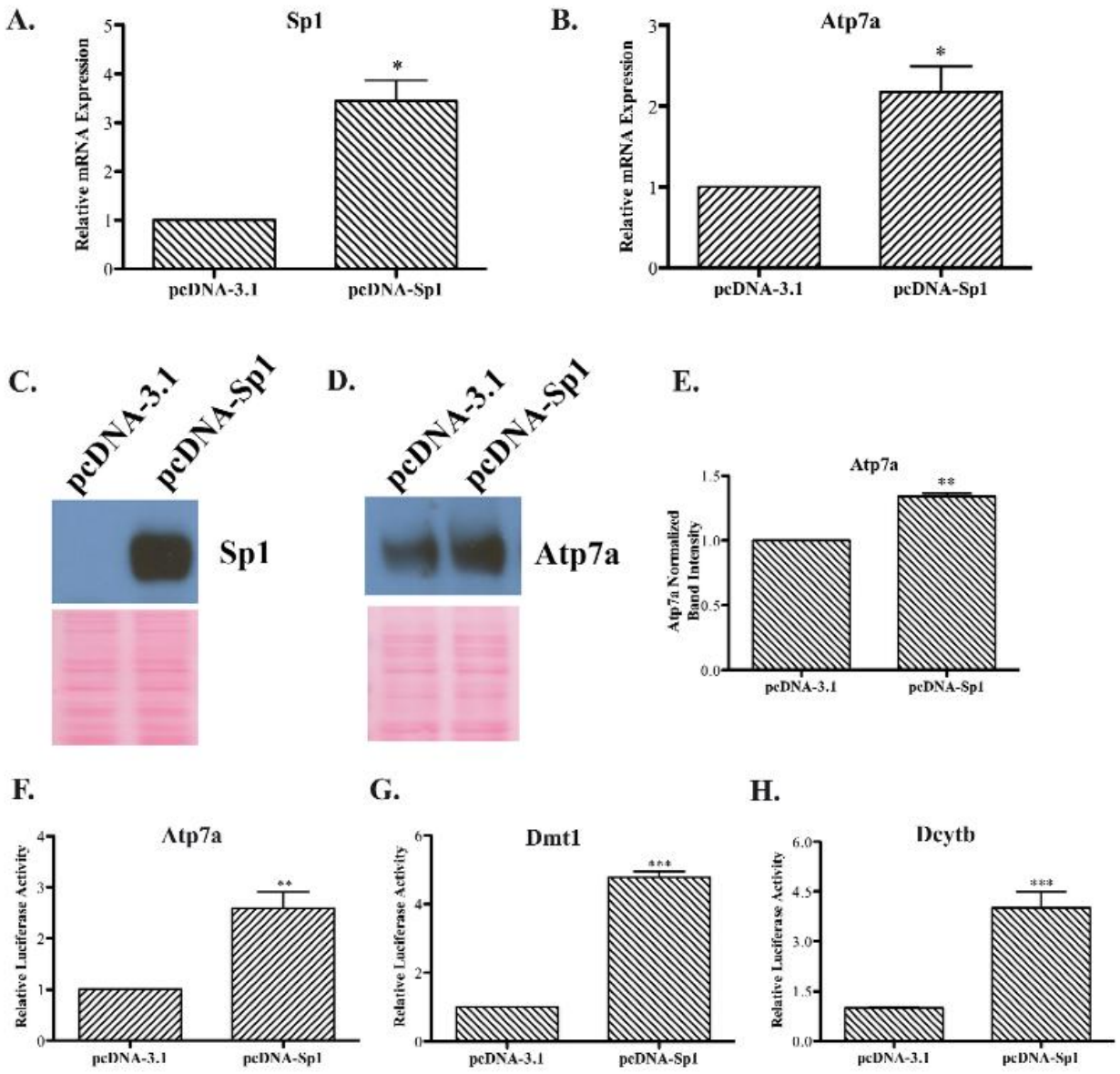

Figure 3-3. Effect of Sp1 over-expression on endogenous Atp7a expression and Atp7a, Dmt1, and Dcytb promoter activity in IEC-6 cells. IEC-6 cells were transfected with HA-tagged Sp1 expression vector. Sp1 and Atp7a mRNA and protein expression were determined. A: relative Sp1 mRNA expression levels. B: relative Atp7a mRNA expression levels. C: HA-tagged Sp1 protein level. D & E: Atp7a protein level. Atp7a, Dmt1, and Dcytb promoter constructs were co-transfected with Sp1 expression vector. F: Atp7a promoter activity. G: Dmt1 promoter activity. H: Dcytb promoter activity. Each bar represents the mean value ± SD. *P<0.05, **P<0.01, ***P<0.005; unpaired Student's t-test, n=3.

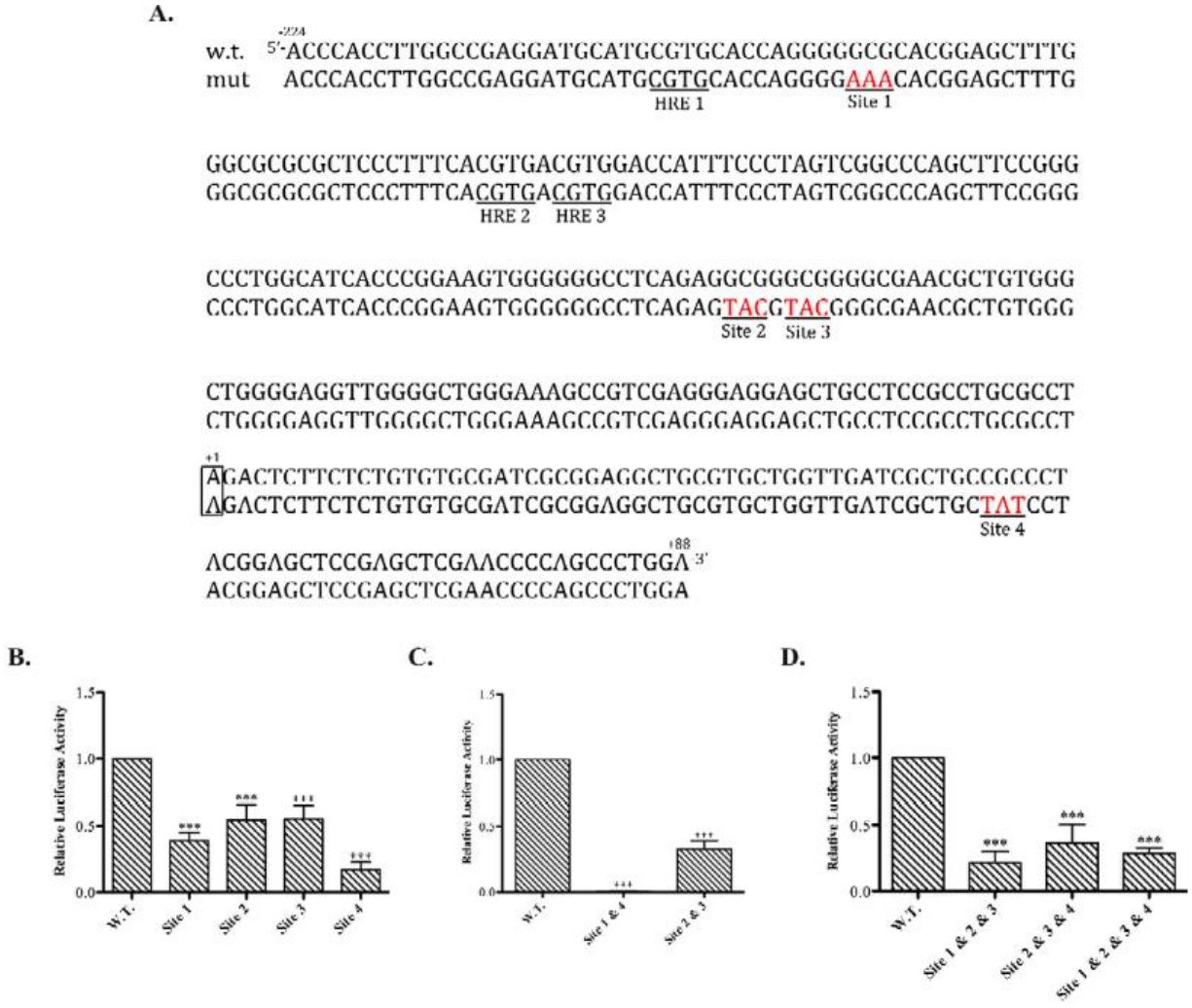

Figure 3-4. Mutation analysis of putative Sp1 binding sites. A: wild-type (WT) and mutated Atp7a promoter sequences from -224 bp to +88 bp are shown. Putative Sp1-binding sites and mutated sequences were annotated. Putative Sp1-binding site was mutated individually or in combination. Either WT or mutated promoter constructs were transfected into IEC-6 cells. B: promoter activity of construct bearing single. C: promoter activity of construct with double mutations. D: promoter activity of constructs with three or four mutations. Each bar represents mean value ± SD. ***P<0.005 unpaired Student's t-test, n=3.

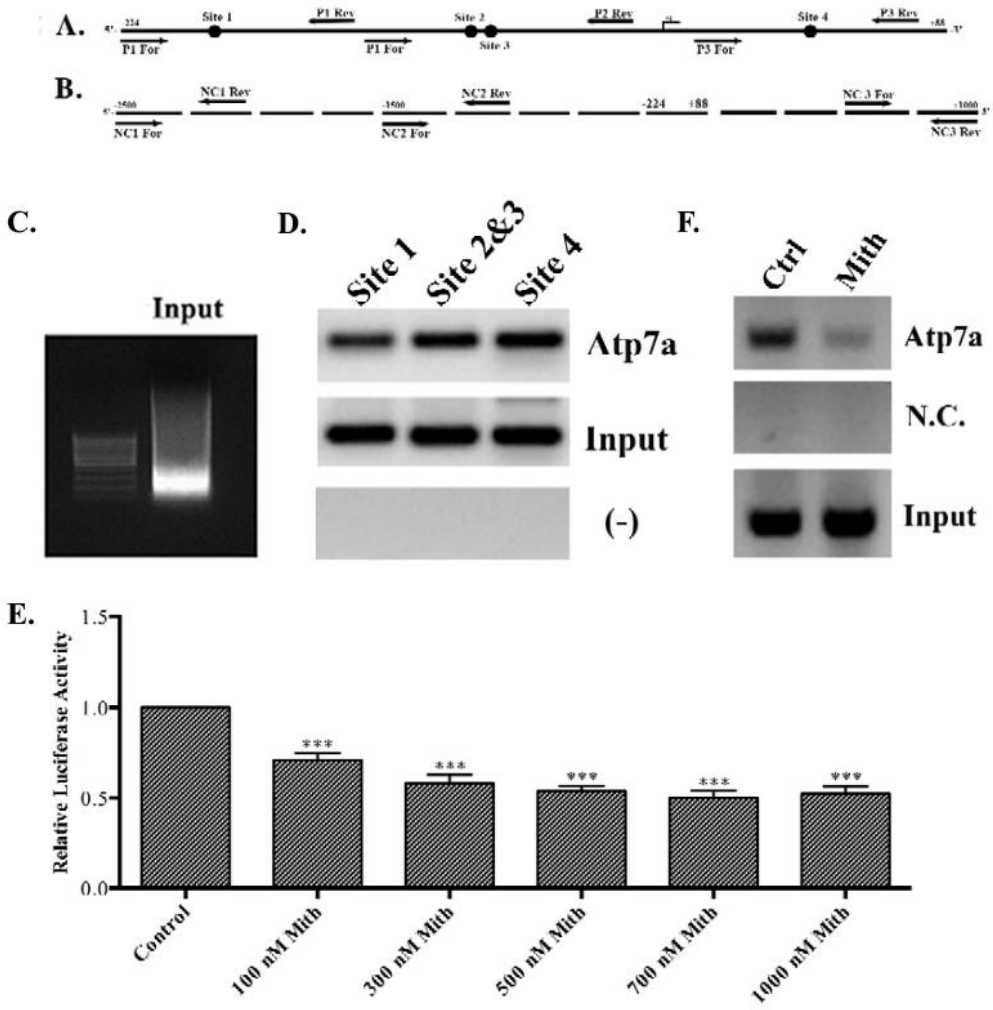

Figure 3-5. Chromatin immunoprecipitation (ChIP) analysis of Sp1 binding to rat Atp7a promoter. A: location of primers used to amplify the Atp7a promoter region containing Sp1-binding site(s). B: location of primers used to amplify Atp7a promoter regions not containing Sp1-binding site. Cross-linked chromosomal DNA was pulled down by ChIP-grade Sp1 antibody from IEC-6 nuclear extracts prepared from control (untreated) or mithramycin-treated cells. Input was amplified from DNA before pull down with primers containing the putative Sp1-binding site. C: the size of DNA fragment after sonication. D: each putative Sp1 binding site was PCR amplified with primers (Atp7a) covering region with putative Sp1 binding site. E: *w.t.* Atp7a promoter was transfected into IEC-6 cells. 12 hours after transfection, IEC-6 cells were treated with mithramycin (from 100 nM to 1000 nM). F: primers containing four Sp1-binding sites were used to determine the effect of mithramycin on Sp1 binding. Each bar represents mean value ± SD, n=3. ***P<0.005, unpaired Student's t-test.

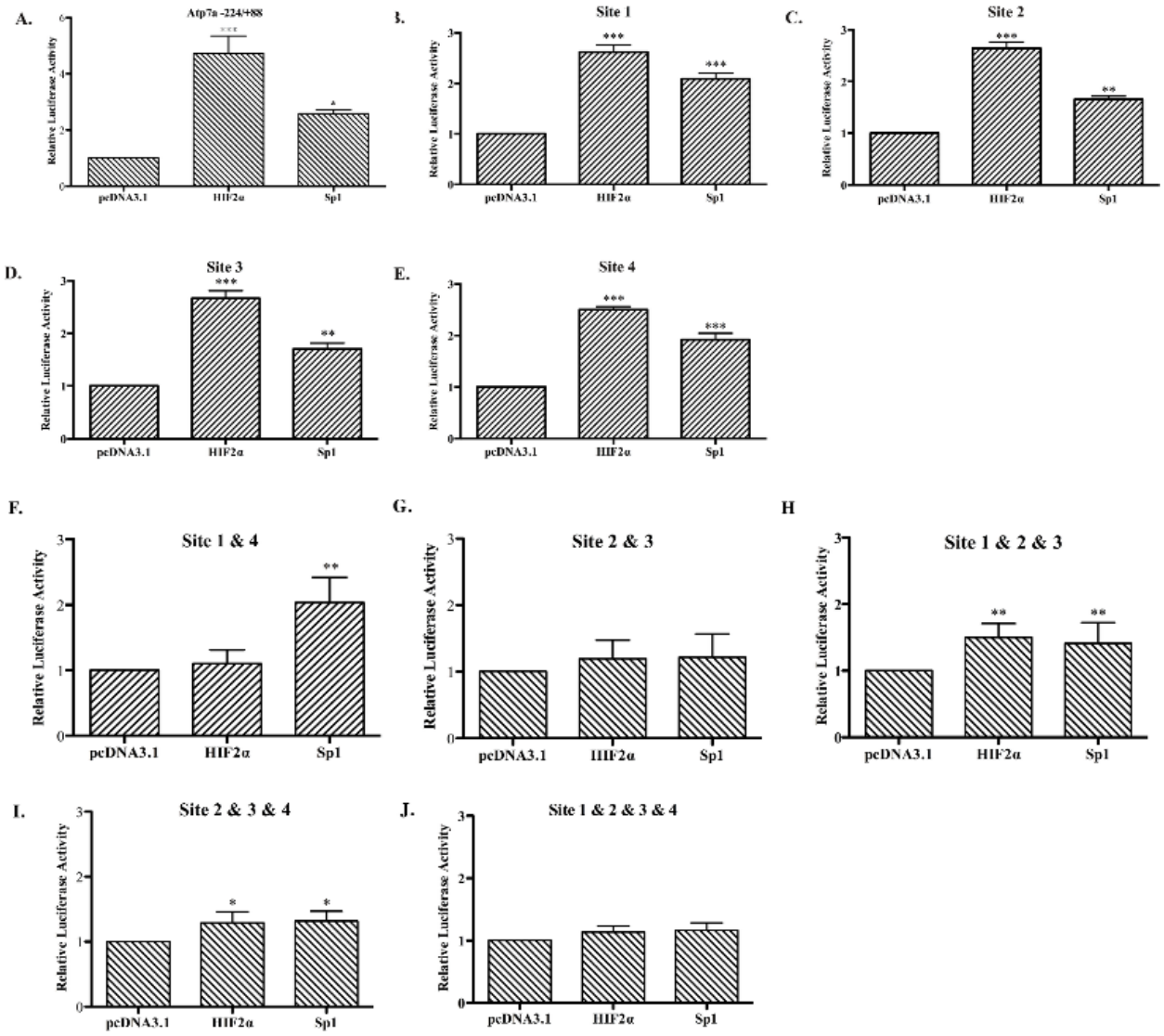

Figure 3-6. Co-transfection of HIF2α or Sp1 expression vector with Atp7a promoter constructs (WT or mutated). *WT* or mutated (individual mutation or mutations in combination) Atp7a promoter construct was co-transfected with HIF2α or Sp1 expression vector (or empty vector as control) into IEC-6 cells. A: *WT* Atp7a promoter construct. B: mutation on site 1. C: mutation on site 2. D: mutation on site 3. E: mutation on site 4. F: mutations on sites 1 & 4. G: mutation on sites 2 & 3. H: mutations on sites 1 & 2 &3. I: mutations on sites 2 & 3 & 4. J: mutations on sites 1 & 2 & 3 & 4. Each bar represents mean value ± SD. *P<0.05, **P<0.01, ***P<0.005 unpaired Student's t-test, n=3.

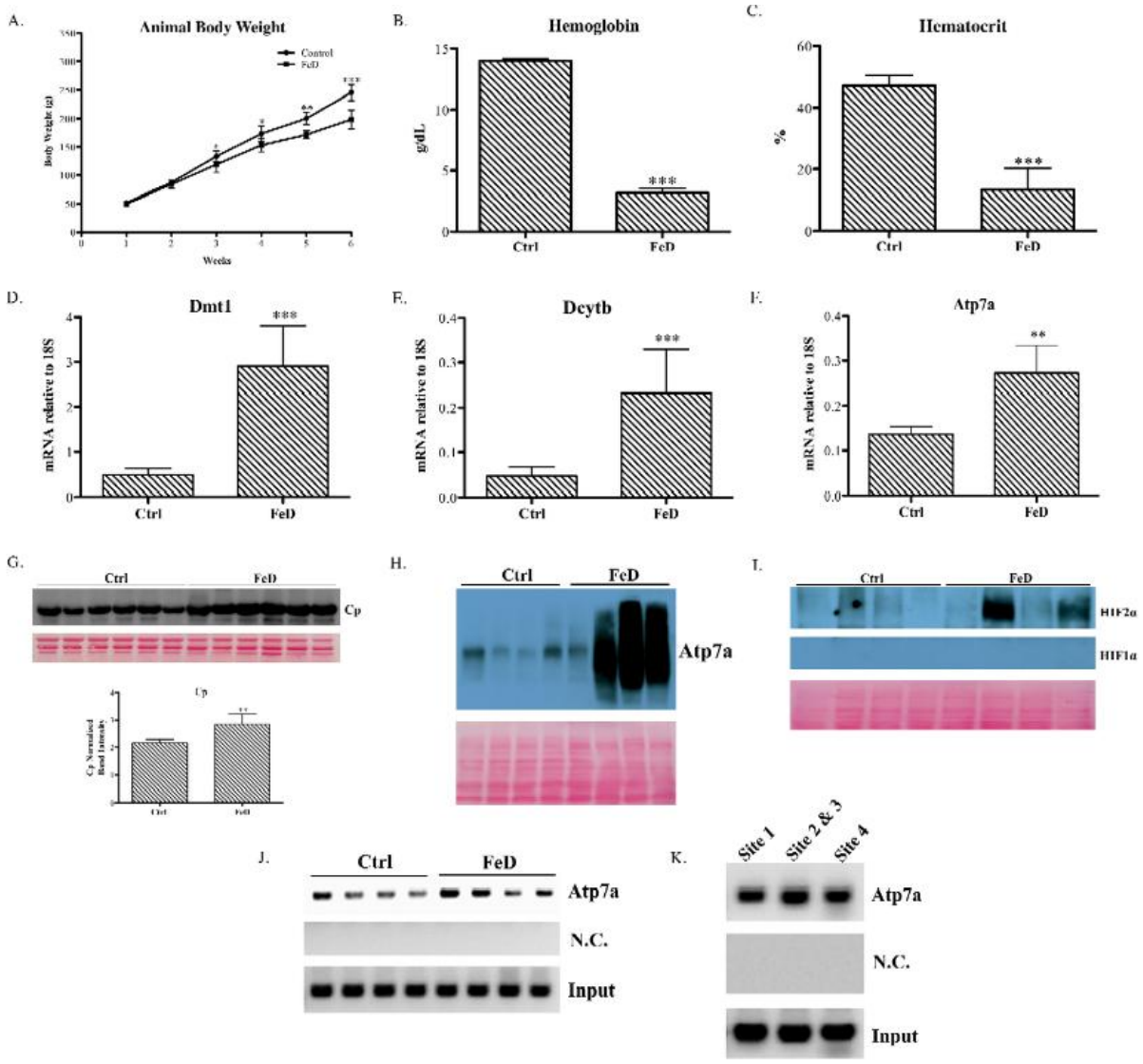

Figure 3-7. ChIP analyses of HIF2α and Sp1 binding to rat Atp7a promoter in rat intestine. 12 rats divided into two groups were placed on control (Ctrl) or iron deficient (FeD) diets for five weeks. At the end of fifth week, rats were sacrificed and duodenal enterocytes were isolated. A: rat body weight was measured each week and growth rate is shown graphically. Hematological status of rats on different diets. B. hemoglobin levels. C: hematocrit levels. Dmt1 (D), Dcytb (E), and Atp7a (F) mRNA expression levels were determined using duodenal enterocytes. G: ceruloplasmin protein level was determined using serum from each group. Each bar represents mean value ± SD. *P<0.05, **P<0.01, ***P<0.005, unpaired Student t-test, n=6. Cytosolic and nuclear proteins were isolated from duodenal enterocytes of each group. H: Atp7a protein level. I: HIF2α and HIF1α protein level. J: Atp7a promoter was PCR-amplified with primers containing HREs. K: Atp7a promoter was PCR-amplified with primers containing each Sp1 binding site.

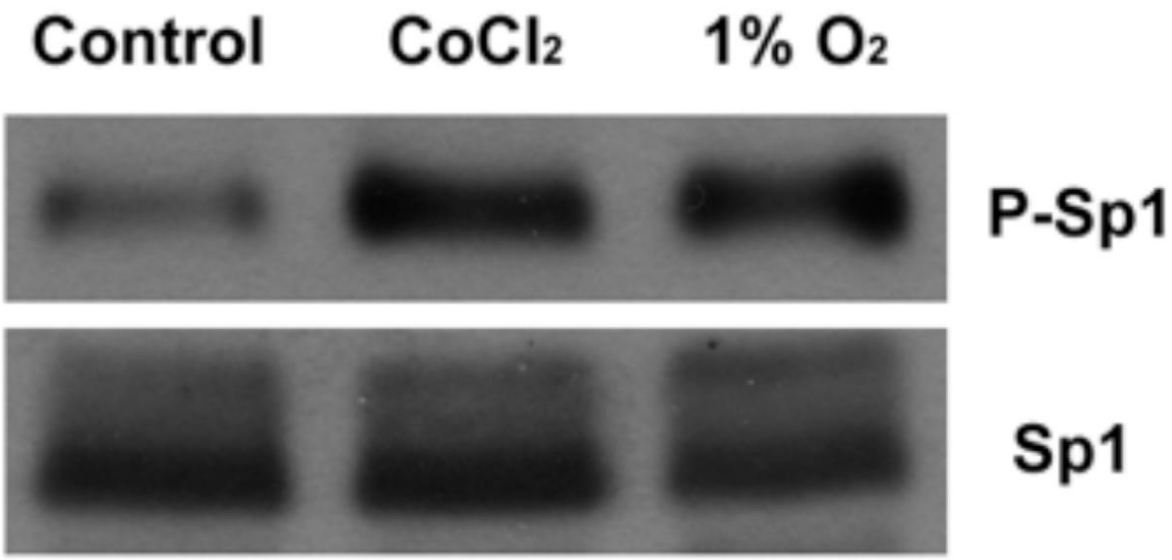

Figure 3-8. Immunoblot analysis of phosphorylated Sp1 (p-Sp1) protein expression in IEC-6 cell with CoCl2 mimetic hypoxia or 1% O2 exposure. IEC-6 cells at 85% confluence were treated with CoCl2 (200 μM) or cultured in hypoxia chamber (1% O2) for 60 hours. P-Sp1 protein level is normalized to total Sp1 protein level. P-Sp1 bands are ~120 kDa and Sp1 bands are ~108 kDa. Blot shown was the representative of three independent experiments.

CHAPTER 4
COPPER STABILIZES THE MENKES COPPER TRANSPORTING ATPASE (ATP7A) PROTEIN EXPRESSED IN RAT INTESTINAL EPITHELIAL (IEC-6) CELLS

Summary

Iron deficiency decreases oxygen tension in the intestinal mucosa, leading to stabilization of hypoxia-inducible transcription factor 2α (Hif2α), and subsequent upregulation of genes involved in iron transport (e.g. Dmt1, Fpn1). Iron deprivation also alters copper homeostasis, reflected by copper accumulation in the intestinal epithelium and induction of an intracellular copper binding protein (Mt) and a copper exporter (Atp7a). Importantly, Atp7a is also a Hif2α target. It was however previously noted that Atp7a protein expression was induced more strongly than mRNA in the duodenum of iron deprived rats, suggesting additional regulatory mechanisms. The current study was thus designed to decipher mechanistic aspects of Atp7a regulation during iron deprivation using an established in vitro model of the mammalian intestine, rat IEC-6 cells. Cells were treated with an iron chelator and/or copper loaded to mimic the in vivo situation. IEC-6 cells exposed to copper showed a dose-dependent increase in Mt expression, confirming intracellular copper accumulation. Iron chelation with copper loading increased Atp7a mRNA and protein levels while unexpectedly, copper alone increased only protein levels. This suggested that copper increased Atp7a protein levels by a post-transcriptional regulatory mechanism. Therefore, to determine if Atp7a protein stability was affected, the translation inhibitor cycloheximide (CHX) was utilized. Experiments in IEC-6 cells revealed that the half-life of the Atp7a protein was ~48 hours and furthermore that intracellular copper accumulation increased steady-state Atp7a

This work has been published: Am J Physiol Cell Physiol2013 Feb; 304(3): C257-62. Permission to reprint is not required.

protein levels. This investigation thus reveals a novel mechanism of Atp7a regulation in which copper stabilizes the protein, possibly complementing Hif2α-mediated transcriptional induction during iron deficiency.

Background

Body iron levels are controlled by intestinal absorption, as no active excretory mechanism exists for this essential trace mineral. As such, intestinal iron transport is tightly regulated by local and systemic factors. Previous studies dating back many decades have implicated copper as being important for control of body iron homeostasis [19, 89]. Relevant observations include hepatic copper loading during iron deficiency [9, 81, 127] and concomitant increased production of a liver-derived, circulating multi-copper ferroxidase, ceruloplasmin (Cp) [81]. It has been noted that serum copper levels increase during iron deficiency in a number of mammalian species [128, 129], likely reflecting higher levels of the *holo*-Cp (i.e. copper-containing) enzyme [10, 35, 130]. Cp is necessary for iron release from body stores [107, 114] and may influence intestinal iron absorption [131]. At the level of the intestine, another multi-copper ferroxidase, hephaestin, is important for iron efflux from enterocytes [33, 132]; its expression however is not strongly regulated by iron levels [133-135]. Additional published studies described perturbations in intestinal copper metabolism during iron deprivation, as exemplified by copper accumulation in the intestinal mucosa [86], and increased expression of a cytoplasmic copper-binding protein (metallothionein [Mt]) and a copper exporter (Menkes copper ATPase [Atp7a]) [85, 86]. Whether copper directly influences intestinal iron absorption or if the metal is simply traversing enterocytes en route to the liver, where copper increases during iron deprivation, is currently not known. In either

case though, it is logical to predict that copper positively influences intestinal iron homeostasis.

The rate-limiting step in acquisition of dietary copper is the copper transporting ATPase, Atp7a, which is necessary for assimilation of absorbed copper. This is reflected by the phenotype of patients with Menkes Disease, in which mutated Atp7a leads to copper accumulation in enterocytes and severe systemic copper deficiency [136, 137]. Interestingly, Atp7a is strongly induced in the duodenum of iron deficient rats [85, 127], in the setting of perturbations in body copper levels. A recent investigation revealed that *Atp7a* was coordinately regulated in intestinal epithelial cells along with genes encoding proteins involved in intestinal iron absorption (e.g. Dmt1, Cybrd1, Fpn1), by a transcriptional mechanism mediated by a hypoxia-inducible *trans*-acting factor, Hif2α [45, 138-140]. It was however noted that Atp7a protein levels were more strongly induced than mRNA levels [86], suggesting that additional regulatory mechanisms exist. The current study was thus undertaken to assess this possibility in an established model of the rodent intestinal epithelium, rat IEC-6 cells, which express proteins involved in intestinal iron and copper absorption, including Dmt1 [141, 142] and Atp7a [143, 144]. Iron deprivation and copper loading studies in IEC-6 cells revealed that copper had a direct influence on Atp7a protein expression independent of changes in mRNA levels.

Materials & Methods

Cell Culture. Rat intestinal epithelial (IEC-6) cells were obtained from the American Type Culture Collection (ATCC; Manassas, VA), and cultured as previously described [113], according to the distributor's recommendations. To determine the Atp7a protein half-life, 7 days post-confluent IEC-6 cells were treated with various

concentrations of a protein translation inhibitor cycloheximide (CHX; 2, 5, or 10 μg/mL) and for different time periods (24, 48, or 60 hours). For Atp7a protein stability experiments, IEC-6 cells were cultured for 7 days post-confluence, followed by CHX, deferoxamine (DFO; an iron chelator) (200 μM) and/or $CuCl_2$ (200 μM) treatment for 48 hours.

Total RNA Isolation and Real-Time Quantitative RT-PCR. IEC-6 cells at ~85% confluence were washed with the ice-cold PBS (pH 7.4) three times. Total RNA was subsequently isolated from cells using TRIzol reagent (Life Technologies; Grand Island, NY) according to the manufacturer's instructions. RNA concentration was determined using a spectrophotometer, and 1 μg total RNA was reverse transcribed with the iScript cDNA Synthesis Kit (BioRad; Hercules, CA) in a 20 μL reaction. After reverse transcription, cDNA was diluted to 120 μL with nuclease-free water, and 3 μL was used for the quantitative, real-time PCR (qRT-PCR) with SYBR Green qRT-PCR master mix (Bio-Rad), as described previously [113]. Expression of experimental genes was normalized to expression of a "housekeeping" gene, 18S rRNA, which fluctuated minimally between samples. The sequences of primers used for the qRT-PCR experiments are listed in Table 4-1. Each primer pair was first validated by performing standard curve reactions whereby linear amplification was observed across a range of template concentrations. Melt curves were also routinely run with each PCR reaction to ensure that single amplicons were produced.

Protein Isolation and Western Blot.Total cellular protein was purified with the Nuclear Extraction Kit (Active Motif; Carlsbad, CA) as described previously with minor modifications [113]. IEC-6 cells at ~85% confluence were washed with the ice-cold PBS

(pH 7.4) and then harvested using a cell scraper, followed by suspension in 1x hypotonic buffer plus protease inhibitor cocktail (2 μM leupeptin, 14 μM E-64, 130 μM bestatin, and 2 mM AEBSF-HCl). Cells were lysed using a tissue homogenizer and membrane-bound proteins were solubilized with NP-40 (0.05%). A total cell lysate, minus nuclear protein, was obtained by centrifuging at 16,000 rpm in a microfuge for 15 minutes at 4° C. Protein concentration in the resulting supernatant was determined using a BCA Protein Assay Kit (Thermo Scientific; Rockford, IL). 30 μg of protein was resolved by 7.5% SDS-PAGE, followed by transfer to a PVDF membrane, which was subsequently blocked in 5% non-fat milk. The membrane was then reacted with a rabbit polyclonal antibody against the rat Atp7a protein (called 54-10), which has been extensively validated [76, 113, 143]. Antibodies against β-actin (600-403-886; Rockland; Gilbertsville, PA) and tubulin (ab-6160; Abcam; Cambridge, MA) were also utilized to detect constitutively-expressed "housekeeping" proteins for normalization. For some experiments, Atp7a protein expression was normalized to total proteins on stained blots, as previously described [84, 145]. Immunoreactive proteins on membranes were visualized using in-house made ECL reagent [81] and x-ray film.

Statistical Analysis. ANOVA (GraphPad, La Jolla, CA) was utilized to statistically compare experimental data across groups; $p < 0.05$ was considered significant.

Results

Atp7a Expression is Upregulated by Iron Chelation and Copper Loading. To model the *in vivo* situation during iron deficiency and to decipher mechanistic aspects of *Atp7a* regulation during iron deficiency, IEC-6 cells were treated with an iron chelator (DFO) and/or extra copper was added to the culture media. Iron chelation increased

Atp7a mRNA expression (~1.6-fold), but had little effect on protein levels (Figure 4-1). Iron chelation (200 µM DFO) plus copper loading ($CuCl_2$; 200 µM) had a more dramatic effect on Atp7a expression, leading to significant induction of mRNA (~2.6-fold) and protein levels (~2-fold). Additionally, copper loading (200 µM for 16 hours) in the absence of iron chelation had no effect on *Atp7a* mRNA expression, but led to a significant increase of protein levels (~1.8-fold) (Figure 4-1). Based upon microscopic observation of cells, none of the treatments led to significant cell death (data not shown).

Effect of Copper Loading on Atp7a Expression. To further investigate the effect of copper loading on Atp7a protein expression, IEC-6 cells were treated with increasing concentrations of copper in the cell culture medium for 16 hours, followed by quantifying Atp7a mRNA and protein expression levels. Increased intracellular copper was confirmed by dose-dependent increases in metallothionein (Mt1a/2a) mRNA expression (Figure 4-2). Mt has been shown to be a sensitive marker of intracellular copper accumulation in a number of mammalian species [68, 77]. Copper treatments from 100-400 µM did not lead to significant cell stress as determined by microscopic observation, but higher levels (e.g. 500 and 600 µM) resulted in notable cell death, as exemplified by detached, floating cells (data not shown). *Atp7a* mRNA expression was not affected by copper treatment at any concentration; however, Atp7a protein levels increased at all copper concentrations, with the maximal response (~2-fold) being seen with 200 µM copper. Higher copper levels (300 and 400 µM) did not lead to further increase of Atp7a protein levels. Furthermore, mRNA levels of additional copper-related genes were also not affected by copper loading, including copper transporter 1 (the

apical copper importer), superoxide dismutase 1 (SOD1; an intracellular, copper-containing antioxidant protein) and antioxidant protein 1 (Atox1; a copper chaperone for Atp7a) (Figure 4-3).

Effect of Copper Loading on Atp7a Protein Stability. Since Atp7a physically interacts with copper as part of its transport function, we next considered the possibility that increased intracellular copper could increase Atp7a protein stability. To do so, a global translation inhibitor, cycloheximide (CHX), was utilized in the IEC-6 cell model. As rapidly dividing IEC-6 cells are very sensitive to CHX treatment (data not shown), these experiments were done in fully confluent cell monolayers (7 days post-confluent). First, IEC-6 cells were treated with increasing CHX concentrations to assess the effect on Atp7a protein levels (Figure 4-4A). A maximal reduction in protein levels (~80%) was observed with 10 µg/mL CHX for 48 hours. Then, to estimate Atp7a protein half-life, cells were treated with 10 µg/mL CHX for time periods ranging from 24 to 60 hours (Figure 4-4B). These experiments revealed that the Atp7a protein half-life was ~48 hours, as at this time point, protein levels had decreased ~50%. Next, to determine if copper loading altered Atp7a protein stability, cells were treated with CHX in the presence and absence of copper (Figure 4-4C). In this study, CHX decreased Atp7a protein levels, while CHX in the presence of copper abolished the decrease. As expected, DFO plus copper also led to an increase of Atp7a protein levels.

Discussion

Consistent with alterations in body copper levels during iron deficiency, intestinal Atp7a mRNA and protein are induced in the setting of increased mucosal copper in iron-deprived rats [85, 86]. To determine the molecular mechanism of this induction, we utilized an established model of the mammalian intestinal epithelium, rat IEC-6 cells.

Cells were treated with $CoCl_2$ or cultured in 1% oxygen to simulate the hypoxic response that typifies iron deprivation [113]. These studies revealed that the *Atp7a* gene was a direct target of a hypoxia-inducible, *trans*-acting factor, Hif2α, which likely mediates increases in Atp7a mRNA expression during iron deprivation [113]. This places Atp7a among a group of iron-related genes (e.g. Cybrd1, Dmt1, Fpn1) that are also Hif2α targets [45, 46, 146]. Furthermore, in iron-deficient rats, we consistently noted that Atp7a protein levels increased more dramatically than mRNA levels, perhaps hinting at an additional regulatory mechanism. This seemed even more plausible given that Atp7a protein levels increased more dramatically in the IEC-6 cell model when cells were treated with an iron chelator in the presence of added copper. The current studies were thus undertaken to consider the possibility that copper has a direct role in stabilizing the Atp7a protein.

In the current and past studies [76], Atp7a mRNA levels increased with DFO treatment in IEC-6 cells, possibly by a HIF-mediated mechanism, as iron chelation is known to stabilize the HIF proteins (similar to low oxygen or $CoCl_2$ exposure) [94, 147, 148]. Induction of mRNA expression was more pronounced in the presence of added copper (Figure 4-1), which presumably increased intracellular copper levels as indicated by induction of Mt1a/2a expression. How intracellular copper accumulation could enhance the effect of DFO on *Atp7a* gene expression is not known. Furthermore, although iron chelation alone did not affect Atp7a protein levels, DFO plus added copper led to an increase. Unexpectedly, copper loading in the absence of DFO also increased Atp7a protein levels, while having no influence on mRNA expression. These observations suggested that two independent regulatory mechanisms were involved in

Atp7a induction in IEC-6 cells: 1) a possible HIF-related transcriptional mechanism that increased mRNA levels, and 2) a post-transcriptional mechanism acting directly on the Atp7a protein. Additional experiments were thus designed to delve into the effect of copper loading on Atp7a protein levels.

Cycloheximide (CHX) is commonly used to globally inhibit protein translation, whereby one can assess the rate of protein decay in the absence of synthesis. In the IEC-6 cell model, we thus utilized CHX to determine: 1) the relative stability of the Atp7a protein and 2) whether it was altered by copper loading of cells. Once a suitable concentration of CHX was identified, which significantly attenuated Atp7a protein expression and was not toxic to the cells (10 μg/mL), a time course was performed to assess Atp7a protein decay rate. Results revealed an approximate 41 hour half-life for the Atp7a protein. Importantly, further experiments showed that Atp7a protein decay was significantly inhibited by loading cells with copper in the presence of CHX, most likely indicating that copper interacted with and stabilized the protein.

Copper has been shown to stabilize proteins in which it plays a catalytic role. For example, *apo*-ceruloplasmin (devoid of copper) is much less stable than the copper-containing form (the *holo* enzyme) [149]. Copper also stabilizes the cytosolic metal storage protein metallothionein [150]. In the current investigation however, copper interaction with the protein is more transient in nature, as Atp7a is a *trans*-membrane copper transporter. Atp7a has 6 cytosolic, N-terminal copper-binding domains [151], although all 6 are not required for copper transport function or trafficking from *trans*-Golgi to plasma membrane in cells [152]. As such, we postulate that increased intracellular copper allows for specific binding to one or more of the intracellular copper-

binding domains, leading to stabilization of the protein. How or if this might influence transport activity or protein trafficking is not known.

This investigation has thus successfully modeled *in vitro* what may be occurring to Atp7a gene and protein expression *in vivo* during iron deprivation, when enterocyte iron levels are low & hypoxia occurs, and mucosal copper levels increase. Iron chelation with DFO, which presumably decreases intracellular iron and stabilizes the HIFs, increased Atp7a mRNA expression, while copper loading had an additional, synergistic effect. Use of a translation inhibitor revealed a direct influence of copper on Atp7a protein stability. A novel paradigm is thus revealed in which Atp7a protein expression increases due to two diverse signals: 1) HIF signaling and 2) via alterations in intracellular copper content. The existence of two independent regulatory mechanisms for copper homeostasis in enterocytes specifically during perturbations in iron levels strengthens the hypothesis that copper has a positive influence on intestinal iron absorption. Whether other copper or iron homeostasis-related proteins may be similarly regulated by interaction with intracellular copper in enterocytes is currently unknown. Interestingly however, the predominant intestinal iron importer, divalent metal transporter 1 (Dmt1) can bind to and transport copper [83], but the physiological significance of such an interaction is not clear.

Table 4-1. Sequences of primers used for qRT-PCR Experiments

Gene Name	Primer Sequence
18S-Forward	5’-TCCAAGGAAGGCAGCAGGC-3’
18S-Reverse	5’-TACCTGGTTGATCCTGCCA-3’
Atp7a-Forward	5’-TGAACAGTCATCACCTTCATCGTC-3’
Atp7a-Reverse	5’-TGCATCTTGTTGGACTCCTGAAAG-3’
Mt1a-Forward	5’-CTTCTTGTCGCTTACACCGTTG-3’
Mt1a-Reverse	5’-CAGCAGCACTGTTCGTCACTTC-3’
Mt2a-Forward	5’-ACTGCCGCCTCCATTCGG-3’
Mt2a-Reverse	5’-TCTTGCAGGAGGTGCATTTGC-3’
Ctr1-Forward	5’-CTACTTTGGCTTTAAGAATGTGGACC-3’
Ctr1-Reverse	5’-AACATTGCTAGTAAAAACACTGCCAC-3’
Sod1-Forward	5’-AGCGGTGAACCAGTTGTGGTG-3’
Sod1-Reverse	5’-TGGACCGCCATGTTTCTTAGAG-3’
Atox1-Forward	5’-GTTCTCTGTGGACATGACCTGTGG-3’
Atox1-Reverse	5’-CAAGGTAGGAGACCGCTTTTCCT-3’

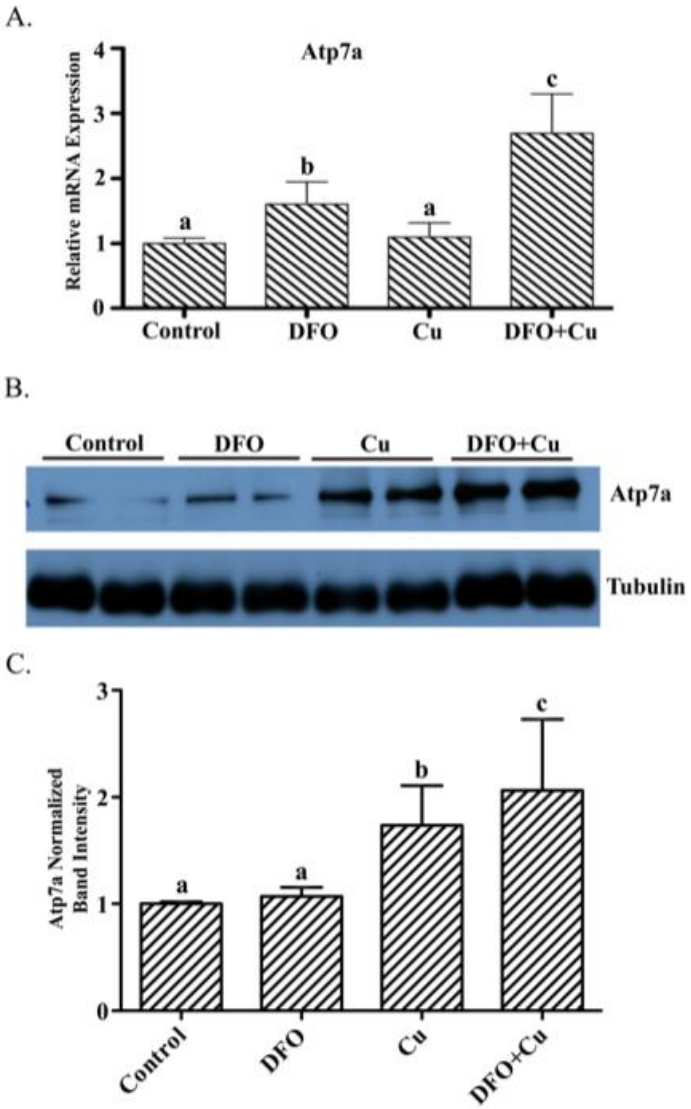

Figure 4-1. Effect of Iron Deprivation and Copper Loading on Atp7a mRNA and Protein Expression in IEC-6 cells. IEC-6 cells at 85% confluence were treated with DFO, $CuCl_2$ or DFO+$CuCl_2$ (all used at 200 μM) for 16 hours. (**A**) Relative Atp7a mRNA expression levels are depicted with the different treatments. Shown are means ± SD; n = 3. (**B**) A representative Atp7a immunoblot is shown, with tubulin used as a constitutively-expressed housekeeping protein for normalization. The Atp7a bands are ~180 kDa, while tubulin bands are ~55 kDa. Quantitative data from 3 independent experiments are presented below in panel **C**, where means ± SD are shown. In panels A and C, letters atop bars indicate significance. Bars sharing the same letter are not statistically different from one another. Bars with different letters are statistically different from one another (ANOVA; $p<0.05$).

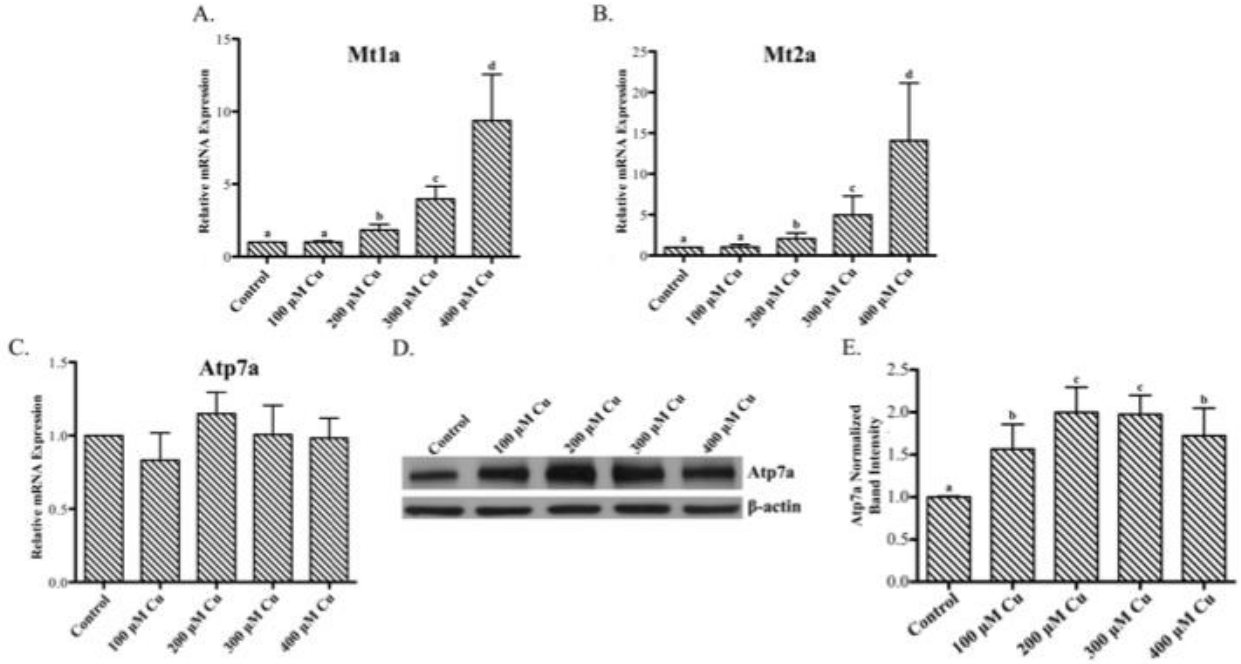

Figure 4-2. Effect of Copper Loading on Mt and Atp7a mRNA Expression. IEC-6 cells at 85% confluence were incubated with $CuCl_2$ at different concentrations (100-400 μM) for 16 hours. Mt1a (**A**), Mt2a (**B**), and Atp7a (**C**) mRNA expression was determined by qRT-PCR. Shown are means ± SD; n=3. (**D**) Atp7a protein levels were determined by immunoblotting with a validated anti-Atp7a polyclonal antibody, utilizing β-actin as a constitutively-expressed housekeeping protein for normalization. The Atp7a bands are ~180 kDa, while β-actin bands are ~50 kDa. A representative blot is shown (D) with quantitative data from 3 independent experiments depicted in panel **E** (where means ± SD are presented). In panels A, B and E, letters atop bars indicate significance. Bars sharing the same letter are not statistically different from one another. Bars with different letters are statistically different from one another (ANOVA; $p<0.05$).

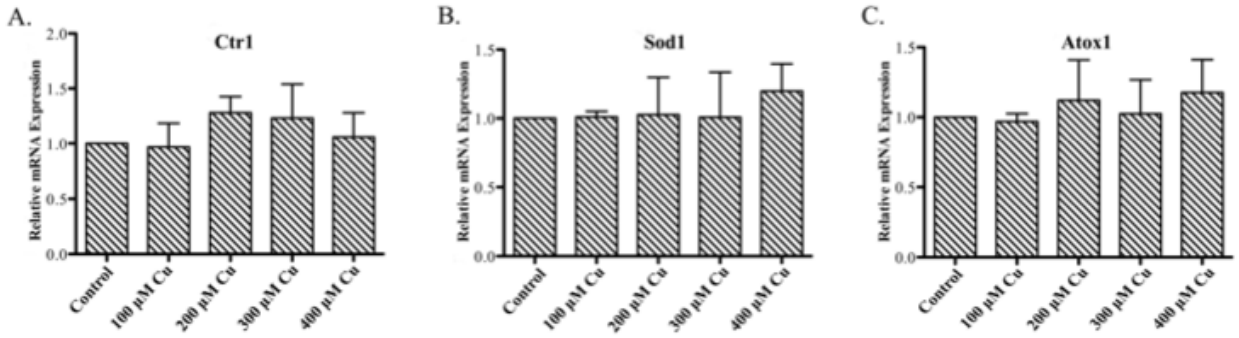

Figure 4-3. Effect of Copper Loading on Expression of Copper-Related Genes**.** IEC-6 cells at 85% confluence were treated with $CuCl_2$ (100-400 µM) for 16 hours. Expression of Ctr1 (A), Sod1 (B), and Atox1 was subsequently determined by qRT-PCR. Each bar represents mean ±SD; n=3.

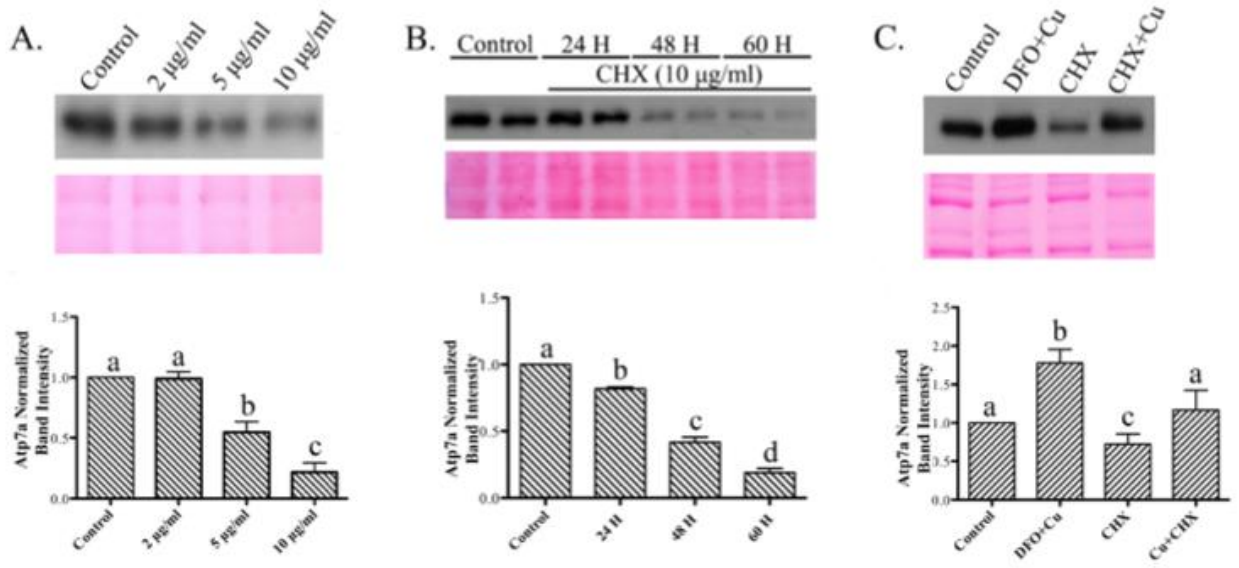

Figure 4-4. Immunoblot Analysis of Atp7a Protein Expression in Cycloheximide (CHX)-Treated IEC-6 cells. IEC-6 cells at 7 days post-confluence were initially treated with CHX for 48 hours at varying concentrations and Atp7a protein expression was quantified (**A**). Shown above is a representative immunoblot with stained protein from the blot shown underneath (which was used to normalize Atp7a protein levels). The Atp7a bands are ~180 kDa. Quantitative data from 3 independent experiments are shown below (mean ± SD; n=3). Subsequently, a time course was performed using 10 µg/mL CHX (**B**). A representative blot and stained proteins are shown above and quantitative data below (mean ± SD; n=3). Cells were then treated with CHX with and without copper loading, and Atp7a protein expression was quantified (**C**). DFO + copper was utilized as a positive control. Again, a representative blot and stained proteins are shown above and quantitative data below (mean ± SD; n=3). In all lower panels, letters atop bars indicate significance. Bars sharing the same letter are not statistically different from one another. Bars with different letters are statistically different from one another(ANOVA; $p<0.05$).

CHAPTER 5
CONCLUSIONS AND FUTURE DIRECTIONS

Conclusions

These studies were designed to delve into the molecular mechanisms of induction of the *Atp7a* gene, which was observed in rat duodenal enterocytes during iron deficiency [85, 86]. The aim of these studies was to identify the specific regulatory mechanisms leading to induction of *Atp7a* gene in rat small intestine. This induction was thus recapitulated in *in vitro* cell culture model, IEC-6 cells. By the completion of these studies, three regulatory mechanisms have been identified: 1) In rat duodenal enterocytes, it was observed that during iron deficiency, *Atp7a* gene expression is strongly induced and its expression parallels that of iron transport-related genes (e.g. *Dmt1*, and *Dcytb*) [85]. It was noted that HIF2α, but not HIF1α, was stabilized in duodenal enterocytes in response to the low iron levels and Atp7a expression is regulated by the HIF2α-mediated signaling pathway. 2) Genes that respond to iron deficiency contain GC-rich sequences in the promoter [87] and these GC-rich sequences are located in close proximity to the region where three evolutionarily conserved HREs are found. Thus, studies were performed to determine if Atp7a is transcriptionally regulated by Sp1 via direct binding to the promoter. Sp1 was shown to be involved in HIF2α-mediated induction of Atp7a expression; 3) During iron deficiency, in the presence of elevated copper levels in duodenal enterocytes, Atp7a protein levels are more robustly induced than its transcript levels [86]. This phenomenon was recapitulated in IEC-6 cells and it was found that copper loading in IEC-6 cells does not affect Atp7a mRNA levels, but increases Atp7a protein levels. Further investigation showed that copper in IEC-6 cells increases Atp7a protein stability.

Future Directions

It was proposed, since the identification of induction of Atp7a expression in duodenal enterocytes during iron deficiency, that induction of Atp7a expression and increased copper absorption in small intestine are considered to be a compensatory mechanism to increase systemic iron levels. Copper is cofactor of two important iron ferroxidases, which may be associated with iron release from enterocytes to portal blood circulation. During iron deficiency, increased copper absorption via small intestine may lead to the accumulation of copper in hepatocytes. This has been observed in *in vivo* animal models, and increased Cp expression and activity are noted in hepatocytes [81]. However, mechanisms of induced Cp expression are still unknown. Further studies can be initiated to reveal the mechanisms by which copper regulates Cp expression in liver. Copper also is cofactor of Hp. During iron deficiency, increased Hp activity is essential to iron release from enterocytes to further increase systemic iron levels. However, whether copper affects Hp expression and how copper is incorporated into Hp are not clear. Studies looking into the functional role of copper in Hp expression in enterocytes and the subcellular Hp synthesis and copper incorporation into Hp can be further investigated.

Genes that respond to low iron have GC-rich sequences in their promoters. Sp-like factors (e.g. Sp1, Sp3, Sp4, and Sp6) may bind to GC-rich sequences. In this study, we characterized one of the Sp-like factors (Sp1) and found that Sp1 transcriptionally regulates Atp7a expression and is involved in the HIF2α-mediated induction of Atp7a expression. However, whether other Sp-like factors could bind to these GC-rich sequences to regulate Atp7a expression is still unknown. Thus, studies to understand whether other Sp-like factors are involved and whether the interaction between Sp1 and

other Sp-like factors exists in response to hypoxia/iron deficiency can be further pursued.

Overall, these studies successfully modeled the observation made in *in vivo* animal models, and several molecular mechanisms have been identified that regulate Atp7a expression during iron deficiency.

LIST OF REFERENCES

1. Aisen, P., C. Enns, and M. Wessling-Resnick, *Chemistry and biology of eukaryotic iron metabolism.* Int J Biochem Cell Biol, 2001. **33**(10): p. 940-59.

2. Nam, W., *High-valent iron(IV)-oxo complexes of heme and non-heme ligands in oxygenation reactions.* Acc Chem Res, 2007. **40**(7): p. 522-31.

3. Hurrell, R.F., *Improvement of trace element status through food fortification: technological, biological and health aspects.* Bibl Nutr Dieta, 1998(54): p. 40-57.

4. Uzel, C. and M.E. Conrad, *Absorption of heme iron.* Semin Hematol, 1998. **35**(1): p. 27-34.

5. Lynch, S.R., *Interaction of iron with other nutrients.* Nutr Rev, 1997. **55**(4): p. 102-10.

6. Lombard, M., E. Chua, and P. O'Toole, *Regulation of intestinal non-haem iron absorption.* Gut, 1997. **40**(4): p. 435-9.

7. Zijp, I.M., O. Korver, and L.B. Tijburg, *Effect of tea and other dietary factors on iron absorption.* Crit Rev Food Sci Nutr, 2000. **40**(5): p. 371-98.

8. Richardson, D.R. and P. Ponka, *The molecular mechanisms of the metabolism and transport of iron in normal and neoplastic cells.* Biochim Biophys Acta, 1997. **1331**(1): p. 1-40.

9. Prus, E. and E. Fibach, *Uptake of non-transferrin iron by erythroid cells.* Anemia, 2011. **2011**: p. 945289.

10. Torti, F.M. and S.V. Torti, *Regulation of ferritin genes and protein.* Blood, 2002. **99**(10): p. 3505-16.

11. McCord, J.M., *Iron, free radicals, and oxidative injury.* J Nutr, 2004. **134**(11): p. 3171S-3172S.

12. Datz, C., et al., *Iron homeostasis in the Metabolic Syndrome.* Eur J Clin Invest, 2013. **43**(2): p. 215-224.

13. Wilson, M.T. and B.J. Reeder, *Oxygen-binding haem proteins.* Exp Physiol, 2008. **93**(1): p. 128-32.

14. Andrews, N.C., *Forging a field: the golden age of iron biology.* Blood, 2008. **112**(2): p. 219-30.

15. Batts, K.P., *Iron overload syndromes and the liver.* Mod Pathol, 2007. **20 Suppl 1**: p. S31-9.

16. Zecca, L., et al., *Iron, brain ageing and neurodegenerative disorders.* Nat Rev Neurosci, 2004. **5**(11): p. 863-73.

17. Zecca, L., et al., *The role of iron and copper molecules in the neuronal vulnerability of locus coeruleus and substantia nigra during aging.* Proc Natl Acad Sci U S A, 2004. **101**(26): p. 9843-8.

18. Kaur, D., et al., *Genetic or pharmacological iron chelation prevents MPTP-induced neurotoxicity in vivo: a novel therapy for Parkinson's disease.* Neuron, 2003. **37**(6): p. 899-909.

19. Wollenberg, P. and W. Rummel, *Dependence of intestinal iron absorption on the valency state of iron.* Naunyn Schmiedebergs Arch Pharmacol, 1987. **336**(5): p. 578-82.

20. Raja, K.B., R.J. Simpson, and T.J. Peters, *Investigation of a role for reduction in ferric iron uptake by mouse duodenum.* Biochim Biophys Acta, 1992. **1135**(2): p. 141-6.

21. McKie, A.T., et al., *An iron-regulated ferric reductase associated with the absorption of dietary iron.* Science, 2001. **291**(5509): p. 1755-9.

22. Gunshin, H., et al., *Cybrd1 (duodenal cytochrome b) is not necessary for dietary iron absorption in mice.* Blood, 2005. **106**(8): p. 2879-83.

23. Latunde-Dada, G.O., et al., *Molecular and functional roles of duodenal cytochrome B (Dcytb) in iron metabolism.* Blood Cells Mol Dis, 2002. **29**(3): p. 356-60.

24. Gunshin, H., et al., *Cloning and characterization of a mammalian proton-coupled metal-ion transporter.* Nature, 1997. **388**(6641): p. 482-8.

25. Fleming, M.D., et al., *The iron transporter Nramp2 is mutated in the anemic belgrade (b) rat.* Blood, 1997. **90**(10): p. 2675-2675.

26. Mackenzie, B. and M.D. Garrick, *Iron Imports. II. Iron uptake at the apical membrane in the intestine.* Am J Physiol Gastrointest Liver Physiol, 2005. **289**(6): p. G981-6.

27. Fleming, M.D., et al., *Nramp2 is mutated in the anemic Belgrade (b) rat: Evidence of a role for Nramp2 in endosomal iron transport.* Proceedings of the National Academy of Sciences of the United States of America, 1998. **95**(3): p. 1148-1153.

28. Fleming, M.D., et al., *Microcytic anaemia mice have a mutation in Nramp2, a candidate iron transporter gene.* Nature Genetics, 1997. **16**(4): p. 383-386.

29. Han, O., *Molecular mechanism of intestinal iron absorption.* Metallomics, 2011. **3**(2): p. 103-9.

30. Abboud, S. and D.J. Haile, *A novel mammalian iron-regulated protein involved in intracellular iron metabolism.* J Biol Chem, 2000. **275**(26): p. 19906-12.

31. McKie, A.T., et al., *A novel duodenal iron-regulated transporter, IREG1, implicated in the basolateral transfer of iron to the circulation.* Mol Cell, 2000. **5**(2): p. 299-309.

32. Frazer, D.M., et al., *Cloning and gastrointestinal expression of rat hephaestin: relationship to other iron transport proteins.* Am J Physiol Gastrointest Liver Physiol, 2001. **281**(4): p. G931-9.

33. Vulpe, C.D., et al., *Hephaestin, a ceruloplasmin homologue implicated in intestinal iron transport, is defective in the sla mouse.* Nat Genet, 1999. **21**(2): p. 195-9.

34. Ranganathan, P.N., et al., *Immunoreactive hephaestin and ferroxidase activity are present in the cytosolic fraction of rat enterocytes.* Biometals, 2012. **25**(4): p. 687-95.

35. Ranganathan, P.N., et al., *Discovery of a cytosolic/soluble ferroxidase in rodent enterocytes.* Proc Natl Acad Sci U S A, 2012. **109**(9): p. 3564-9.

36. Morgan, E.H., *The role of plasma transferrin in iron absorption in the rat.* Q J Exp Physiol Cogn Med Sci, 1980. **65**(3): p. 239-52.

37. Trenor, C.C., et al., *The molecular defect in hypotransferrinemic mice.* Blood, 2000. **96**(3): p. 1113-1118.

38. Holmberg, C.G. and C.B. Laurell, *Histaminolytic activity of a copper protein in serum.* Nature, 1948. **161**(4085): p. 236.

39. Prohaska, J.R., *Impact of Copper Limitation on Expression and Function of Multicopper Oxidases (Ferroxidases).* Advances in Nutrition: An International Review Journal, 2011. **2**(2): p. 89-95.

40. Muckenthaler, M.U., B. Galy, and M.W. Hentze, *Systemic iron homeostasis and the iron-responsive element/iron-regulatory protein (IRE/IRP) regulatory network.* Annu Rev Nutr, 2008. **28**: p. 197-213.

41. Casey, J.L., et al., *Iron-responsive elements: regulatory RNA sequences that control mRNA levels and translation.* Science, 1988. **240**(4854): p. 924-8.

42. Lee, P.L., et al., *The human Nramp2 gene: characterization of the gene structure, alternative splicing, promoter region and polymorphisms.* Blood Cells Mol Dis, 1998. **24**(2): p. 199-215.

43. Caughman, S.W., et al., *The iron-responsive element is the single element responsible for iron-dependent translational regulation of ferritin biosynthesis. Evidence for function as the binding site for a translational repressor.* J Biol Chem, 1988. **263**(35): p. 19048-52.

44. Anderson, C., I. Aronson, and P. Jacobs, *Erythropoiesis: Erythrocyte Deformability is Reduced and Fragility increased by Iron Deficiency.* Hematology, 2000. **4**(5): p. 457-460.

45. Shah, Y.M., et al., *Intestinal hypoxia-inducible transcription factors are essential for iron absorption following iron deficiency.* Cell Metab, 2009. **9**(2): p. 152-64.

46. Mastrogiannaki, M., et al., *HIF-2alpha, but not HIF-1alpha, promotes iron absorption in mice.* J Clin Invest, 2009. **119**(5): p. 1159-66.

47. Taylor, M., et al., *Hypoxia-Inducible Factor-2Œ± Mediates the Adaptive Increase of Intestinal Ferroportin During Iron Deficiency in Mice.* Gastroenterology, 2011. **140**(7): p. 2044-2055.

48. Park, C.H., et al., *Hepcidin, a urinary antimicrobial peptide synthesized in the liver.* J Biol Chem, 2001. **276**(11): p. 7806-10.

49. Donovan, A., et al., *Positional cloning of zebrafish ferroportin1 identifies a conserved vertebrate iron exporter.* Nature, 2000. **403**(6771): p. 776-81.

50. Kim, B.E., T. Nevitt, and D.J. Thiele, *Mechanisms for copper acquisition, distribution and regulation.* Nat Chem Biol, 2008. **4**(3): p. 176-85.

51. Collins, J.F. and L.M. Klevay, *Copper.* Adv Nutr, 2011. **2**(6): p. 520-2.

52. Nose, Y., B.E. Kim, and D.J. Thiele, *Ctr1 drives intestinal copper absorption and is essential for growth, iron metabolism, and neonatal cardiac function.* Cell Metabolism, 2006. **4**(3): p. 235-244.

53. Ohgami, R.S., et al., *The Steap proteins are metalloreductases.* Blood, 2006. **108**(4): p. 1388-94.

54. Wyman, S., et al., *Dcytb (Cybrd1) functions as both a ferric and a cupric reductase in vitro.* FEBS Lett, 2008. **582**(13): p. 1901-6.

55. Amaravadi, R., D.M. Glerum, and A. Tzagoloff, *Isolation of a cDNA encoding the human homolog of COX17, a yeast gene essential for mitochondrial copper recruitment.* Hum Genet, 1997. **99**(3): p. 329-33.

56. Casareno, R.L., D. Waggoner, and J.D. Gitlin, *The copper chaperone CCS directly interacts with copper/zinc superoxide dismutase.* J Biol Chem, 1998. **273**(37): p. 23625-8.

57. Larin, D., et al., *Characterization of the interaction between the Wilson and Menkes disease proteins and the cytoplasmic copper chaperone, HAH1p.* J Biol Chem, 1999. **274**(40): p. 28497-504.

58. Yamaguchi, Y., et al., *Biochemical characterization and intracellular localization of the Menkes disease protein.* Proc Natl Acad Sci U S A, 1996. **93**(24): p. 14030-5.

59. Petris, M.J., et al., *Ligand-regulated transport of the Menkes copper P-type ATPase efflux pump from the Golgi apparatus to the plasma membrane: a novel mechanism of regulated trafficking.* EMBO J, 1996. **15**(22): p. 6084-95.

60. Linder, M.C. and M. Hazegh-Azam, *Copper biochemistry and molecular biology.* Am J Clin Nutr, 1996. **63**(5): p. 797S-811S.

61. Kubow, S., T.M. Bray, and W.J. Bettger, *Effects of dietary zinc and copper on free radical production in rat lung and liver.* Can J Physiol Pharmacol, 1986. **64**(10): p. 1281-5.

62. Menkes, J.H., *Maple syrup disease; isolation and identification of organic acids in the urine.* Pediatrics, 1959. **23**(2): p. 348-53.

63. Vulpe, C., et al., *Isolation of a candidate gene for Menkes disease and evidence that it encodes a copper-transporting ATPase.* Nat Genet, 1993. **3**(1): p. 7-13.

64. Mercer, J.F., et al., *Isolation of a partial candidate gene for Menkes disease by positional cloning.* Nat Genet, 1993. **3**(1): p. 20-5.

65. Chelly, J., et al., *Isolation of a candidate gene for Menkes disease that encodes a potential heavy metal binding protein.* Nat Genet, 1993. **3**(1): p. 14-9.

66. Blalock, T.L., M.A. Dunn, and R.J. Cousins, *Metallothionein gene expression in rats: tissue-specific regulation by dietary copper and zinc.* J Nutr, 1988. **118**(2): p. 222-8.

67. Minghetti, M., et al., *Copper induces Cu-ATPase ATP7A mRNA in a fish cell line, SAF1.* Comp Biochem Physiol C Toxicol Pharmacol, 2011. **154**(2): p. 93-9.

68. Suzuki, K.T., et al., *Roles of metallothionein in copper homeostasis: responses to Cu-deficient diets in mice.* J Inorg Biochem, 2002. **88**(2): p. 173-82.

69. Petris, M.J., et al., *Copper-stimulated endocytosis and degradation of the human copper transporter, hCtr1.* J Biol Chem, 2003. **278**(11): p. 9639-46.

70. West, E.C. and J.R. Prohaska, *Cu,Zn-superoxide dismutase is lower and copper chaperone CCS is higher in erythrocytes of copper-deficient rats and mice.* Exp Biol Med (Maywood), 2004. **229**(8): p. 756-64.

71. Bertinato, J. and M.R. L'Abbe, *Copper modulates the degradation of copper chaperone for Cu,Zn superoxide dismutase by the 26 S proteosome.* J Biol Chem, 2003. **278**(37): p. 35071-8.

72. Caruano-Yzermans, A.L., T.B. Bartnikas, and J.D. Gitlin, *Mechanisms of the Copper-dependent Turnover of the Copper Chaperone for Superoxide Dismutase.* Journal of Biological Chemistry, 2006. **281**(19): p. 13581-13587.

73. Lutsenko, S., et al., *Function and Regulation of Human Copper-Transporting ATPases.* Physiological Reviews, 2007. **87**(3): p. 1011-1046.

74. Robinson, N.J. and D.R. Winge, *Copper Metallochaperones.* Annual Review of Biochemistry, 2010. **79**(1): p. 537-562.

75. Linz, R. and S. Lutsenko, *Copper-transporting ATPases ATP7A and ATP7B: cousins, not twins.* J Bioenerg Biomembr, 2007. **39**(5-6): p. 403-7.

76. Collins, J.F., et al., *Alternative Splicing of the Menkes Copper Atpase (Atp7a) Transcript in the Rat Intestinal Epithelium.* Am J Physiol Gastrointest Liver Physiol, 2009.

77. Pase, L., et al., *Copper stimulates trafficking of a distinct pool of the Menkes copper ATPase (ATP7A) to the plasma membrane and diverts it into a rapid recycling pool.* Biochem. J., 2004. **378**(3): p. 1031-1037.

78. Takahashi, N., T.L. Ortel, and F.W. Putnam, *Single-chain structure of human ceruloplasmin: the complete amino acid sequence of the whole molecule.* Proc Natl Acad Sci U S A, 1984. **81**(2): p. 390-4.

79. Martin, F., et al., *Copper-dependent activation of hypoxia-inducible factor (HIF)-1: implications for ceruloplasmin regulation.* Blood, 2005. **105**(12): p. 4613-9.

80. Mukhopadhyay, C.K., B. Mazumder, and P.L. Fox, *Role of hypoxia-inducible factor-1 in transcriptional activation of ceruloplasmin by iron deficiency.* J Biol Chem, 2000. **275**(28): p. 21048-54.

81. Ranganathan, P.N., et al., *Serum ceruloplasmin protein expression and activity increases in iron-deficient rats and is further enhanced by higher dietary copper intake.* Blood, 2011. **118**(11): p. 3146-53.

82. Tennant, J., et al., *Effects of copper on the expression of metal transporters in human intestinal Caco-2 cells.* FEBS Lett, 2002. **527**(1-3): p. 239-44.

83. Arredondo, M., et al., *DMT1, a physiologically relevant apical Cu1+ transporter of intestinal cells.* Am J Physiol Cell Physiol, 2003. **284**(6): p. C1525-30.

84. Jiang, L., et al., *Exploration of the Copper Related Compensatory Response in the Belgrade Rat Model of Genetic Iron Deficiency.* American journal of physiology. Gastrointestinal and liver physiology, 2011.

85. Collins, J.F., et al., *Identification of differentially expressed genes in response to dietary iron deprivation in rat duodenum.* Am J Physiol Gastrointest Liver Physiol, 2005. **288**(5): p. G964-71.

86. Ravia, J.J., et al., *Menkes Copper ATPase (Atp7a) is a novel metal-responsive gene in rat duodenum, and immunoreactive protein is present on brush-border and basolateral membrane domains.* J Biol Chem, 2005. **280**(43): p. 36221-36227.

87. Collins, J.F. and Z. Hu, *Promoter analysis of intestinal genes induced during iron-deprivation reveals enrichment of conserved SP1-like binding sites.* BMC Genomics, 2007. **8**: p. 420.

88. Zoller, H., et al., *Expression of the duodenal iron transporters divalent-metal transporter 1 and ferroportin 1 in iron deficiency and iron overload.* Gastroenterology, 2001. **120**(6): p. 1412-9.

89. Collins, J.F., J.R. Prohaska, and M.D. Knutson, *Metabolic crossroads of iron and copper.* Nutr Rev, 2010. **68**(3): p. 133-47.

90. Collins, J.F., *Gene chip analyses reveal differential genetic responses to iron deficiency in rat duodenum and jejunum.* Biol Res, 2006. **39**(1): p. 25-37.

91. Ravia, J.J., et al., *Menkes copper ATPase (Atp7a) is a novel metal-responsive gene in rat duodenum, and immunoreactive protein is present on brush-border and basolateral membrane domains.* Journal of Biological Chemistry, 2005. **280**(43): p. 36221-36227.

92. Ece, A., et al., *Increased serum copper and decreased serum zinc levels in children with iron deficiency anemia.* Biol Trace Elem Res, 1997. **59**(1-3): p. 31-9.

93. Collins, J.F., M. Wessling-Resnick, and M.D. Knutson, *Hepcidin regulation of iron transport.* J Nutr, 2008. **138**(11): p. 2284-8.

94. Hu, Z., S. Gulec, and J.F. Collins, *Cross-species comparison of genomewide gene expression profiles reveals induction of hypoxia-inducible factor-responsive genes in iron-deprived intestinal epithelial cells.* Am J Physiol Cell Physiol, 2010. **299**(5): p. C930-8.

95. Benita, Y., et al., *An integrative genomics approach identifies Hypoxia Inducible Factor-1 (HIF-1)-target genes that form the core response to hypoxia.* Nucleic Acids Res, 2009. **37**(14): p. 4587-602.

96. Piret, J.P., et al., *CoCl2, a chemical inducer of hypoxia-inducible factor-1, and hypoxia reduce apoptotic cell death in hepatoma cell line HepG2.* Ann N Y Acad Sci, 2002. **973**: p. 443-7.

97. Collins, J.F., et al., *Induction of arachidonate 12-lipoxygenase (Alox15) in intestine of iron-deficient rats correlates with the production of biologically active lipid mediators.* Am J Physiol Gastrointest Liver Physiol, 2008. **294**(4): p. G948-62.

98. Yuan, Y., et al., *Cobalt inhibits the interaction between hypoxia-inducible factor-alpha and von Hippel-Lindau protein by direct binding to hypoxia-inducible factor-alpha.* J Biol Chem, 2003. **278**(18): p. 15911-6.

99. Maxwell, P.H., et al., *The tumour suppressor protein VHL targets hypoxia-inducible factors for oxygen-dependent proteolysis.* Nature, 1999. **399**(6733): p. 271-5.

100. Cockman, M.E., et al., *Hypoxia inducible factor-alpha binding and ubiquitylation by the von Hippel-Lindau tumor suppressor protein.* J Biol Chem, 2000. **275**(33): p. 25733-41.

101. Hu, Z., B. Hu, and J.F. Collins, *Prediction of synergistic transcription factors by function conservation.* Genome Biol, 2007. **8**(12): p. R257.

102. Chandel, N.S., et al., *Mitochondrial reactive oxygen species trigger hypoxia-induced transcription.* Proc Natl Acad Sci U S A, 1998. **95**(20): p. 11715-20.

103. Giordano, F.J., *Oxygen, oxidative stress, hypoxia, and heart failure.* The Journal of Clinical Investigation, 2005. **115**(3): p. 500-508.

104. Videla, L.A., et al., *Oxidative stress-mediated hepatotoxicity of iron and copper: Role of Kupffer cells.* Biometals, 2003. **16**(1): p. 103-111.

105. Gunshin, H., et al., *Slc11a2 is required for intestinal iron absorption and erythropoiesis but dispensable in placenta and liver.* J Clin Invest, 2005. **115**(5): p. 1258-66.

106. Harris, Z.L., et al., *Targeted gene disruption reveals an essential role for ceruloplasmin in cellular iron efflux.* Proc Natl Acad Sci U S A, 1999. **96**(19): p. 10812-7.

107. Hellman, N.E., et al., *Hepatic iron overload in aceruloplasminaemia.* Gut, 2000. **47**(6): p. 858-60.

108. Takami, T. and I. Sakaida, *Iron regulation by hepatocytes and free radicals.* J Clin Biochem Nutr, 2011. **48**(2): p. 103-6.

109. Walden, W.E., et al., *Structure of dual function iron regulatory protein 1 complexed with ferritin IRE-RNA.* Science, 2006. **314**(5807): p. 1903-8.

110. Wang, G.L. and G.L. Semenza, *General involvement of hypoxia-inducible factor 1 in transcriptional response to hypoxia.* Proc Natl Acad Sci U S A, 1993. **90**(9): p. 4304-8.

111. Wang, G.L., et al., *HYPOXIA-INDUCIBLE FACTOR-1 IS A BASIC-HELIX-LOOP-HELIX-PAS HETERODIMER REGULATED BY CELLULAR O-2 TENSION.* Proceedings of the National Academy of Sciences of the United States of America, 1995. **92**(12): p. 5510-5514.

112. Jiang, B.H., et al., *Dimerization, DNA binding, and transactivation properties of hypoxia-inducible factor 1.* J Biol Chem, 1996. **271**(30): p. 17771-8.

113. Xie, L. and J.F. Collins, *Transcriptional regulation of the Menkes copper ATPase (Atp7a) gene by hypoxia-inducible factor (HIF2{alpha}) in intestinal epithelial cells.* Am J Physiol Cell Physiol, 2011. **300**(6): p. C1298-305.

114. Xie, L. and J.F. Collins, *Copper stabilizes the Menkes copper-transporting ATPase (Atp7a) protein expressed in rat intestinal epithelial cells.* Am J Physiol Cell Physiol, 2013. **304**(3): p. C257-62.

115. Mizukami, Y., et al., *Hypoxia-inducible factor-1-independent regulation of vascular endothelial growth factor by hypoxia in colon cancer.* Cancer Res, 2004. **64**(5): p. 1765-72.

116. Carroll, V.A. and M. Ashcroft, *Role of Hypoxia-Inducible Factor (HIF)-1α versus HIF-2α in the Regulation of HIF Target Genes in Response to Hypoxia, Insulin-Like Growth Factor-I, or Loss of von Hippel-Lindau Function: Implications for Targeting the HIF Pathway.* Cancer Research, 2006. **66**(12): p. 6264-6270.

117. Sleiman, S.F., et al., *Mithramycin Is a Gene-Selective Sp1 Inhibitor That Identifies a Biological Intersection between Cancer and Neurodegeneration.* The Journal of Neuroscience, 2011. **31**(18): p. 6858-6870.

118. Barceló, F., et al., *DNA Binding Characteristics of Mithramycin and Chromomycin Analogues Obtained by Combinatorial Biosynthesis.* Biochemistry, 2010. **49**(49): p. 10543-10552.

119. Miller, D.M., et al., *Mithramycin selectively inhibits transcription of G-C containing DNA.* Am J Med Sci, 1987. **294**(5): p. 388-94.

120. Liang, Z.D., et al., *Specificity protein 1 (sp1) oscillation is involved in copper homeostasis maintenance by regulating human high-affinity copper transporter 1 expression.* Mol Pharmacol, 2012. **81**(3): p. 455-64.

121. Wada, T., S. Shimba, and M. Tezuka, *Transcriptional regulation of the hypoxia inducible factor-2alpha (HIF-2alpha) gene during adipose differentiation in 3T3-L1 cells.* Biol Pharm Bull, 2006. **29**(1): p. 49-54.

122. Emili, A., J. Greenblatt, and C.J. Ingles, *Species-specific interaction of the glutamine-rich activation domains of Sp1 with the TATA box-binding protein.* Mol. Cell. Biol., 1994. **14**(3): p. 1582-1593.

123. Taylor, I.C. and R.E. Kingston, *Factor substitution in a human HSP70 gene promoter: TATA-dependent and TATA-independent interactions.* Mol Cell Biol, 1990. **10**(1): p. 165-75.

124. Tan, N.Y. and L.M. Khachigian, *Sp1 phosphorylation and its regulation of gene transcription.* Mol Cell Biol, 2009. **29**(10): p. 2483-8.

125. Koizume, S., et al., *HIF2α-Sp1 interaction mediates a deacetylation-dependent FVII-gene activation under hypoxic conditions in ovarian cancer cells.* Nucleic Acids Research, 2012.

126. Ke, X., et al., *Hypoxia upregulates CD147 through a combined effect of HIF-1alpha and Sp1 to promote glycolysis and tumor progression in epithelial solid tumors.* Carcinogenesis, 2012. **33**(8): p. 1598-607.

127. Hurrell, R.F., et al., *Iron absorption in humans as influenced by bovine milk proteins.* Am J Clin Nutr, 1989. **49**(3): p. 546-52.

128. Andrews, N.C., M.D. Fleming, and J.E. Levy, *Molecular insights into mechanisms of iron transport.* Curr Opin Hematol, 1999. **6**(2): p. 61-4.

129. Kundu, S., et al., *On the reactivity of mononuclear iron(V)oxo complexes.* J Am Chem Soc, 2011. **133**(46): p. 18546-9.

130. Heeney, M.M. and N.C. Andrews, *Iron homeostasis and inherited iron overload disorders: an overview.* Hematol Oncol Clin North Am, 2004. **18**(6): p. 1379-403, ix.

131. Cherukuri, S., et al., *Unexpected role of ceruloplasmin in intestinal iron absorption.* Cell Metab, 2005. **2**(5): p. 309-19.

132. Anderson, G.J., et al., *The ceruloplasmin homolog hephaestin and the control of intestinal iron absorption.* Blood Cells Mol Dis, 2002. **29**(3): p. 367-75.

133. Lewin, J.S., et al., *Interactive MRI-guided radiofrequency interstitial thermal ablation of abdominal tumors: clinical trial for evaluation of safety and feasibility.* J Magn Reson Imaging, 1998. **8**(1): p. 40-7.

134. Linderman, R.J. and J.M. Siedlecki, *Selective Copper-Catalyzed Coupling Reactions of (alpha-Acetoxyhexyl)tricyclohexyltin.* J Org Chem, 1996. **61**(19): p. 6492-6493.

135. Wang, F., et al., *A novel murine protein with no effect on iron homoeostasis is homologous with transferrin and is the putative inhibitor of carbonic anhydrase.* Biochem J, 2007. **406**(1): p. 85-95.

136. Williams, D.M. and C.L. Atkin, *Tissue copper concentrations of patients with Menke's kinky hair disease.* Am J Dis Child, 1981. **135**(4): p. 375-6.

137. Danks, D.M., et al., *Menkes kinky-hair syndrome. An inherited defect in the intestinal absorption of copper with widespread effects.* Birth Defects Orig Artic Ser, 1974. **10**(10): p. 132-7.

138. Taylor, M., et al., *Hypoxia-inducible factor-2alpha mediates the adaptive increase of intestinal ferroportin during iron deficiency in mice.* Gastroenterology, 2011. **140**(7): p. 2044-55.

139. Boaz, T.L., et al., *MR monitoring of MR-guided radiofrequency thermal ablation of normal liver in an animal model.* J Magn Reson Imaging, 1998. **8**(1): p. 64-9.

140. Hider, R.C., D. Bittel, and G.K. Andrews, *Competition between iron(III)-selective chelators and zinc-finger domains for zinc(II).* Biochem Pharmacol, 1999. **57**(9): p. 1031-5.

141. Thomas, C. and P.S. Oates, *Differences in the uptake of iron from Fe(II) ascorbate and Fe(III) citrate by IEC-6 cells and the involvement of ferroportin/IREG-1/MTP-1/SLC40A1.* Pflugers Arch, 2004. **448**(4): p. 431-7.

142. Thomas, C. and P.S. Oates, *IEC-6 cells are an appropriate model of intestinal iron absorption in rats.* J Nutr, 2002. **132**(4): p. 680-7.

143. Lu, Y., C. Kim, and J.F. Collins, *Multiple Menkes copper ATPase (Atp7a) transcript and protein variants are induced by iron deficiency in rat duodenal enterocytes.* J Trace Elem Med Biol, 2012. **26**(2-3): p. 109-14.

144. Collins, J.F., et al., *Alternative splicing of the Menkes copper Atpase (Atp7a) transcript in the rat intestinal epithelium.* Am J Physiol Gastrointest Liver Physiol, 2009. **297**(4): p. G695-707.

145. Lynch, S.R., et al., *The effect of dietary proteins on iron bioavailability in man.* Adv Exp Med Biol, 1989. **249**: p. 117-32.

146. Lewin, J.S., et al., *Interactive MR imaging-guided biopsy and aspiration with a modified clinical C-arm system.* AJR Am J Roentgenol, 1998. **170**(6): p. 1593-601.

147. Bunn, H.F. and R.O. Poyton, *Oxygen sensing and molecular adaptation to hypoxia.* Physiol Rev, 1996. **76**(3): p. 839-85.

148. Semenza, G.L., *Hypoxia-inducible factor 1 and the molecular physiology of oxygen homeostasis.* J Lab Clin Med, 1998. **131**(3): p. 207-14.

149. Hellman, N.E. and J.D. Gitlin, *Ceruloplasmin metabolism and function.* Annu Rev Nutr, 2002. **22**: p. 439-58.

150. Cols, N., et al., *In vivo copper- and cadmium-binding ability of mammalian metallothionein beta domain.* Protein Eng, 1999. **12**(3): p. 265-9.

151. Lutsenko, S., et al., *N-terminal domains of human copper-transporting adenosine triphosphatases (the Wilson's and Menkes disease proteins) bind copper selectively in vivo and in vitro with stoichiometry of one copper per metal-binding repeat.* J Biol Chem, 1997. **272**(30): p. 18939-44.

152. Goodyer, I.D., et al., *Characterization of the Menkes protein copper-binding domains and their role in copper-induced protein relocalization.* Hum Mol Genet, 1999. **8**(8): p. 1473-8.

BIOGRAPHICAL SKETCH

Liwei Xie was born in Xi'an, China, an old city with more than 2000 years of history, and raised by his grandparents and father, who helped him to grow to be a strong, silent, and independent man. He believes this was the most precious gift that he received from his family. Before college, He spent most of his time with his grandfather who sparked his passion for science. The two most valued things he learned from his grandfather were hard work and creative thinking.

His high school biology teacher was also extremely influential in his life. Her help changed his perspectives of biological sciences, and molded his understanding of it by demonstrating to him the importance and necessity of biomedical research in disease therapies, such as AIDS, cancer, and diabetes. She ignited his passion, and inspired his dream of becoming a scientist, and it was her influence later on in his life that led him to switch from electrical engineering to biological sciences. As a result, he began pursuing his true passion at the State University of New York at Buffalo, where he obtained his second bachelor's degree in biological sciences. While there, he gained research experience working with Dr. Collins's in the Department of Exercise and Nutritional Sciences as an undergraduate volunteer. After the summer of 2008, he split his time between two new labs, which exposed him to several other interesting studies such as inflammatory response and function of protein-methylation. These experiences provided him with different perspectives for areas of his graduate studies, and he decided nutritional sciences would be his major focus.

In 2009, he moved to the University of Florida to pursue his Doctor of Philosophy in nutritional science. He felt so excited to be part of an energetic and productive team. Besides working on the excellent research projects, he also had the opportunity to learn

about nutrition from professors who are prominent experts in the area of vitamins and minerals. His Doctor of Philosophy training focused on understanding the molecular mechanisms of mineral absorption, and more broadly, it provided him with a fundamental and precise understanding of nutrition. His future plan is to bridge his training in nutrition to human diseases. Epidemiological studies have shown that dietary changes can have a critical effect on a vast number of diseases beyond obesity and metabolic syndromes, such as cancer. He plans to shift his focus to studying the molecular mechanisms of carcinogenesis, and further exploring the strategy for cancer prevention and treatment. Dr. Shah's lab at the University of Michigan Ann Arbor has rich experience and excellent resources to study the progression of colon cancer. The post-doctoral training he receives will allow him to connect his understanding of metal homeostasis with colon carcinogenesis.